Waveforms MOdels for Machine Type CommuNication inteGrating 5G Networks (WONG5) Document Number D2.1 Critical and comparative study of waveforms in C-MTC context

Yahia Medjahdi, Sylvain Traverso, Jean-Baptiste Doré, Hmaied Shaiek, Daniel Roviras, Robin Gerzaguet, Rafik Zayani, David Demmer, Pascal Chevalier, Yves Louët, et al.

Waveforms MOdels for Machine Type CommuNication inteGrating 5G Networks

(WONG5)

Document Number D2.1

Critical and comparative study of waveforms in C-MTC context

Contractual date of delivery:	12/01/2017
Project Number and Acronym:	ANR-15-CE25-0005, WONG5
Editor:	Yahia Medjahdi (CNAM)
Authors:	*Yahia Medjahdi (CNAM), Sylvain Traverso (TCS), Jean-Baptiste Dore (CEA), Hmaied Shaiek (CNAM), Daniel Roviras (CNAM), Robin Gerzaguet (CEA), Rafik Zayani (CNAM), David Demmer (CEA), Pascal Chevalier (TCS), Yves Louet (CS), Mouna Ben Mabrouk (CS), Rostom Zakaria (CNAM), Didier Le Ruyet (CNAM)*
Participants:	CNAM, TCS, CEA, CS
Workpackage:	WP2
Security:	Public(PU)
Nature:	Report
Version:	0.7
Total Number of Pages:	90

Abstract:

This report is the first one of task WP2 (Critical comparative analysis of post-OFDM waveforms) titled 'Waveforms for C-MTC'. The aim of this deliverable is to analyze and compare post-OFDM waveforms for 5G systems following different criteria (PSD, spectral efficiency, latency, complexity, time and frequency offset behavior, PAPR) and to define a restricted set of WF adapted to the C-MTC context.

Keywords: C-MTC, CP-OFDM, post-OFDM, WOLA-OFDM, UFMC, UF-OFDM, Filtered-OFDM, FMT, N-Continuous-OFDM, FBMC-OQAM, Lapped-OFDM, WCP-COQAM, FBMC-QAM, GFDM, PSD, spectral efficiency, latency, timing offset, CFO, PAPR, complexity

Document Revision History

Version	Date	Author	Summary of main changes
0.0	09.11.2016	Yahia Medjahdi	Initial structure of the document
0.1	07.12.2016	Jean Baptiste Dore	CEA contribution
0.2	07.12.2016	Sylvain Traverso	TCS contribution
0.3	15.12.2016	Yahia Medjahdi	CNAM contribution
0.4	09.01.2017	Sylvain Traverso	TCS contribution (update)
0.5	01.02.2017	Jean Baptiste Dore	CEA contribution (update)
0.6	02.02.2017	Yahia Medjahdi	Draft version
0.7	01.03.2017	Yahia Medjahdi	Final version

Executive Summary

The goals of the WONG5 project are to study and propose the most appropriate post-OFDM waveforms (WF) that could be adapted to critical machine type communications (C-MTC). Deliverable D2.1 analyses most of available post-OFDM WF that are in the race for 5G systems standardization. The WF candidates studied in D2.1 are: CP-OFDM as a comparison basis, Weighted Overlap and Add-OFDM (WOLA-OFDM), Universal Filtered Multicarrier (UFMC), N-continuous OFDM, Filtered Multi-Tone (FMT), Filter Bank Multicarrier-Offset QAM (FBMC-OQAM), Lapped-OFDM, Windowed Cyclic Prefix-COQAM (WCP-COQAM), Filter Bank Multicarrier-QAM (FBMC-QAM) and Generalized Frequency Division Multiplexing (GFDM). In Part 2 of the deliverable, WF are classified and presented. The system model used for all comparisons is presented in Part 3, while Part 4 of the document is devoted to WF comparison. Comparisons are conducted using the same system model for all WF, following the different criteria: Spectral efficiency, Latency, Asynchronous access related to both Timing offset and Carrier Frequency Offset, PAPR, Complexity and finally MIMO issues. Part 5 of the deliverable gathers and compare the different WF in the light of C-MTC requirements and a set of candidate WFs is defined for further studies in task 2.2 (Study of new WF for C-MTC), task 3 (Non-linear issues) and task 4 (MIMO issues).

Table of Contents

1. Introduction

1.1 Context

The objective the WONG5 project is to study and propose the most appropriate post-OFDM waveforms (WF) for critical machine type communications (C-MTC). Requirements for C-MTC systems have been described in D1.1 [DRT16] and can be summarized as follows: low latencies, very high reliability and data integrity, high energy efficiency for mobile systems and resistance to asynchronous users (time and frequency). The aim of deliverable D2.1 is to analyze available post-OFDM WF and to compare them under the requirements of C-MTC systems. The output of the comparison will be a restricted set of possible candidates WFs for C-MTC. These WFs will be further studied in WONG5 project. In task 2.2, studies will be conducted in order to enhance their properties related to C-MTC context. In task 3, energy efficiency improvement will be studied together with their adaptation to analog RF components. During task 4, adaptation of candidate WFs to MIMO systems will be developed.

1.2 Objectives

The main objective of deliverable D2.1 is to analyze and compare available post-OFDM WF and to define a set of suitable candidates for C-MTC systems.

The WF studied in D2.1 are:

- CP-OFDM as a comparison basis,
- Weighted Overlap and Add-OFDM (WOLA-OFDM),
- Universal Filtered Multicarrier (UFMC),
- N-continuous OFDM,
- Filtered Multi Tone (FMT),
- Filter Bank Multicarrier-Offset QAM (FBMC-OQAM),
- Lapped-OFDM,
- Windowed Cyclic Prefix-Circular OQAM (WCP-COQAM),
- Filter Bank Multicarrier-QAM (FBMC-QAM)
- Generalized Frequency Division Multiplexing (GFDM).

In the above list, all WFs candidates to 5G systems available in literature, at the time of this deliverable redaction, have been included.

A common system model has been adopted for all WFs comparisons. This system model takes into account the fact that asynchronous users will be present in a C-MTC system. The resource blocks (RB) assigned to the user of interest (UOI) are surrounded by RB assigned to other users that can have time and frequency offsets related to the UOI.

The different comparison criteria are:

- Power spectral density,

- Spectral efficiency,
- Latency,
- Asynchronous access related to Timing Offset,
- Asynchronous access related to Carrier Frequency Offset (CFO),
- Peak to Average Power Ratio (PAPR),
- Complexity.

This deliverable gathers and compares the different WF in the light of C-MTC requirements and a set of candidate WFs will be defined for further studies in WONG5 project.

2. Candidate Waveforms

2.1 WF Classification

Before presenting the different WF candidates for the physical layer of the future 5G C-MTC networks, it should be interesting to classify them based on a crucial aspect which is the orthogonality between the transmitted data symbols. In this section, we will define the orthogonality condition in the complex and real domains. Then we will introduce the need for non orthogonal WFs.

It is well known that one of the main drawbacks of the CP-OFDM is the poor frequency localization of the filters associated with its synthesized subcarrier signals (at the transmitter : $g_T(t)$) and analyzed subcarrier signals (at the receiver: $g_R(t)$). In order to overcome this problem, a finite pulse shape filter with smooth edges for $g_T(t)$ and $g_R(t)$ different from the rectangular pulse [FB11] used in CP-OFDM can be used. With these modifications, we obtain the windowing-based OFDM WFs [ZMSR16] and the filtering-based OFDM WF [AJM15]. With these WFs and over distortion free propagation channels, the transmitted data symbols are separable at the receiver side, if the following condition is fulfilled:

$$\int_{\mathbb{R}} g_T(t - mT) e^{j2\pi kt/T} g_R(t - m'T) e^{-j2\pi k't/T} dt = \delta_{m,m'}\delta_{k,k'} \tag{2.1}$$

where $\delta_{k,k'}$ is the Kronecker delta function and is equal to : 1 if $k = k'$ and 0 elsewhere. As the transmitted symbols are complex (belong to a QAM constellation), the condition given by equation 2.1, is called complex orthogonality condition.

Another drawback of the CP-OFDM and some of the windowing/filtering-based OFDM WFs is the loss of spectral efficiency due to the use of CP or specific guard band. This leads to a symbol density lower than 1. Thus, in order to avoid this drawback, we have to choose a WF with symbol density of one. However, it is theoretically proven, based on the Balian Low theorem [Sal67], that it is not possible to fulfill simultaneously the following conditions :

- the prototype function $g_T(t)$ and $g_R(t)$ are well-localized in time and frequency,
- the transmitted data symbols satisfy the complex orthogonality condition given in (2.1),
- maintain a symbol density $\rho = 1$.

In order to achieve the above mentioned objectives, it is possible to restrict the orthogonality condition to the real domain. In this case and over a distortion-free propagation channel, it is possible to recover the data at the receiver side when real-valued (or purely imaginary) PAM constellation symbols are transmitted, instead of QAM symbols. With this solution and in order to maintain a symbol density equal to 1, we should transmit two real-valued symbols per unit area of the time-frequency lattice. One of the pioneering solution, fulfilling the Balian Low theorem, and called FBMC-OQAM (FBMC based on transmitting Offset-QAM symbols), was proposed by Saltzberg [Sal67] in the mid 1960s. With this modulation, the orthogonality condition is restricted to the real domain and the prototype filter : $g(t) = g_T(t) = g_T(-t)$ is designed such as, over distortion free propagation channel, we have :

$$\Re\left[\int_{\mathbb{R}} g(t - mT/2) e^{j2\pi kt/T} e^{j(m+k)\pi/2} g^*(t - m'T/2) e^{-j2\pi k't/T} e^{-j(m'+k')\pi/2} dt\right] = \delta_{m,m'}\delta_{k,k'} \tag{2.2}$$

WFs with orthogonality in $\mathbb{C}$	WFs with orthogonality in $\mathbb{R}$	WFs without orthogonality
• CP-OFDM • WOLA-OFDM • UFMC • Filtered-OFDM • N-continuous OFDM • FMT	• FBMC-OQAM • Lapped-OFDM-OQAM • WCP-COQAM	• FBMC-QAM • GFDM

Table 2-1: Classification of the WFs candidates based on the orthogonality condition

where,$\Re[.]$ is the real part operator.

It has also been demonstrated that the FBMC-OQAM based WFs are more robust, than the OFDM based counterparts, to users asynchronism [MTLR+11]. This criterion was highlighted to be fundamental in the WONG5 project context as stressed in deliverable D1.2. However, the concept of transmitting real data instead of complex one, makes more complex the MIMO adaptation of the OQAM based techniques due to the high level of inherent interference brought by the prototype filter as well as channel estimation schemes. For these reasons, other solutions have been proposed in order to optimize the prototype filter response and transmitting complex QAM symbols rather than real ones. It is straightforward that, with such FBMC transmission technique, the orthogonality condition given by equation 2.2 is no more valid.

In Table 2-1 we have classified the different WFs candidate for the physical layer of the future 5G C-MTC networks based on the orthogonality condition.

In the following sections we will describe and study all the WFs listed in Table 2-1.

2.2 WF with complex orthogonality

2.2.1 CP-OFDM

CP-OFDM is the most well documented multicarrier waveform. It is widely used in several wireless standards (e.g. IEEE 802.11. a/g/n and 3GPP-LTE). It consists of splitting up of a stream of complex symbols at high-rate into several lower-rate streams transmitted on a set of orthogonal subcarriers which are implemented using the inverse fast Fourier transform (IFFT). The OFDM transmitted signal can be written as,

$$\underbrace{\mathbf{x_n}}_{[N\times 1]} = \underbrace{\mathbf{F^{-1}}}_{[N\times N]} \underbrace{\mathbf{s_n}}_{[N\times 1]} \tag{2.3}$$

where, $\mathbf{F^{-1}}$ and $\mathbf{s_n}$ stand for the $N \times N$ IFFT matrix and a $N \times 1$ vector of complex input data symbols, respectively.

Accordingly, as illustrated in Figure 2-1, the OFDM receiver can be implemented using the fast Fourier transform (FFT). In order to keep the orthogonality between subcarriers, a cyclic

prefix (CP) is usually inserted transforming thus the linear channel convolution into circular convolution if the CP is longer than the channel impulse response. Therefore, after the FFT operation, the channel equalization becomes trivial through a single coefficient per subcarrier.

2.2.2 WOLA-OFDM

The weighted overlap and add (WOLA) could be applied to CP-OFDM to obtain WOLA-OFDM. WOLA was initially introduced in [Qua] by Qualcomm Incorporated and has been studied in [ZMSR16] with OFDM in asynchronous 5G scenario.

In the WOLA transmitter process, a time domain windowing operation is performed producing thus soft edges at the beginning and the end of original transmitted block. These soft edges are added to the cyclic extension of the OFDM symbol of length $N_s = N$. Indeed, the smooth transition between the last sample of a given symbol and the first sample of the next symbol is provided with point-to-point multiplication of the windowing function and the symbol with cyclic prefix and cyclic suffix (see Figure 2-2). The samples corresponding to CP (of size CP) from the last part of a given symbol are copied and appended to its beginning. Besides, the first W_{Tx} samples of the symbol are added to the end, corresponding to the cyclic suffix. Thus, the WOLA-OFDM time domain symbols are cyclically extended from N_s samples to $N_s + CP + W_{Tx}$.

After the cyclic extensions insertion, a window of length $L = N_s + CP + W_{Tx}$ samples is applied. In fact, many windowing functions have been studied and compared [BT07] in terms of enhancing side lobe suppression. Straightforward solution is to define edge of the time domain window as a root raised-cosine (RRC) pulse. In this report, we consider the Meyer-RRC pulse combining the RRC time domain pulse with the Meyer auxiliary function [GMM$^+$15].

In addition to the transmit windowing, which is used to improve the spectral confinement of the transmitted signal, the WOLA processing is also applied at the receiver side in order to enhance asynchronous inter-user interference suppression, as illustrated in Figure 2-3. Note that the applied receive window is independent of the transmit one and its length is equal to $N_s + 2W_{Rx}$. This windowing is followed by Overlap and Add processing which minimizes the effects of windowing on the useful data. As shown in Figure 2-3, it is worth emphasizing that the first window part $[0, 2W_{Rx}]$ applied at the receiver must be symmetrical w.r.t the point $(W_{Rx}, \frac{1}{2})$, in order to correctly recover the weighted samples.

2.2.3 UFMC (UF-OFDM)

Universal Filtered MultiCarrier (UFMC) has recently been proposed by Alcatel-Lucent Bell Laboratories [VWS$^+$13], and it is also referred to UF-OFDM in the literature [WSC14]. The block diagram of UFMC is depicted in Figure 2-4. UFMC is a combination of ZP-OFDM (traditional CP-OFDM where the CP is replaced by a Zero Padding (ZP)) and filtered-OFDM which is further detailed in Section 2.2.4: each OFDM symbol at the output of the IDFT is filtered and the ZP is used to absorb the filter transient response. In the absence of a multipath channel, UFMC holds the orthogonality of the subcarriers. Nevertheless, the orthogonality is no longer sustained as the time spreading of the channel increases and only soft protection against multipath effects is possible at the receiver. At the reception, the multiuser interferences coming from time and frequency asynchronism are first reduced by applying a window on the received UFMC block symbols [SW14a]. This windowing is similar to the one used for WOLA-OFDM. It has to be noted that this processing destroys the subcarrier orthogonality even if the channel is perfect. Finally a FFT of size two times greater than the IFFT used at the transmission is

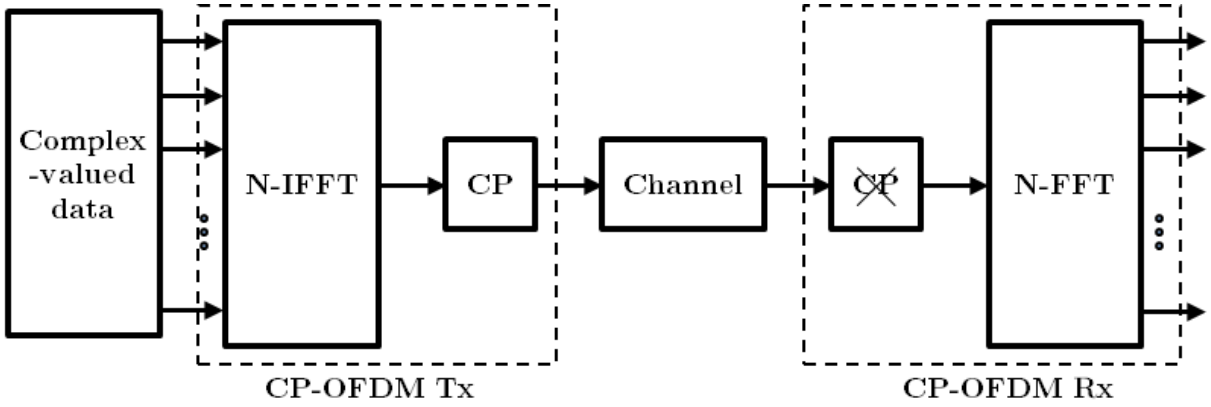

Figure 2-1: CP-OFDM transceiver

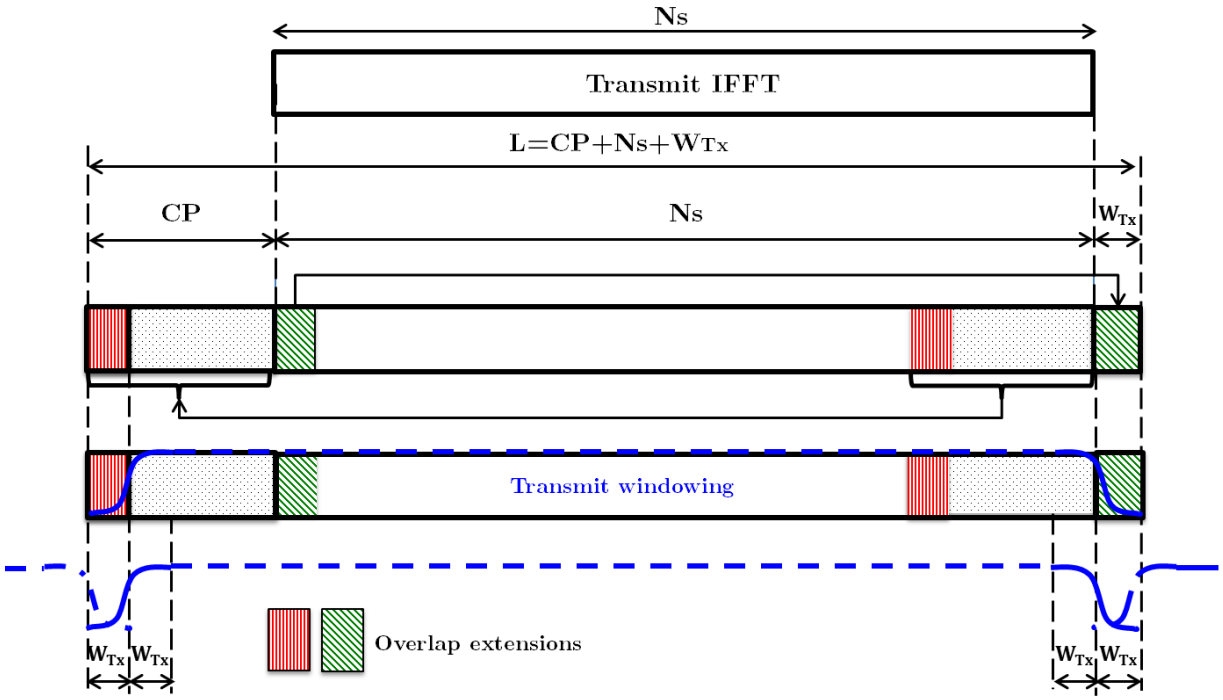

Figure 2-2: WOLA processing: Transmitter side

applied to the received UFMC block symbols and only even subcarrier indexes are kept. It is important to note that the complexity of the receiver can be reduced by collecting additional samples corresponding to the length of the ZP and using an overlap-and-add method to obtain the circular convolution property [MWG+02]. In this case, the required FFT size is identical to the size of the IFFT used at the transmission. All existing and already developed OFDM-based designs are applicable to UFMC such as MIMO, channel estimation/equalization, pilot, synchronization, PAPR reduction (DFT precoding or any others approaches).

The filter is predefined and set to reduce the out of band radiation of a single resource block composed of 12 subcarriers. Any bandpass filter that covers the subcarriers of the user of interest may be used. The Dolph-Chebyshev filter has been initially proposed [VWS+13] because it provides a good trade-off between filter length and out of band reduction. However other choices are also possible [WWS15, WWSdS14], for instance methods to design filters that provide improved robustness to carrier frequency offset (CFO) and timing offset (TO) also have been reported.

The main similarities and differences between UFMC and filtered-OFDM are provided in the next Section.

2.2.4 Filtered-OFDM

Filtered-OFDM (f-OFDM) has been recently proposed as a 5G candidate at the 3GPP RAN1 workgroup [AJM15, HiS16]. This scheme is based on traditional CP-OFDM and follows a pragmatic approach (see Figure 2-5) to overcome problems raised by the use of asynchronous communications for which traditional CP-OFDM is known to provide poor performance:

- At the transmission, the poor out-of-band radiation of traditional CP-OFDM is improved using a filter at the output of a CP-OFDM transmitter,

- At the reception, the interferences coming from time and frequency asynchronous adjacent users are lowered thanks to the filtering (signal of interest is supposed to be centered at 0 Hz) at the input of a CP-OFDM receiver.

The advantage of f-OFDM is to keep traditional CP-OFDM as its core waveform at both transmission and reception. All existing and already developed OFDM-based designs are applicable to f-OFDM such as MIMO, channel estimation/equalization, pilot, synchronization, PAPR reduction (DFT precoding or any others approaches). In addition, an important advantage of f-OFDM is to enable the co-existence of different time-frequency granularities (i.e. numerologies), such as different subcarrier spacings, cyclic prefix sizes, burst lengths, ...

The filtering process required by the f-OFDM scheme introduces some drawbacks such as complexity, potential inter block interference and an increase of the burst length and consequently an increase of the latency. This issues are respectively addressed in sections 2.2.4.1 and 2.2.4.2.

UFMC (also called UF-OFDM) and f-OFDM have in common the use of a low pass filter applied to a group of subcarriers, nevertheless these two schemes have important differences which are summarized below:

- A ZP is used in UFMC whereas a CP is used in f-OFDM.

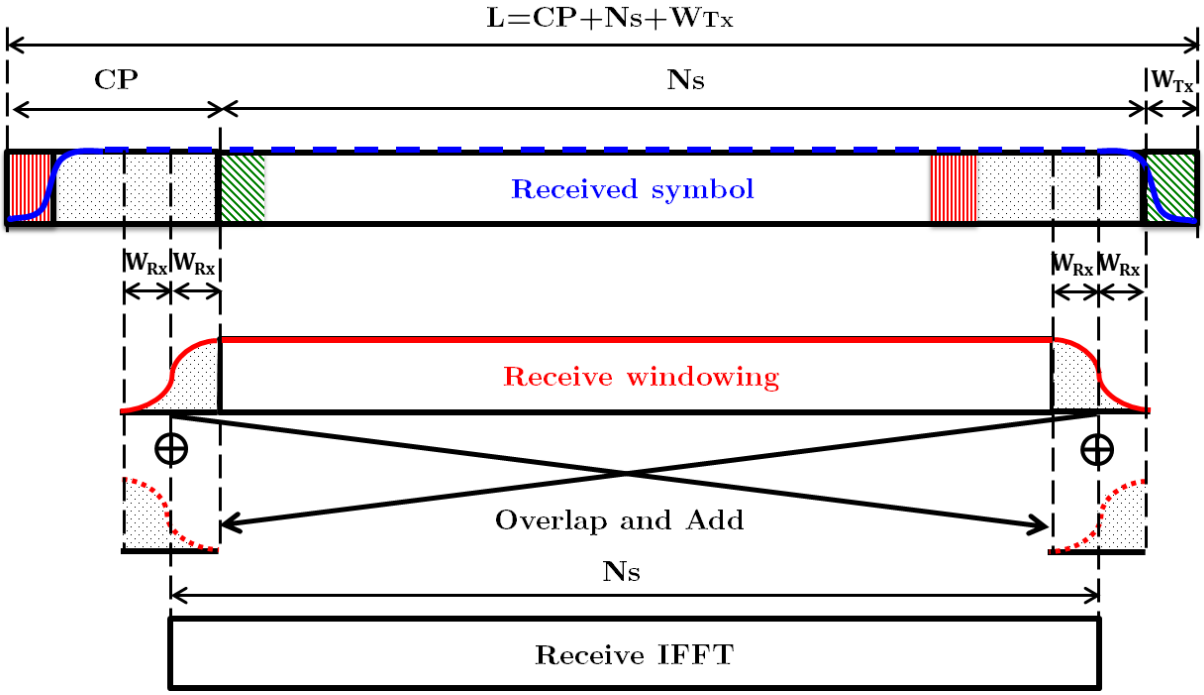

Figure 2-3: WOLA processing: Receiver side

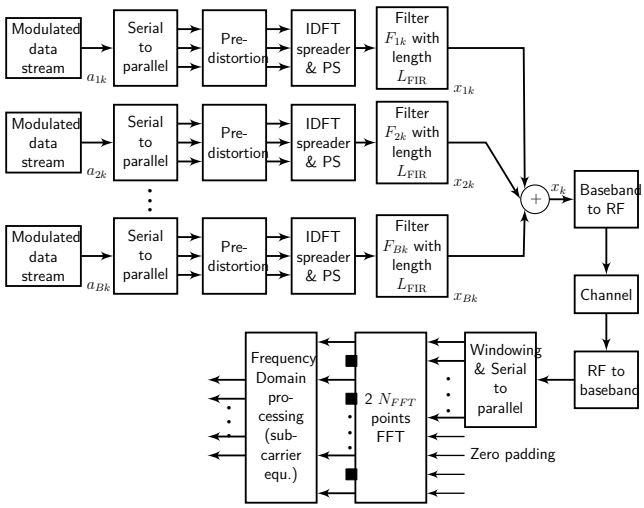

Figure 2-4: Block diagram of UFMC Tx and Rx processing [SW14b].

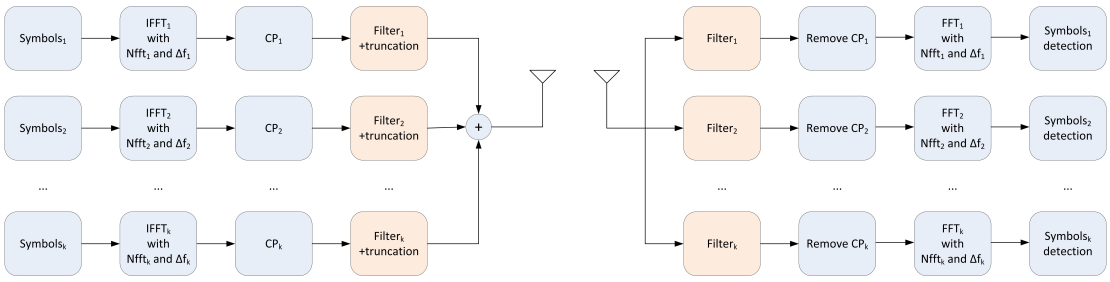

Figure 2-5: Block diagram of f-OFDM Tx and Rx processing.

- UFMC limits the filter length to the size of the ZP. If the channel is perfect (no multipath and noise) then perfect reconstruction of the transmitted signal is possible. However, if the channel has a delay spread greater than 1 sample duration then inter-symbol interference is present at the receiver. The filter length of f-OFDM is usually greater than the size of the ZP leading to systematic (but reasonable) inter block interference.

- UFMC receiver limits the interferences due to unsynchronized users thanks to the use of a time windowing technique before FFT processing. In f-OFDM, the interferences are limited thanks to the use of a filter at the receiver (similar to the one used at the transmitter).

- The filter used for UFMC is fixed and its bandwidth covers a fixed group of subcarriers (one resource block, namely 12 subcarriers). If a user uses more than one resource block then multiple signal generations and summation are required. For f-OFDM, the filter is adapted (on-line, or off-line if pre-computed) to the number of subcarriers used by a user.

2.2.4.1 Filter Design

The filter used for f-OFDM has to satisfy the following criteria [HiS16]:

1. The pass-band of the filter should be as flat as possible over the subcarriers contained in the subband. This ensures that the distortion of the filter on the data subcarriers, especially the subband edge subcarriers, is minimal.

2. The frequency roll-off of filter should start from the edges of the pass-band and also the transition band of the filter should be sharp. This ensures the system bandwidth is utilized as efficient as possible, i.e. with minimal guard band overhead. Also, the neighboring subband signals with different numerologies can be placed next to each other in frequency with minimal number of guard subcarriers.

3. The filter should have enough stop-band attenuation to ensure that the interference leakage between the neighboring subbands is negligible.

A filter design example that can achieve a reasonable balance between frequency- and time-localization is presented in [HiS16]. The filter design is based on soft truncation of a prototype filter using a time-domain window with smooth transitions. A *sinc* function is first generated:

$$p_B(n) = sinc\left([W + 2 \cdot \partial W] \cdot \frac{n}{N}\right) \tag{2.4}$$

where W is the number of assigned subcarriers, ∂W is a small excess bandwidth or tone-offset, $n = [-L/2 : +L/2]$ is the time index, L is the filter length and N is the IFFT size.

Then the normalized lowpass filter coefficients are given by:

$$f_B(n) = \frac{p_B(n) \cdot w(n)}{\sum_n p_B(n) \cdot w(n)} \tag{2.5}$$

where $w(n)$ is a window function defined as:

$$w(n) = \left[\frac{1 + \cos(\frac{2\pi n}{L-1})}{2}\right]^{0.6} \tag{2.6}$$

Finally, and if required, the bandpass filter coefficients $f'_B(n)$ are obtained by shifting the lowpass filter to appropriate central frequency f_0, which is the central frequency of the assigned data subcarriers in the baseband:

$$f'_B(n) = f_B(n) \cdot \exp^{-j\frac{2\pi n f_0}{N\Delta f}} \tag{2.7}$$

where Δf is the subcarrier spacing.

Complexity issue

Both time-domain and frequency domain implementation of filtering are possible. The complexity of frequency-domain implementation techniques such as overlap-and-save (OLS) or overlap-and-add (OLA), is lower than time-domain, since they use cost-efficient FFT/IFFT, which are insensitive to the number of filter taps.

Interblock interference

An example of the impact of the Tx filtering on traditional CP-OFDM is presented in Figure 2-6. We can observe that a filter length greater than the CP length generates interblock interferences even if an ideal channel is considered. Nevertheless, most of the filter energy is concentrated into a small portion of samples (much less than the CP length) leading to reasonably small interblock interferences. Furthermore, a well-designed filter has an almost-flat frequency response over the entire subband's bandwidth (including the edge subcarriers) at both Tx and Rx. Therefore, majority of subcarriers within the subband will not get impacted by the Tx and Rx filterings and thus will not experience any time-spread due to the filtering. It is the side lobe suppression of only few edge subcarriers that will cause a minor time-spread, which is much smaller than the CP length. Therefore, the effective CP length to combat the multipath channel's delay spread is reduced negligibly due to the end-to-end subband filtering.

2.2.4.2 Burst Truncation

The length of a f-OFDM burst which has not been truncated could have long ramp-up and ramp-down time shaping, increasing the overhead and the latency (see Figure 2-7). To solve this issue, a pragmatic approach consists in hard truncating (at the beginning and the end of the burst) with an appropriate length in order to reduce the burst size (see Figure 2-7). Indeed, the original f-OFDM signal burst tails are very well localized in time, thus truncation provides reasonable increasing of out-of-band emission. Both simulations and [HiS16] show that a truncation length equals to half the CP length provides good performance in the case of a LTE scenario.

2.2.5 N-continuous OFDM

The N-continuous OFDM scheme has been introduced for the first time in [vdBB09b]. Basically, the idea consists in creating consecutive adjacent OFDM symbols which are continuous in the time domain in order to improve the poor out of band radiation of traditional CP-OFDM. The construction of OFDM symbols will render the transmitted signal $s(t)$ and its first N derivatives continuous using a precoding matrix which is placed between the symbol mapping and the IFFT

(see Figure 2-8). Similarly to f-OFDM, one advantage of N-continuous OFDM scheme is to have traditional CP-OFDM as its core waveform at both transmission and reception.

Nevertheless, in its basic form, this scheme requires the transmission of side information (precoding matrix) to the receiver in order to recover the data. A solution to cope with this problem has been proposed in [vdBB09a] and consists in using a systematic precoding matrix at the price of an increase of the transmitted signal quality (e.g. Error Vector Magnitude (EVM)).

2.2.6 FMT

Filtered multitone (FMT) is a multicarrier modulation technique that has been specifically developed for DSL applications [CEOC00] In FMT, a conventional method of frequency division multiplexing is used, i.e. the subcarrier bands are juxtaposed. Each band can be seen as a traditional single carrier modulation which respects the Nyquist criteria (Figure 2-9). It is well known that the optimal repartition (in terms of Signal to Noise Ratio at the demodulation input) of the Nyquist filter is a square-root Nyquist filter at both emission and reception sides.

Square root Nyquist filters limit the effective transmission bandwidth of each band to $B = (1 + \alpha) \cdot F_s$, where F_s is the sampling frequency and α is the excess bandwidth coefficient (also called roll off factor). The use of a $\alpha > 0$ can be seen as suboptimal since the spectral efficiency decreases by the same amount. One can imagine that small α is a good solution, but the time/frequency duality requires large square root Nyquist filter length which drastically increases the latency and the overhead. Some recent works have proposed new filters [Tra16] in order to cope as much as possible with this problem providing a good compromise between out of band radiation and group delay. FMT transmitter and receiver can be efficiently implemented using polyphase filter and (I)FFT [HDR03] (see Figure 2-10) only if the spacing between subcarrier is fixed (which is usually the case).

2.3 WF with real orthogonality

2.3.1 FBMC-OQAM

Despite the large success of CP-OFDM as the multicarrier benchmark, it has to deal with the many requirements envisaged in future generation physical layer. Indeed, the capability of using non-contiguous spectrum with a relaxed synchronization are the main challenges of the desired future waveform that OFDM cannot fulfill. In fact, the poor localized frequency response of rectangular transmit filter of CP-OFDM induces high level of Out-Of-Band (OOB) radiation. Besides, the rectangular receive filter also brings an important amount of interference from other asynchronous users [FBM16]. In order to overcome the main OFDM shortcomings, Filter-Bank based MultiCarrier (FBMC) systems have been proposed as an alternative to OFDM offering better frequency localization and flexible access to the available resources.

The key-idea of FBMC is to use well-frequency localized prototype filters (like PHYDYAS [VIS+09] and IOTA [LFAB95]), instead of the OFDM rectangular one, providing thus better adjacent channel leakage performance compared to OFDM. In order to ensure orthogonality between adjacent symbols and adjacent subcarriers, while keeping maximum spectral efficiency, Nyquist constraints on the prototype filter combined with Offset Quadrature Amplitude Modulation (OQAM) are used. As shown in Figure 2-11, in OQAM, the in-phase and the quadrature components of a given QAM symbol are time staggered by half a symbol period, $N/2$ (i.e. $T/2$). The duration of the prototype filters is usually a multiple of the FFT size ($L = KN$), where K is called the overlapping factor.

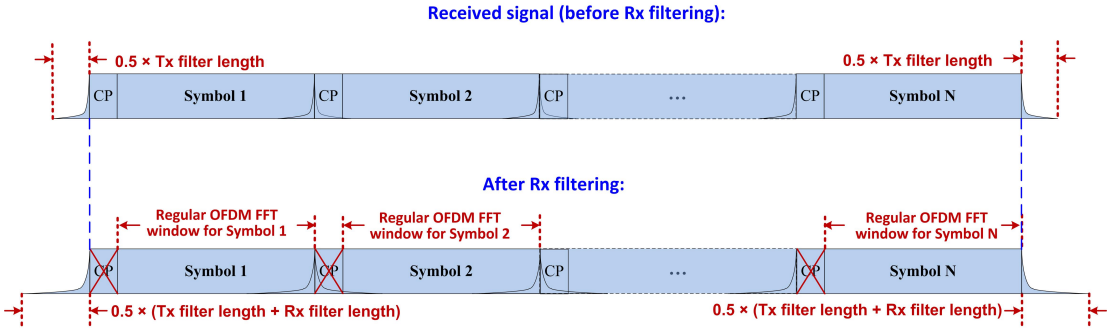

Figure 2-6: Impact for f-OFDM of filtering on transmitted (up) and received (down) bursts [HiS16].

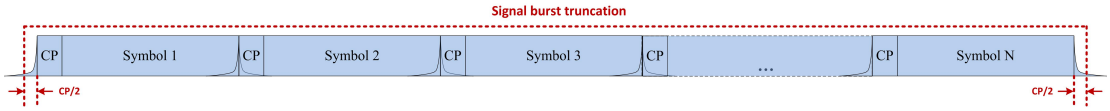

Figure 2-7: Burst truncation for f-OFDM [HiS16].

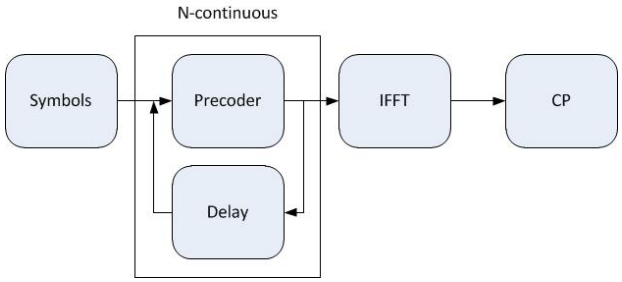

Figure 2-8: Block diagram of N-continuous OFDM scheme.

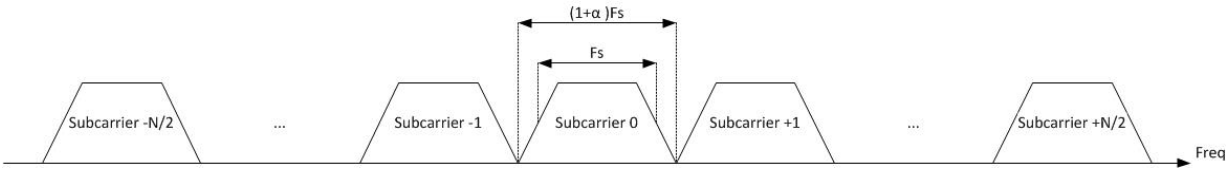

Figure 2-9: Frequency representation of FMT scheme.

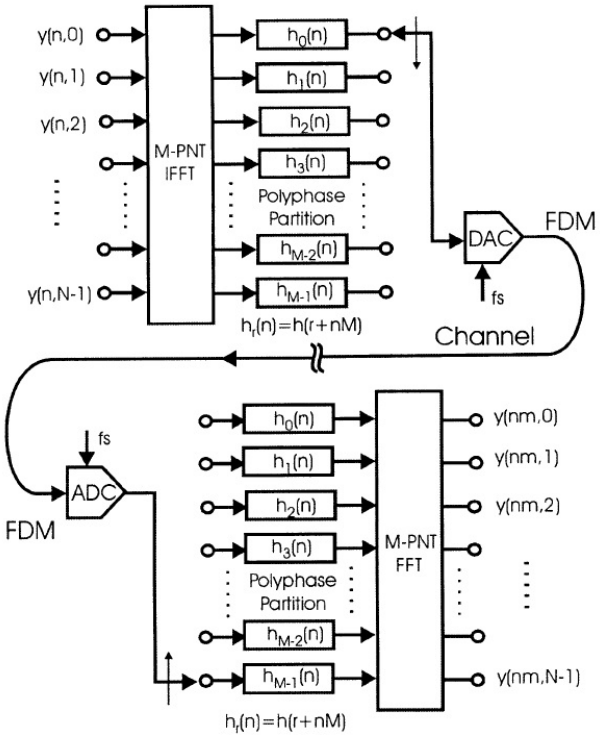

Figure 2-10: Efficient Polyphase and (I)FFT implementation of FMT scheme [HDR03].

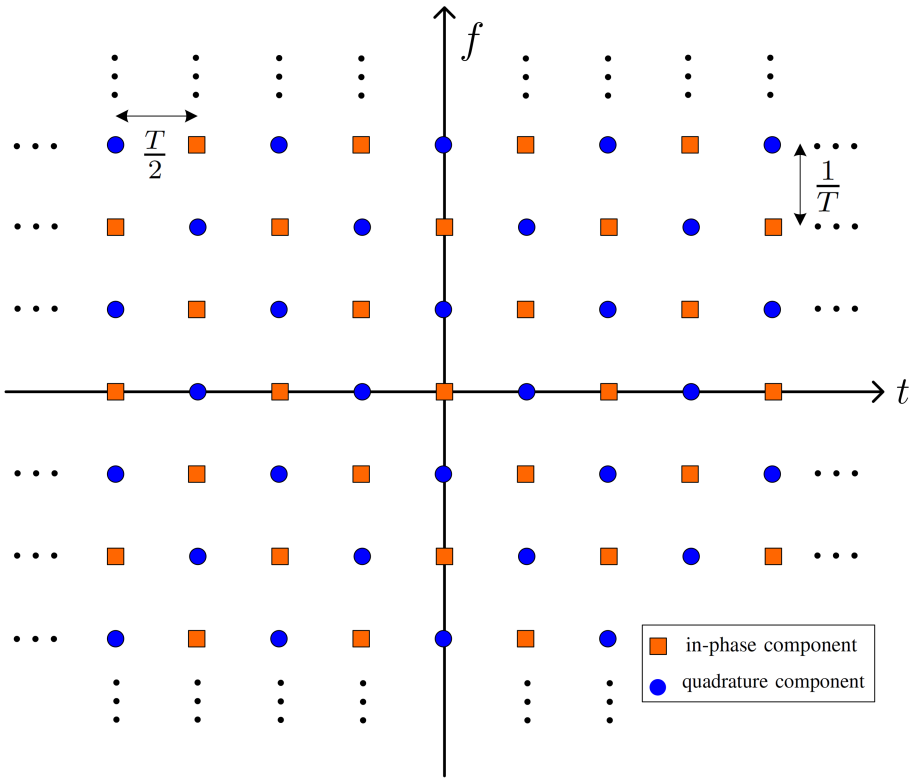

Figure 2-11: Time-frequency phase-space lattice representation of OQAM modulation

In the literature, we distinguish two architectures of FBMC system:

- PPN-FBMC (PolyPhase Network-FBMC): In this case, the transmitter (also called Synthesis Filter Bank) is implemented by an N-IFFT followed by the polyphase decomposition of the prototype filters. Similarly to the transmitter, the implementation of the receiver (also called Analysis Filter Bank) relies on cascading polyphase network with N-FFT. Interested readers are referred to [Med12] for more details.

- FS-FBMC (Frequency Spreading-FBMC):In this document, we focus on this implementation technique which is shown in Figure 2-12.

Using OQAM modulation, the real-valued input symbols are phase-shifted by multiples of $\pi/2$ along both time and frequency axis. The pre-processed data is then filtered in the frequency domain (i.e. Frequency spread filtering). Actually, since FBMC prototype filters are usually designed by applying the frequency sampling technique, the number of non-zero samples in the frequency response is given by $P = 2K-1$ i.e. the number of multicarrier symbols which overlap in the time domain [Bel12]. An example of the Frequency spread filtering is illustrated in Figure 2-13 when the overlapping factor is $K = 4$.

For each N input data symbols, we obtain KN samples at the output of FS-filtering that are then fed to an KN-IFFT. Note that, for each block of N real-valued symbols, we obtain at the output of the IFFT a block of KN samples. Following the OQAM principle, a delay of $N/2$ (i.e. $T/2$) is introduced between two successive blocks as displayed in Figure 2-14. At a given time, the block of interest will be added to $K-1$ previous blocks and $K-1$ next blocks. This operation is called overlap&sum which is equivalent to a sliding window that selects KN samples in the time domain every $N/2$ samples [BDN14]. Note that the resulting FBMC signal is identical to the one synthesized by a PPN-FBMC.

As shown in Figure 2-15 and following the overlap-&-sum operation performed at the transmitter, the FS-FBMC receiver applies a KN-FFT on KN samples of the received signal every $N/2$ sample-period. Similar to the FS-filtering applied at the transmitter, the matched filtering is done in the frequency domain. Note that in the presence of channel, the equalization is combined with the frequency domain matched filtering. More precisely, in order to obtain the data symbol transmitted on the m-th subcarrier, the $2K-1$ FFT-outputs with indices $(m-1)K+1:1:(m+1)K-1$ are, respectively, weighted by the following coefficients: $\{G_k H_{k'}, k \in [K-1:-1:0] \cup [1:1:K-1], k' \in [(m-1)K+1:1:(m+1)K-1]\}$ and summed where G_k denote the frequency response of the prototype filter and $H_{k'}$ stands for the k'-th the channel frequency response. It is worth emphasizing that the main advantage of FS-FBMC receiver is that no additional delay is required for channel equalization, in contrast to the per-subcarrier multi-tap equalization.

2.3.2 Lapped-OFDM

Actually, the lapped-OFDM waveform is an FBMC-OQAM system with a particular prototype filter. Its name is derived from the lapped orthogonal transform defined by [BMT15]:

$$T(n,k) = h(n)\cos\left[\left(n-\frac{1}{2}+\frac{N}{2}\right)\left(k-\frac{1}{2}\right)\right], 1 \le n \le 2N, 1 \le k \le N \tag{2.8}$$

$$h(n) = -\sin\left[\left(n-\frac{1}{2}\right)\frac{\pi}{2M}\right] \tag{2.9}$$

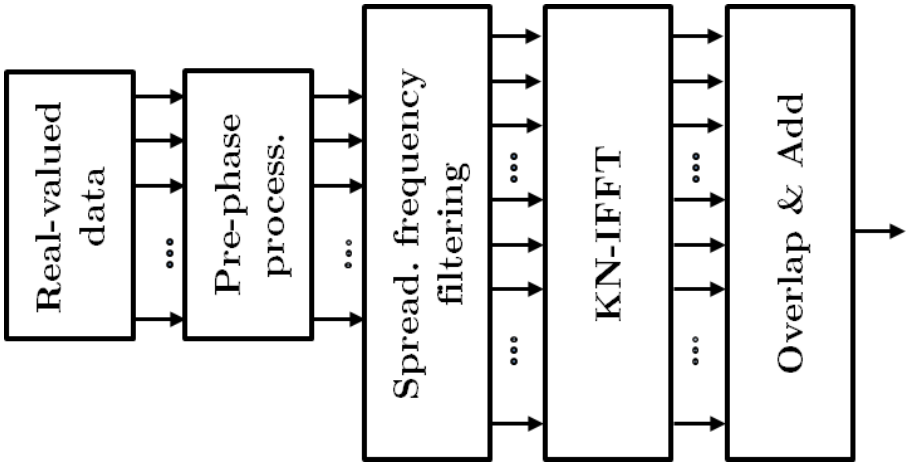

Figure 2-12: FBMC-OQAM transmitter: FS implementation

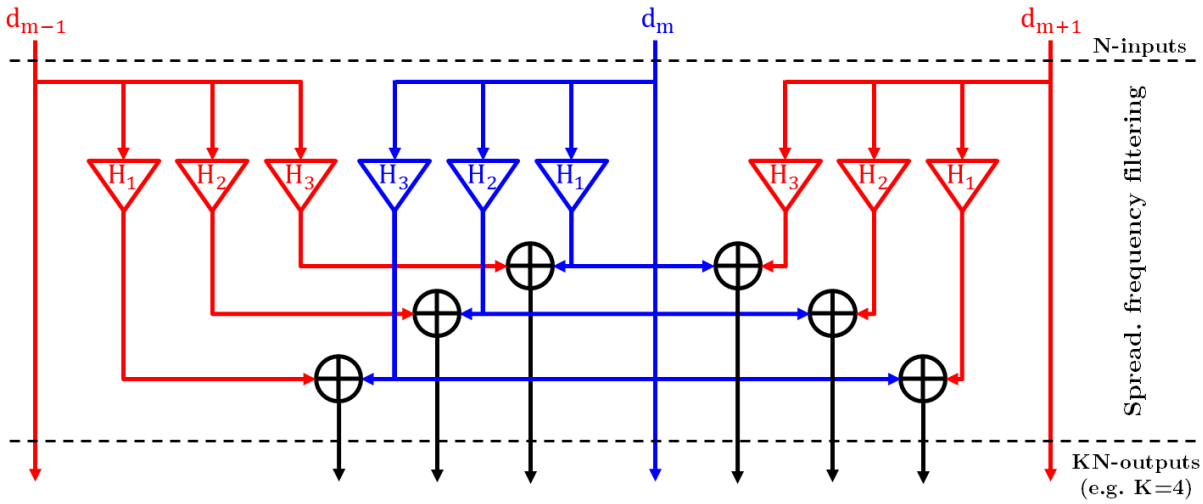

Figure 2-13: Frequency spread filtering

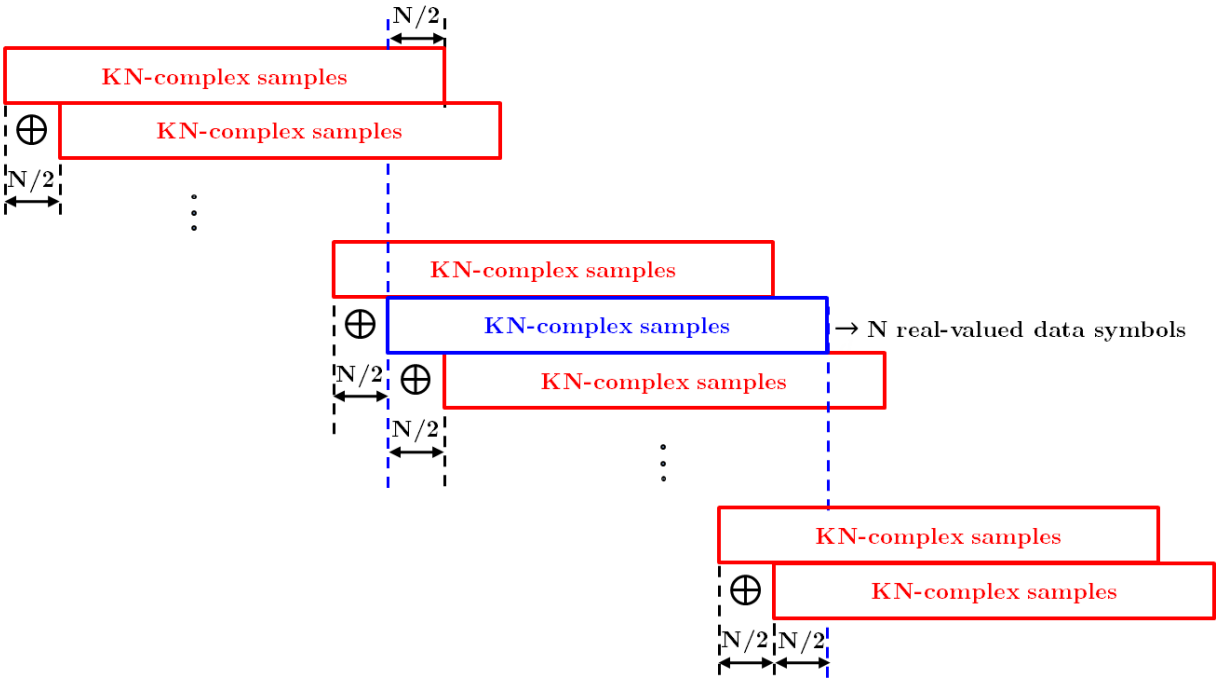

Figure 2-14: FBMC-OQAM transmitted signal

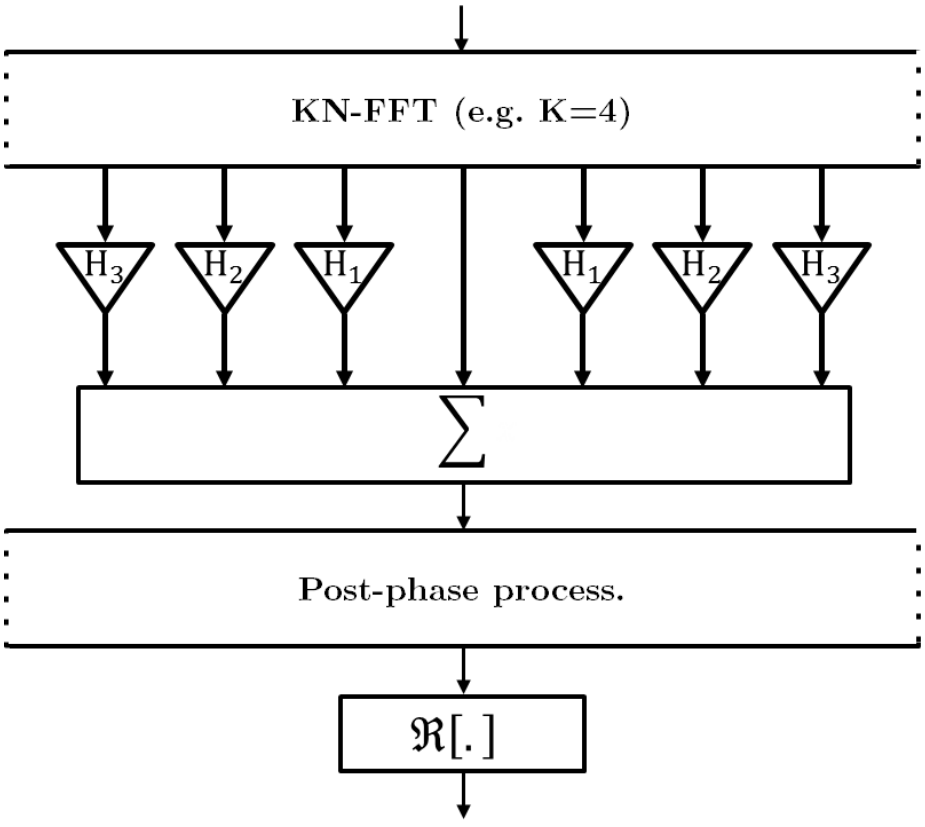

Figure 2-15: FBMC-OQAM receiver: FS implementation

After some algebraic manipulations, the lapped transform can be implemented with a $2N$-FFT followed by a sine filter having the 2 coefficients $[1, -1]$ [BMT15]. As in any FBMC-OQAM system, the input data must be phase-shifted by multiples of $\pi/2$.

Since PHYDYAS is the prototype filter that is widely used in the literature, it is wise to compare lapped-OFDM to PHYDYAS-FBMC-OQAM (referred in this document as FBMC-OQAM) in terms of:

- Time response: Looking at Figure 2-16-(a), one can see that, in contrast to PHYDYAS which is defined on $L = 4N$ sample periods, the lapped-OFDM filter is defined on a shorter duration $L = 2N$. In other works, the overlapping factor of lapped-OFDM is $K = 2$, instead of $K = 4$ in PHYDYAS case.

- Frequency response: Since PHYDYAS filter is longer than lapped-OFDM one, FBMC-OQAM frequency response is more localized compared Lapped-OFDM one. Actually, the latter decreases as $1/f^2$, instead of $1/f$ for OFDM rectangular filter [BMT15] (see Figure 2-16-(b)).

- Transceiver impulse response: In the time axis, the filter response spreads over $(2K - 1)\, N/2$ sample periods. Accordingly, as shown in Figure 2-17, one can see that the lapped-OFDM response is more localized in the time domain compared to FBMC-OQAM (spreads over $3N/2$ sample periods, instead of $7N/2$ in PHYDYAS). However, it spreads on higher number of subcarriers in comparison to FBMC-OQAM (more than 9 subcarriers, instead of 3 subcarriers in PHYDYAS case). It is also worth pointing out the fact that lapped-OFDM achieves a perfect reconstruction instead of a near perfect reconstruction in PHYDYAS case. In other words, the lapped-OFDM response is free of real-valued intrinsic interference while some negligible real-valued interference terms can be found in the FBMC-OQAM transceiver response (see Figure 2-17).

As aforementioned, note that FBMC-OQAM and lapped-OFDM belong to the same waveform class with two different prototype filters (PHYDYAS for FBMC-OQAM and Sinus for Lapped-OFDM).

2.3.3 WCP-COQAM

Despite the various advantages of FBMC systems, the long prototype filters could be questionable for low-latency communications [SWC14]. Besides, FBMC signals are not suitable to short packet transmission due to long ramp-up/down of FBMC signal leading thus to a non-negligible loss in spectral efficiency. In order to overcome this situation, burst truncation can reduce this loss but it has detrimental effects like additional interference and significant OOB radiation [Bel10]. Circular convolution with time-windowing was proposed in [AJM13], [LS14] to remove the overhead signal while maintaining smooth transition at the burst edges. This solution is known as Windowed Cyclic Prefix-based Circular-OQAM (WCP-COQAM). This section is devoted to describe the built-in properties of this waveform. The WCP-COQAM signal construction process consists of the following steps:

- Circular convolution:

The circular-OQAM (COQAM) signal, defined in a block interval $m \in [0, KN-1]$, is expressed as,

$$x_{\mathrm{COQAM}}[m] = \sum_{n=0}^{N-1} \sum_{k=0}^{2K-1} a_k[n]\, \tilde{g}(m - kN/2)\, e^{j\frac{2\pi}{N}n\left(m-\frac{D}{2}\right)} e^{j\phi_{n,k}}, \tag{2.10}$$

where, the filter $\tilde{g}$ stands for circular convolution (see Figure 2-18) with the prototype filter g of length $KN = D+1$. More precisely, $\tilde{g}$ is obtained by the periodic repetition of duration KN of g [LS14], so that,

$$\tilde{g}(m) = g(mod[m, KN]) \tag{2.11}$$

Note, that the prototype filter g is originally designed for FBMC-OQAM systems. This means that the input data symbols $a_k[n]$ are real-valued, since the orthogonality only applies to the real field. The phase term $\phi_{n,k}$ at subcarrier n and symbol index k can be expressed as $\frac{\pi}{2}(n+k)$. It is introduced on both transmitter and receiver side, in order to make the intrinsic interference purely imaginary-valued thus orthogonal to the useful data which is real-valued.

- CP add and Time-windowing:

In order to avoid multipath channel interference, a CP can easily be inserted since COQAM corresponds to a block transform [LS14]. Thanks to circular convolution, the continuity of CP-COQAM signal is maintained inside a given CP-COQAM block (See Figure 2-18). However, since signal discontinuities can be observed between different CP-COQAM blocks, there is no remarkable difference between the CP-COQAM spectrum and CP-OFDM one [FBM16]. Note that this behavior is independent of how well is localized the prototype filter frequency response. Accordingly, a windowing is necessary to reduce the significant OOB radiation induced by inter-block discontinuities. Therefore, the resulting WCP-COQAM block ($KN + CP$ samples) can be derived from the COQAM (KN samples) one by,

$$x_{\mathrm{WCP-COQAM}}[m] = x_{\mathrm{COQAM}}[mod(m - CP, KN)] \times w[m] \tag{2.12}$$

where the coefficients $w[m]$ are computed based on the windowing function $f(m)$,

$$w[m] = \begin{cases} f(m), & m = 0, ..., 2W_{\mathrm{Tx}} - 1 \\ 1, & m = 2W_{\mathrm{Tx}}, ..., KN + CP - 2W_{\mathrm{Tx}} - 1 \\ w(KN + CP - 1 - m), & \text{otherwise} \end{cases} \tag{2.13}$$

In the receiver side, the CP is removed, windowed samples are compensated and the receive circular convolution is applied afterwards. The OQAM decision is then made to recover the desired useful data symbols. Interested readers are referred to [LS14] for more details.

2.4 WF without orthogonality

2.4.1 FBMC-QAM

As previously discussed, filter-bank based waveforms use a per-subcarrier filtering, reducing thus out-of-band emission and providing more flexibility to meet the future physical layer requirements. As emphasized earlier, such enhancements are at the price of orthogonality condition

Table 2-2: Samsung Type-I vs. PHYDYAS:

Freq. coeff.	**PHYDYAS**	**Samsung Type-I**
G_0	1	1
G_1	0.971960	$-0.6901 + 0.9051i$
G_2	$\sqrt{2}/2$	$+0.2041 - 0.5234i$
G_3	0.235147	$-0.0140 + 0.0472i$
self-SIR	7.5dB	10.6dB

that only holds in the real domain and is no longer valid in the presence of practical channels. Indeed, the self-interference inherent to OQAM-based schemes can be as strong as the useful signal power [BLRR+10], [ZLRM12]. This is a major problem when considering spatial multiplexing with maximum likelihood detection [ZR14]. In fact, the proposed iterative interference cancellation schemes are limited by error propagation induced by the residual interference signal. In order to overcome this problem, it has been demonstrated, in [AS97] and [VBRB06], that the interference power must be small and should be kept under a certain threshold, in order to counteract the error propagation phenomenon and consequently make more efficient the interference cancellation scheme. In order to achieve this objective and reduce the interference level, the authors in [ZLRM12] were the first to propose the utilization of QAM modulation, instead of OQAM one, in FBMC systems. Actually, a significant part of self-interference is avoided by only transmitting QAM symbols every signalling period $nT, n \in \mathbb{Z}$. In other words, the interference induced by OQAM symbols transmitted in $(2n+1)\frac{T}{2}, n \in \mathbb{Z}$ is no longer considered [ZR14]. Such a combination is called FBMC-QAM systems. In order to improve the performance of FBMC-QAM symbols, new prototype filters have been designed, optimizing simultaneously spectrum localization, self-interference level, and overall spectral efficiency [YKK+15]. In this report, we consider one of these prototype filters which is called 'Samsung Type-I'. In the Table 2-2, the frequency domain coefficients of the latter are compared to PHYDYAS ones [YKK+15]. As shown in the same table, the signal to interference (SIR) levels are also given, where Samsung Type-I outperforms PHYDYAS by a gain of 3dB.

In Figure 2-19, both PHYDYAS and Samsung Type-I frequency responses are depicted. One can see that Samsung Type-I is slightly more frequency localized in comparison to PHYDYAS. It is worth mentioning that, in contrast to PHYDYAS, the filter Samusung Type-I does not satisfy the Nyquist criteria.

2.4.2 GFDM

GFDM was introduced in 2009 by Vodafone Chair Mobile Communications Systems [FKB09] and is based on the time-frequency filtering of a data block, which leads to a flexible but non-orthogonal waveform. A data block is composed of K subcarriers and M time slots, and transmit N= KM complex modulated data. Each data is filtered by a filter that is translated into both frequency and time domains. Thus, as the symbols overlap both in frequency and in time, interference (between sub-symbols and between symbols) occurs. To avoid inter-symbol interference, a CP is added at the end of each symbol of size KM. The GFDM waveform is parametrized by its shaping filter, which is usually chosen to be a Root Raised Cosine (RRC) filter [MGK+12]. To further lower the ACL, a windowing process can be added in the transmission

stage. It however increases the interference level, that can be mitigated at the receiver stage with a tail-biting approach [FKB09]. Several receiver architectures can be used. In the litterature, two main receivers have been considered: the matched filter (MF) and the zero forcing (ZF) schemes [MKLF12]. In the MF approach, each received block is filtered by the same time and frequency translated filters as in the transmission stage. This approach has a low complexity but, as the modulation is non orthogonal, offers poor performance due to inter-subsymbol interference. It is thus necessary to implement an interference cancellation scheme [DMLF12], which improves the performance but severely increases the complexity of the receiver (as the IC scheme is based on the reconstruction of the a-priori transmitted GFDM signal). In the ZF approach, the signal is decoded with the pseudo-inverse of the transmitter matrix. The ZF-receiver does not introduce self-interference but suffers from noise amplification and its performance depends on the properties of the transmitter matrix [MGK$^+$12]. The GFDM transceiver is described in Figure 2-20. More recently, OQAM was also considered in GFDM to allow the use of less complex linear receivers instead of IC [GMM$^+$15].

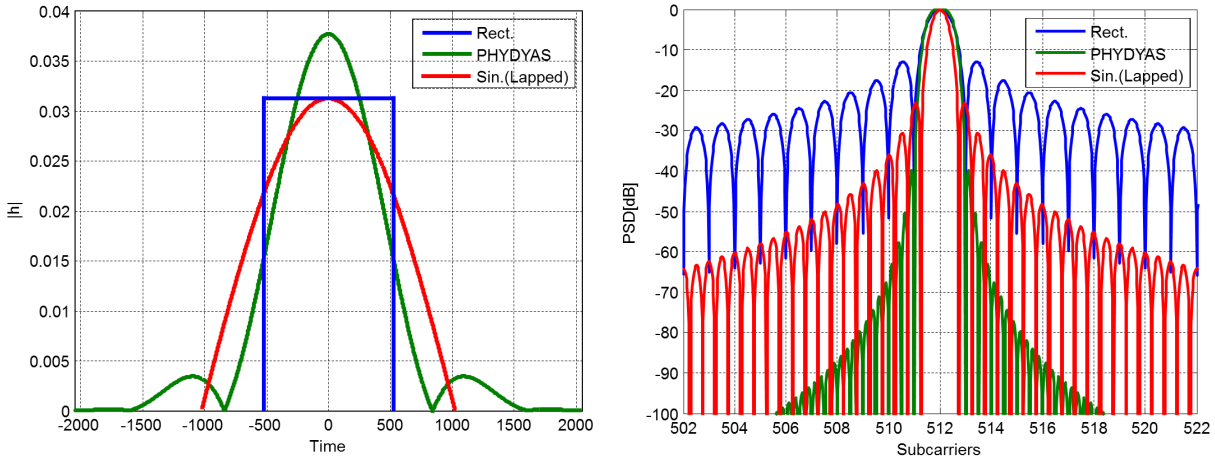

(a) (b)

Figure 2-16: Lapped-OFDM vs. PHYDYAS: (a) Time, (b) Frequency

Time

	n-1	n	n+1
m-4	- 0.021i	0	0.0212i
m-3	0	0	0
m-2	0.1061i	0	-0.106i
m-1	0.2500i	-0.5i	0.2500i
m	0.3183i	1	-0.318i
m+1	0.2500i	0.5i	0.2500i
m+2	0.1061i	0	-0.106i
m+3	0	0	0
m+4	- 0.021i	0	0.0212i

Frequency

(a)

Time

	n-3	n-2	n-1	n	n+1	n+2	n+3
m-1	0.043i	0.125i	0.206i	0.239i	0.206i	0.125i	0.043i
m	0.067i	0.0002	0.56i	1	0.56i	0.0002	0.067i
m+1	0.043i	0.125i	0.206i	-0.239i	0.206i	0.125i	0.043i

Frequency

(b)

Figure 2-17: Tansceiver impulse response: (a) Lapped-OFDM, (b) PHYDYAS

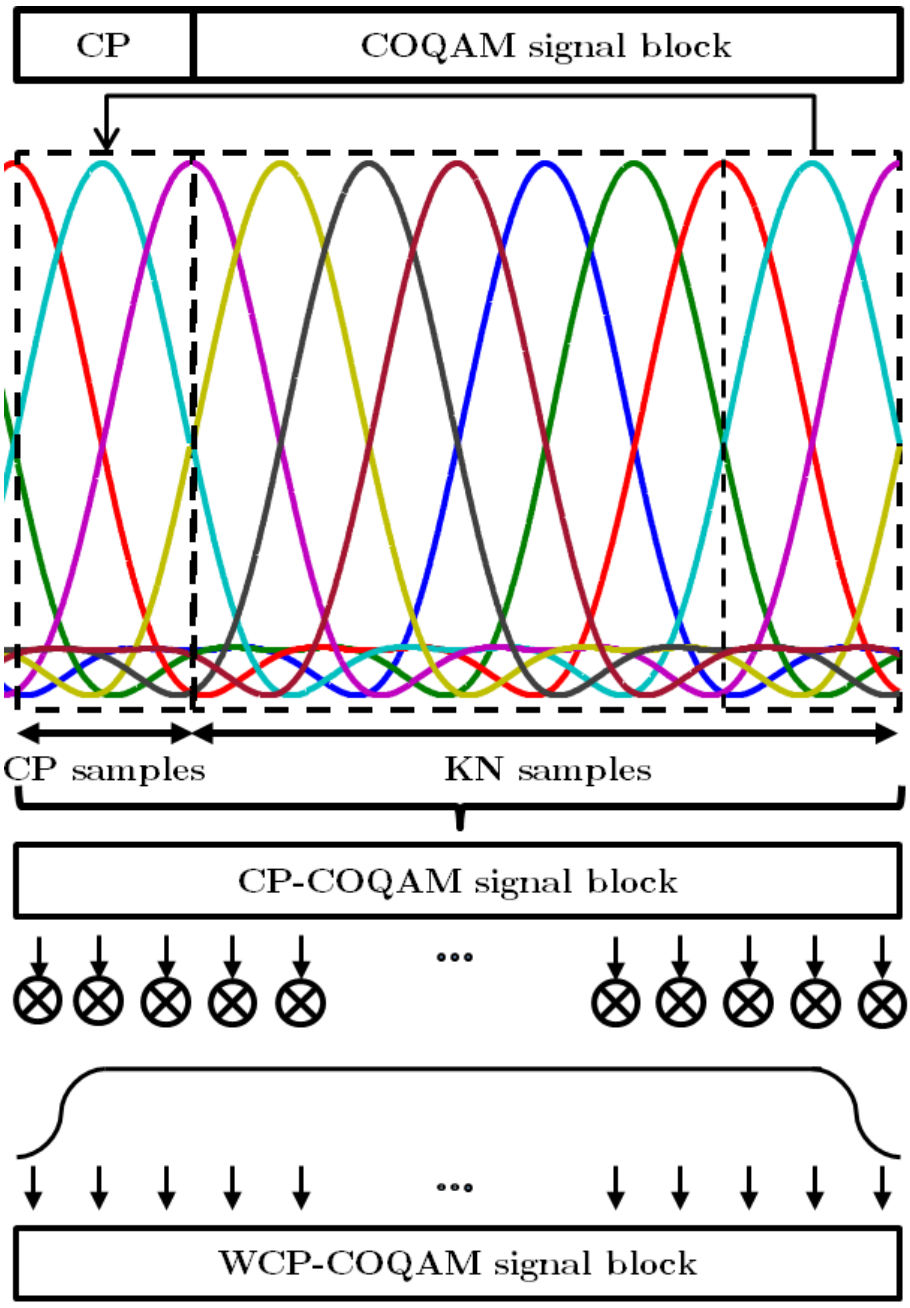

Figure 2-18: WCP-COQAM signal construction

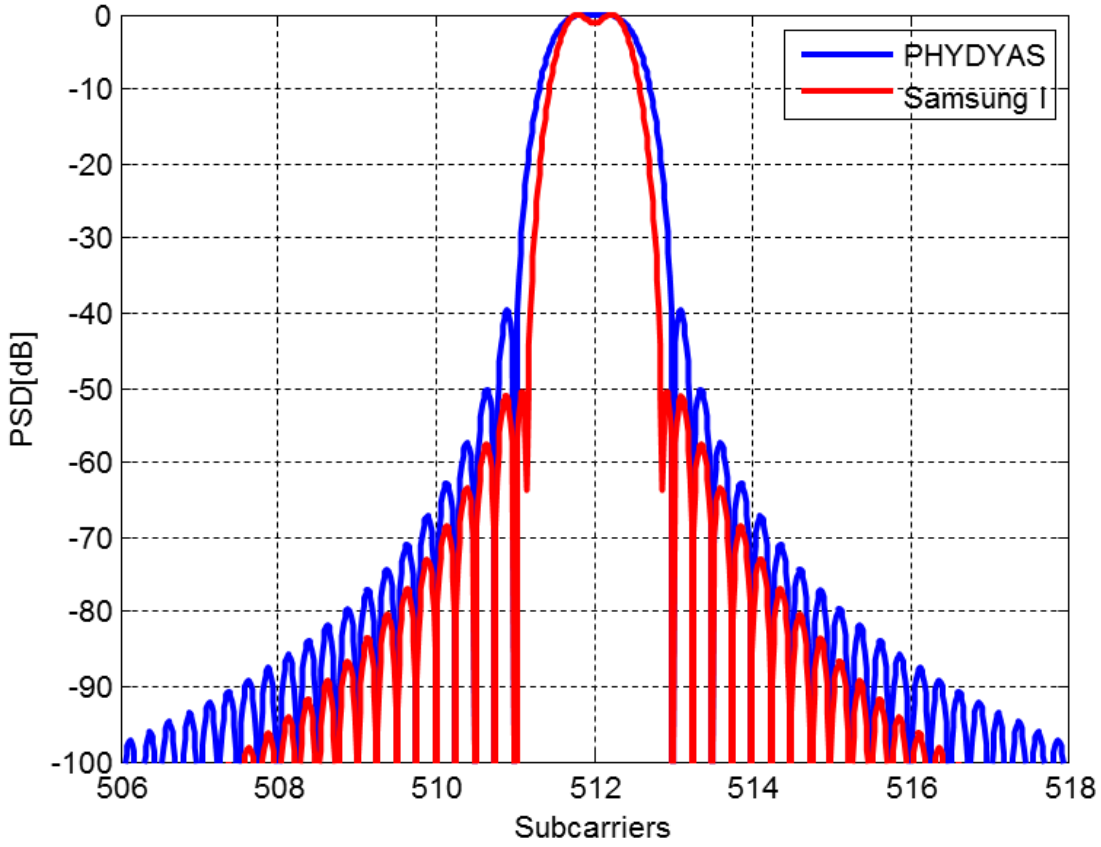

Figure 2-19: Samsung Type-I vs. PHYDYAS: frequency response

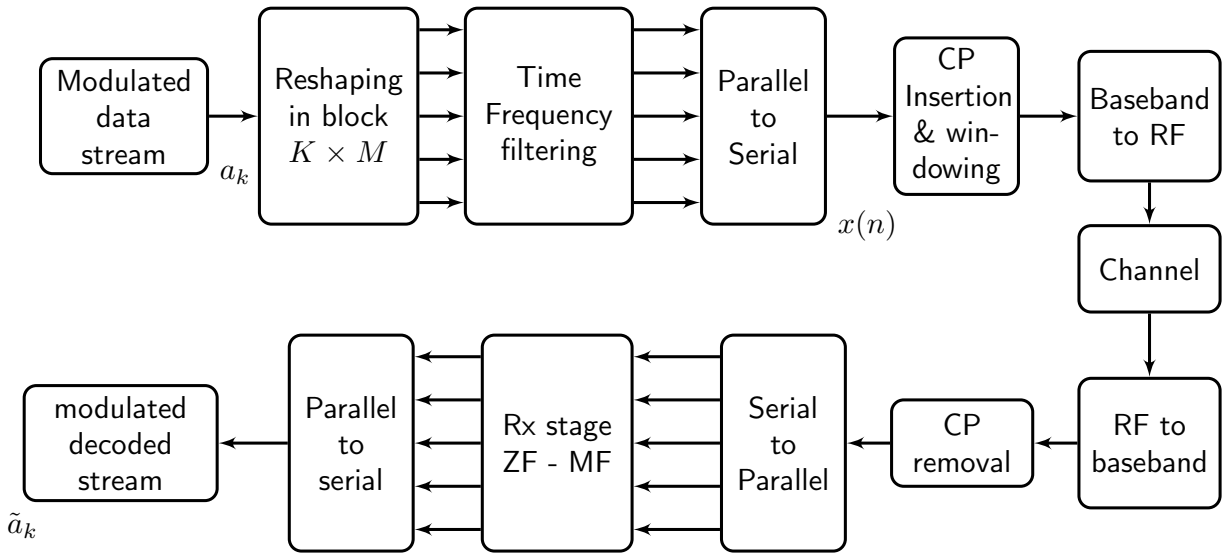

Figure 2-20: GFDM transceiver scheme.

3. System Model

3.1 Coexistence scenario

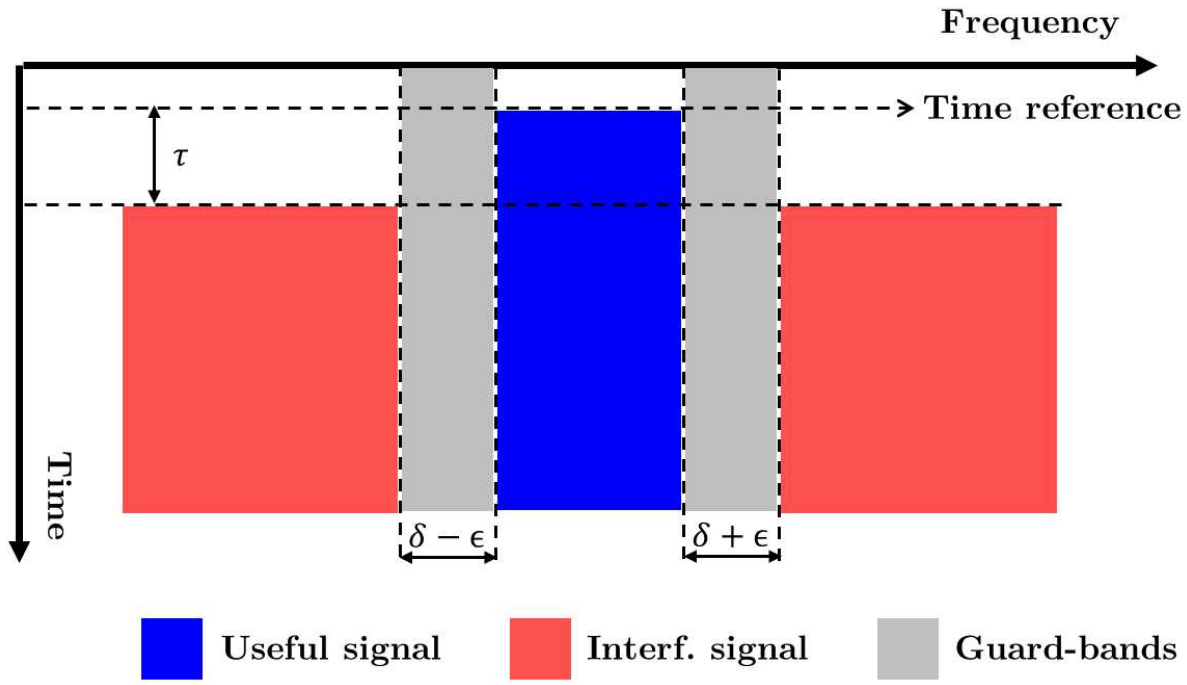

Figure 3-1: Coexistence scenario: two asynchronous users with τ [s] timing offset, ϵ [kHz] carrier frequency offset and free guard-bands of δ [kHz].

In this study, we consider a scenario of two coexisting users sharing the available frequency band as depicted in Figure 3-1, where the blue colored area and the red colored one correspond to the time/frequency resources allocated to the user of interest and the other one, respectively. The useful signal occupies a frequency band of 540 kHz equivalent to 3 LTE resource blocks (LTE-RB bandwidth = 180 kHz) while 1.62 MHz (i.e. 9 LTE-RB) are allocated to the other user on each side of the useful frequency band. A guard-band of δ kHz , illustrated by a gray colored area, is separating the frequency bands of both users. Several cases are considered for guard-bands: no guard band, 15 kHz, 45 kHz and 75 kHz.

The receiver of interest is assumed to be perfectly synchronized, in both time and frequency domains (i.e. neither timing offset nor frequency offset are considered), and is situated at equal distance from both transmitters[1]. However, as illustrated in Figure 3-1, a time/frequency synchronization misalignment (τ and ε denote timing and carrier frequency offsets, respectively) can occur between the receiver of interest and the other user. Note that we consider a timing offset distributed between $-T/2$ and $+T/2$, where T is the OFDM symbol duration ($T = 66.66\mu s$). Due to this synchronization mismatch, the receiver of interest suffers from the interference inducing thus performance degradation. It is worth mentioning that the CFO induces a shift of both red-colored areas of the interfering signal spectrum by ε kHz where the resulting guard bands become $\delta - \varepsilon$ kHz on one side and $\delta + \varepsilon$ kHz on the other side. In order to highlight the impact of this interference, we consider free-distortion channels (perfect and

[1]Note that in this work, we assume the same transmit power per subcarrier for both useful and interfering users

Table 3-1: General parameters

General	
RB bandwidth	180 kHz
Useful bandwidth of user of interest (UOI)	540 kHz
Interfering bandwidth	2×1.62 MHz
Timing offset (τ)	[-33.33,+33.33]μs
CFO (ε)	[-1.5,+1.5]kHz
Input data	16-QAM
Gaurd-band δ	[0, 15, 45, 75] kHz

noiseless channels) between both transmitters on one side and the victim receiver on the other side.

3.2 Parameters

In this section, we provide the general parameters of the scenario previously described (see Table 3-1) as well as specific parameters related to the different waveforms considered in this document:

- Waveforms with complex orthogonality: Tables 3-2 and 3-3,
- Waveforms with real orthogonality: Table 3-4,
- Non-orthogonal: Table 3-5.

Table 3-2: Waveforms with complex orthogonality (1/2)

CP-OFDM / WOLA-OFDM	
FFT size	1024
CP length	72
Windowing	Raised cosine
Window length (W_e,W_r)	$(20, 32)$
Subcarrier spacing	15 kHz
Sampling Frequency	15.36 MHz
UFMC (UF-OFDM)	
FFT size	1024
Filter	Dolph-Chebyshev
Filter length ($\mathrm{L_{FIR}}$ =ZP+1)	73
Zero padding length	72
Stop-band attenuation	40 dB
Receive windowing	Raised cosine
Subcarrier spacing	15 kHz
Sampling Frequency	15.36 MHz
f-OFDM	
FFT size	1024
Filter	the same at both Tx and Rx sides
Filter length	512
CP length	72
Transition band	2.5 $\times$ 15 kHz
Burst truncation	CP/2 on each side
Subcarrier spacing	15 kHz
Sampling Frequency	15.36 MHz

Table 3-3: Waveforms with complex orthogonality (2/2)

N-Continuous OFDM	
FFT size	1024
CP length	72
Continuity order	2 (second derivative)
Precoding matrix knowledge at Rx	none
Subcarrier spacing	15 kHz
Sampling Frequency	15.36 MHz
FMT	
Filter	[Tra16]
Roll-off factor α	0.25
Filter length	$16(1+\alpha)1024$
FFT size	$(1+\alpha)1024$
Subcarrier spacing	15 kHz
Sampling Frequency	15.36 MHz

Table 3-4: Waveforms with real orthogonality

FBMC-OQAM	
Prototype Filter	PHYDYAS
Overlapping factor (K)	4
FFT size	1024
Subcarrier spacing	15 kHz
Sampling Frequency	15.36 MHz
Lapped-OFDM	
Prototype Filter	sinus
Overlapping factor (K)	2
FFT size	1024
Subcarrier spacing	15 kHz
Sampling Frequency	15.36 MHz
WCP-COQAM	
CP	72
Transmit windowing	Raised cosine
Window length (W_e)	20
Prototype Filter	PHYDYAS
Overlapping factor (K)	4
FFT size	1024
Subcarrier spacing	15 kHz
Sampling Frequency	15.36 MHz

Table 3-5: Non orthogonal waveforms

FBMC-QAM	
Prototype Filter	Samsung Type I [YKK+15]
Overlapping factor (K)	4
FFT size	1024
Subcarrier spacing	15 kHz
Sampling Frequency	15.36 MHz
GFDM	
FFT size	1024
Block size (M)	7
Subcarrier spacing	15 kHz
Sampling Frequency	15.36 MHz

4. Waveform Comparison

4.1 Introduction

This section is devoted to compare the performance of the waveform candidates described in Section 2 in terms of:

- PSD: the out-of-band radiation of the interfering signal is evaluated.
- Spectral efficiency function of the number of transmitted symbols per frame.
- Physical layer latency: corresponds to the time delay between the transmission of a given information and the recovery of the latter.
- Time and frequency synchronization errors between the interfering transmitter and the receiver of interest.
- Power fluctuation: both Instantaneous-to-Average Power Ratio (IAPR) and Peak-to-Average Power Ratio (PAPR) are analyzed.
- Transceiver complexity: only the number of multiplications per unit of time of modulation/demodulation process is considered.

4.2 PSD

It is well established that traditional CP-OFDM has poor frequency domain localization. For instance, LTE system requires the use of 10% of the system bandwidth as guard bands. These large guard bands located at both edges of the spectrum are necessary in order to reach enough attenuation to meet LTE spectrum mask requirement. It is expected that future 5G systems use more efficiently the allocated bandwidth and large guard bands can be seen as a waste of spectral efficiency. Thus, good or excellent spectral containment will be a key parameter for future 5G waveform in order to support neighboring and non orthogonal signals.

We present in figure 4-1 the PSD (Power Spectral Density) comparison of the considered waveforms. We choose to plot only the contribution of the interference users so that we can observe at the same time the level of out-of band emission and the level of emission within a spectral hole. As expected, the worst PSD performance is given by the traditional CP-OFDM waveform. The far-end PSD is dominated by the waveforms which have their filtering applied to each subcarrier, namely Lapped-OFDM, FBMC-QAM, FBMC-OQAM and FMT. N-continuous OFDM has a relatively slow decaying but provides good far-end PSD. UFMC and f-OFDM apply a filter to a group of subcarriers and we can observe that their performances are in the same order of magnitude. WCP-COQAM presents moderate far-end PSD performance due to time domain transition between successive blocks. The time domain windowing applied to transmitted OFDM blocks (WOLA-OFDM) improves by about 20 dB the performance of traditional CP-OFDM, but its far-end PSD performance remains moderate. Similar to WCP-COQAM, GFDM is not very well localized in the frequency domain due to the block construction of GFDM signal generating time domain transitions between blocks.

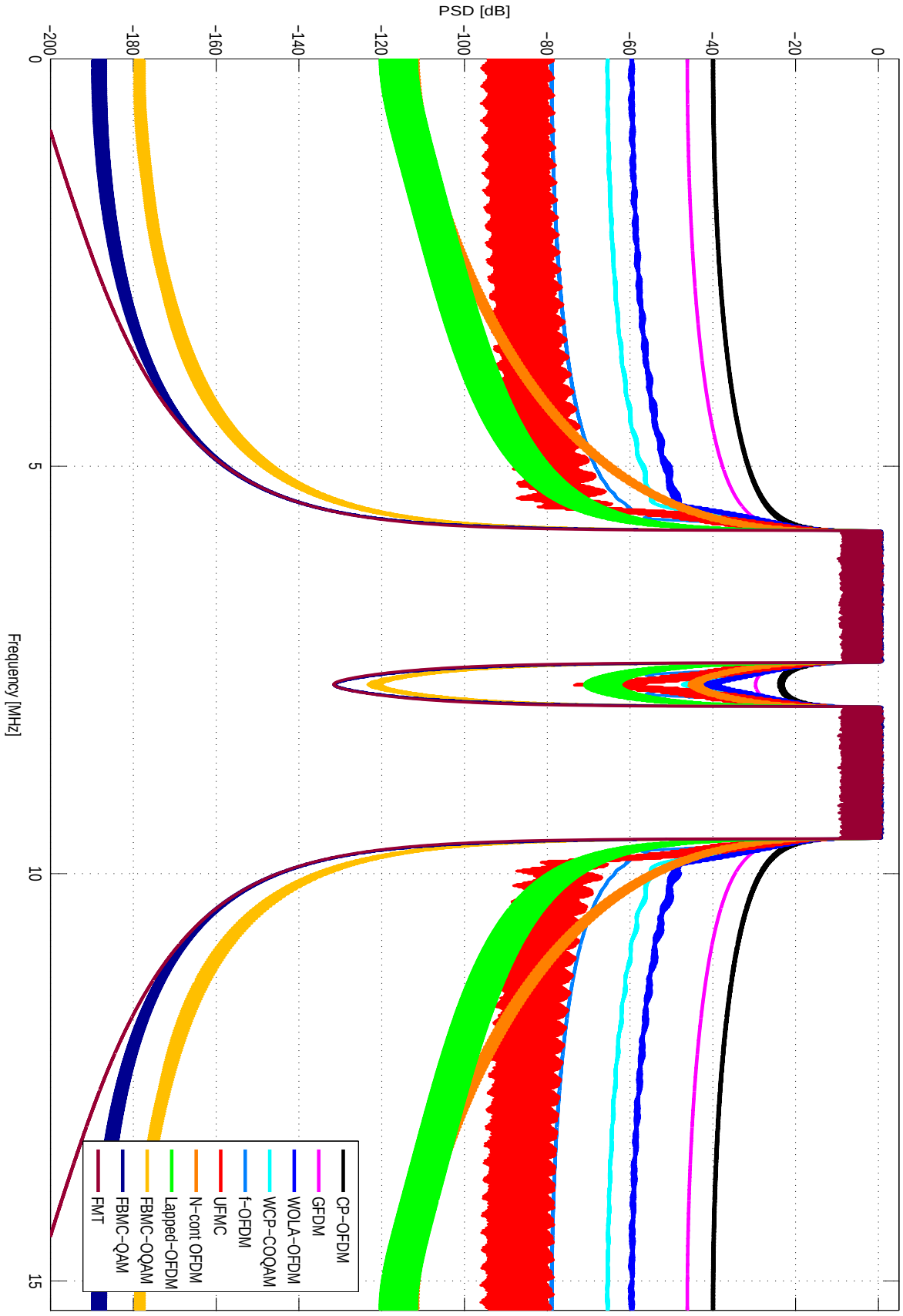

Figure 4-1: Interference users PSD comparison.

In figure 4-2, we present a zoom of the PSD at one edge of the spectrum. The waveforms which have their filter applied to each subcarrier provide the best PSD performance: FBMC-QAM, FBMC-OQAM and FMT provide an extremely fast spectrum decaying and only one subcarrier spacing is necessary to achieve very low PSD levels. Nevertheless, and due to shorter prototype filter duration ($K = 2$), Lapped-OFDM has lower spectrum decaying compared to the aforementioned waveforms. The PSD of f-OFDM requires few subcarriers to be drastically improved with respect to traditional CP-OFDM due to the transition bandwidth of the filter which has been set to $\partial W = 2.5$ subcarriers. Finally, all other waveforms provides moderate performance and requires more than one resource block (12 subcarriers) to reach an attenuation of -40 dB.

4.3 Spectral efficiency/ Latency

Spectral efficiency (SE) given in bits/s/Hz is a key parameter for high data rate systems since it gives a clear idea of achievable data rates for a given bandwidth. In Table 4-1, we present the SE according to the number of transmitted parallel vector symbols S, and also its asymptotic version called "Asymptotic Spectral Efficiency" where S tends toward infinity. The required number of parallel vectors is different for each waveform and depends on the number of complex QAM symbols N_{QAM} to be transmitted, but also on the way a block symbol is built. The exact number of S is given in Table 4-2 for each considered waveform, where $\lceil . \rceil$ refers to the ceiling operation and N_u is the number of used subcarriers. We can observe that for small values of S, the waveforms which have their filter applied to each subcarrier have a spectral efficiency penalty due to their longer impulse response. This is especially true for FMT since the overlap factor K is usually much longer: for instance $K_{FMT} = 16$ for a roll off factor of 0.25, while $K = 4$ for FBMC-OQAM and FBMC-QAM). All the waveforms which require a kind of guard interval (CP or ZP) suffer from the fact that this guard interval does not transmit any useful information. When S tends toward infinity, only FBMC derivatives (Lapped-OFDM, FBMC-OQAM and QAM) achieve full capacity.

The latency of a waveform is also another key parameter, especially when considering very low response systems such as tactile Internet. In this deliverable, we use the "End-to-End Physical layer latency" criteria ($E2E$) defined as the time delay from which the FEC (Forward Error Correction) is capable to decode the bits corresponding to the N_{QAM} transmitted symbols. In other words, it refers to the time between the availability of the bits at the output of the FEC at the transmitter side, and the beginning of the channel decoding at the receiver side. Thus it is important to note that $E2E$ criteria does not take into account the time required by channel coding and decoding and the potential delay introduced by the channel. $E2E$ comparison is provided by Table 4-3 and is also graphically presented in figure 4-3 according to N_{QAM} and for a user which uses 3 RB corresponding to $N_u = 36$ subcarriers. In this figure, we can observe that the large group delay of the FMT prototype filter and the loss of spectral efficiency due to the roll off factor drastically increase the latency of FMT scheme. All other waveforms latencies are in the same order of magnitude. In order to better assess the performance of the other waveforms, we present in figure 4-4 the End-to-End Physical layer latency ratio with respect to traditional CP-OFDM scheme. We can observe that for small N_{QAM} values, the latencies are in general (much) greater than traditional OFDM, and there exist only few waveforms and few settings which provide better performance. When N_{QAM} increases, FBMC derivative waveforms become a little bit better than OFDM, and the other waveforms have much more settings which

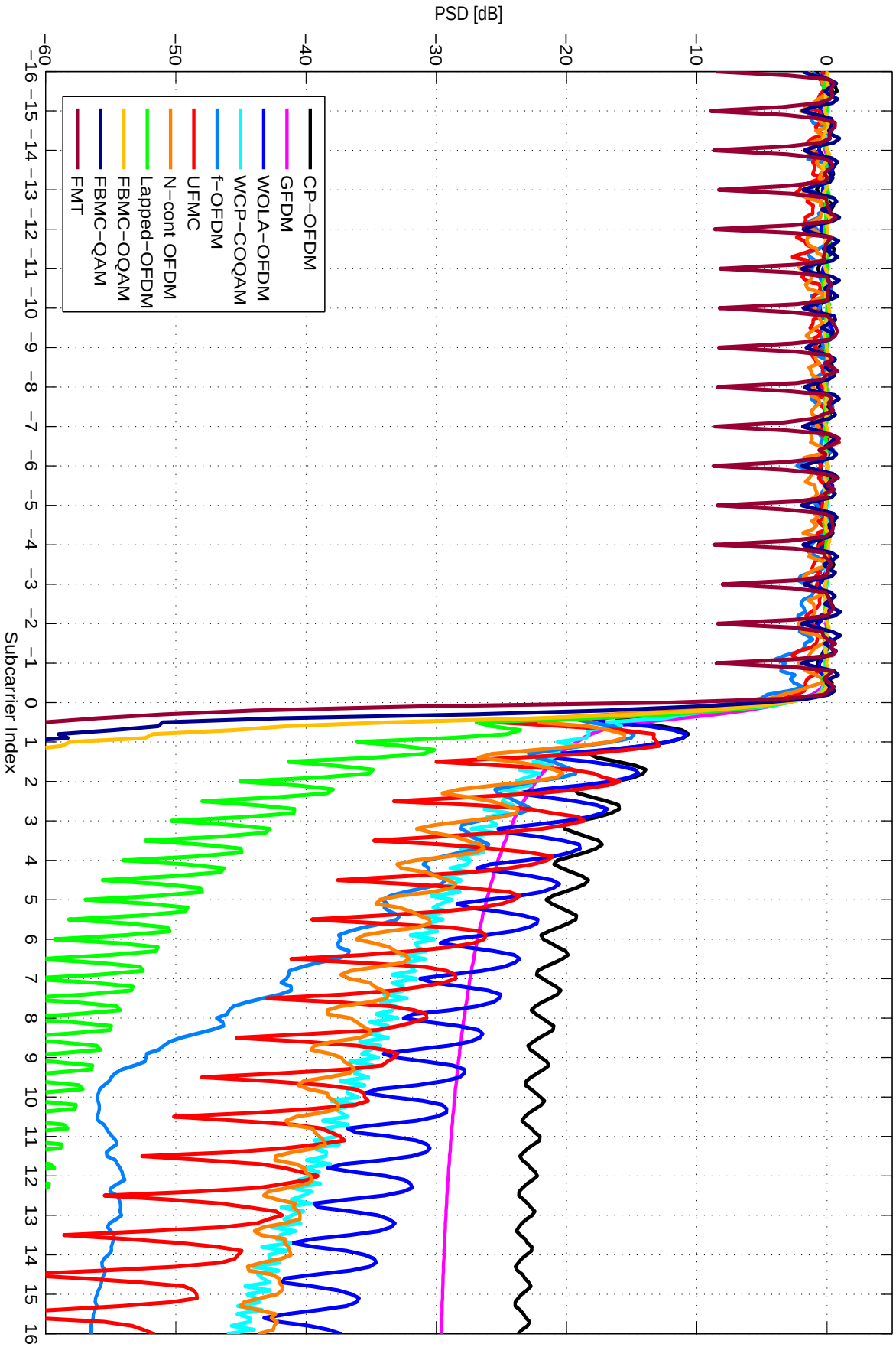

Figure 4-2: Comparison of the interference users PSD edge according to the subcarrier index.

Table 4-1: Spectral Efficiency comparison

Waveform	Spectral efficiency	Asymptotic Spectral Efficiency
OFDM	$\eta = m\frac{N_{\mathrm{FFT}}}{N_{\mathrm{FFT}}+L_{\mathrm{CP\,OFDM}}}$	$\eta' = m\frac{N_{\mathrm{FFT}}}{N_{\mathrm{FFT}}+L_{\mathrm{CP\,OFDM}}}$
WOLA-OFDM	$\eta = m\frac{SN_{\mathrm{FFT}}}{S(N_{\mathrm{FFT}}+L_{\mathrm{CP\,WOLA}})+W_{\mathrm{Tx}}}$	$\eta' = m\frac{N_{\mathrm{FFT}}}{N_{\mathrm{FFT}}+L_{\mathrm{CP\,WOLA}}}$
UFMC	$\eta = m\frac{N_{\mathrm{FFT}}}{N_{\mathrm{FFT}}+L_{\mathrm{ZP\,UFMC}}}$	$\eta' = m\frac{N_{\mathrm{FFT}}}{N_{\mathrm{FFT}}+L_{\mathrm{ZP\,UFMC}}}$
f-OFDM	$\eta = m\frac{SN_{\mathrm{FFT}}}{S(N_{\mathrm{FFT}}+L_{\mathrm{CP\,f-OFDM}})+L_{\mathrm{Trunc}}}$	$\eta' = m\frac{N_{\mathrm{FFT}}}{N_{\mathrm{FFT}}+L_{\mathrm{CP\,f-OFDM}}}$
N-Cont OFDM	$\eta = m\frac{N_{\mathrm{FFT}}}{N_{\mathrm{FFT}}+L_{\mathrm{CP\,N-Cont\,OFDM}}}$	$\eta' = m\frac{N_{\mathrm{FFT}}}{N_{\mathrm{FFT}}+L_{\mathrm{CP\,N-Cont\,OFDM}}}$
FMT	$\eta = m\frac{S}{(S+K_{\mathrm{FMT}}-1)(1+\alpha)}$	$\eta' = \frac{m}{1+\alpha}$
FBMC-OQAM	$\eta = m\frac{S}{S+K_{\mathrm{FBMC-OQAM}}-1/2}$	$\eta' = m$
WCP-COQAM	$\eta = m\frac{KN_{\mathrm{FFT}}}{K_{\mathrm{WCP-COQAM}}N_{\mathrm{FFT}}+L_{\mathrm{CP\,WCP-COQAM}}}$	$\eta' = m\frac{KN_{\mathrm{FFT}}}{K_{\mathrm{WCP-COQAM}}N_{\mathrm{FFT}}+L_{\mathrm{CP\,WCP-COQAM}}}$
FBMC-QAM	$\eta = m\frac{S}{S+K_{\mathrm{FBMC-QAM}}-1}$	$\eta' = m$
GFDM	$\eta = m\frac{s_{\mathrm{GFDM}}N_{\mathrm{FFT}}}{s_{\mathrm{GFDM}}N_{\mathrm{FFT}}+L_{\mathrm{CP\,GFDM}}}$	$\eta' = m\frac{s_{\mathrm{GFDM}}N_{\mathrm{FFT}}}{s_{\mathrm{GFDM}}N_{\mathrm{FFT}}+L_{\mathrm{CP\,GFDM}}}$

Table 4-2: Number of transmitted parallel vectors in the time domain according to the number of complex QAM symbols N_{QAM}

Waveform	Number of transmitted parallel vector in the time domain
OFDM	$S = \lceil \frac{N_{QAM}}{N_U} \rceil$
WOLA-OFDM	$S = \lceil \frac{N_{QAM}}{N_U} \rceil$
UFMC	$S = \lceil \frac{N_{QAM}}{N_U} \rceil$
f-OFDM	$S = \lceil \frac{N_{QAM}}{N_U} \rceil$
N-Cont OFDM	$S = \lceil \frac{N_{QAM}}{N_U} \rceil$
FMT	$S = \lceil \frac{N_{QAM}}{N_U} \rceil$
FBMC-OQAM	$S = \lceil \frac{N_{QAM}}{N_U} \rceil$
WCP-COQAM	$S = \lceil \frac{N_{QAM}}{N_U K_{\mathrm{WCP-OQAM}}} \rceil$
FBMC-QAM	$S = \lceil \frac{N_{QAM}}{N_U} \rceil$
GFDM	$S = \lceil \frac{N_{QAM}}{7 \cdot N_U} \rceil$

Table 4-3: End-to-End PHY latency comparison

Waveform	End-to-End PHY latency ($E2E$)
OFDM	$E2E = S\frac{N_{\mathrm{FFT}}+L_{\mathrm{CP\,OFDM}}}{F_{\mathrm{s\,OFDM}}}$
WOLA-OFDM	$E2E = \frac{S(N_{\mathrm{FFT}}+L_{\mathrm{CP\,WOLA}})+W_{\mathrm{Tx}}}{F_{\mathrm{s\,WOLA}}}$
UFMC	$E2E = S\frac{N_{\mathrm{FFT}}+L_{\mathrm{ZP\,UFMC}}}{F_{\mathrm{s\,UFMC}}}$
f-OFDM	$E2E = \frac{S(N_{\mathrm{FFT}}+L_{\mathrm{CP\,f-OFDM}})+L_{\mathrm{Trunc}}}{F_{\mathrm{s\,f-OFDM}}}$
N-Cont OFDM	$E2E = S\frac{N_{\mathrm{FFT}}+L_{\mathrm{CP\,N-Cont\,OFDM}}}{F_{\mathrm{s\,N-Cont\,OFDM}}}$
FMT	$E2E = \frac{(S-1+K_{\mathrm{FMT}})N_{\mathrm{FFT}}}{F_{\mathrm{s\,FMT}}}$
FBMC-OQAM	$E2E = N_{\mathrm{FFT}}\frac{S-\frac{1}{2}+K_{\mathrm{FBMC-OQAM}}}{F_{\mathrm{s\,FBMC-OQAM}}}$
WCP-COQAM	$E2E = S\frac{K_{\mathrm{WCP-OQAM}}N_{\mathrm{FFT}}+L_{\mathrm{CP\,WCP*COQAM}}}{F_{\mathrm{s\,WCP-OQAM}}}$
FBMC-QAM	$E2E = N_{\mathrm{FFT}}\frac{S-1+K_{\mathrm{FBMC-QAM}}}{F_{\mathrm{s\,FBMC-QAM}}}$
GFDM	$E2E = S\frac{7\cdot N_{\mathrm{FFT}}+L_{\mathrm{CP\,GFDM}}}{F_{\mathrm{s\,GFDM}}}$

give better latency performance.

We remind hereafter the notations used in this section:

- m is the modulation efficiency (including both the modulation order and the coding rate)
- $L_{CP\,\mathbf{X}}$ and $L_{ZP\,\mathbf{X}}$ are respectively the number of symbols of the CP and the ZP of waveform $\mathbf{X}$
- $K_{\mathbf{X}}$ is the overlapping factor of the filter used by waveform $\mathbf{X}$[1]
- $F_{\mathrm{s}\,\mathbf{X}}$ is the sampling frequency of waveform $\mathbf{X}$
- N_{FFT} is the number of available subcarriers
- W_{Tx} is the number of symbols used to perform the WOLA processing at the transmitter side
- L_{Trunc} is the number of symbols kept at both edges of a f-OFDM burst after truncation
- α is the roll off factor used for each FMT subcarrier

4.4 Asynchronous access

In this section, as mentioned previously, we discuss the performance of the considered waveforms in multi-user asynchronous access. In order to focus on the asynchronous interference impact on the performance of various waveform schemes, we propose to measure the normalized mean

[1]It is important to note that K_{FMT} is usually much greater than the overlapping factor of the other waveforms due to the fact that the roll off factor is usually $\alpha < 0.3$.

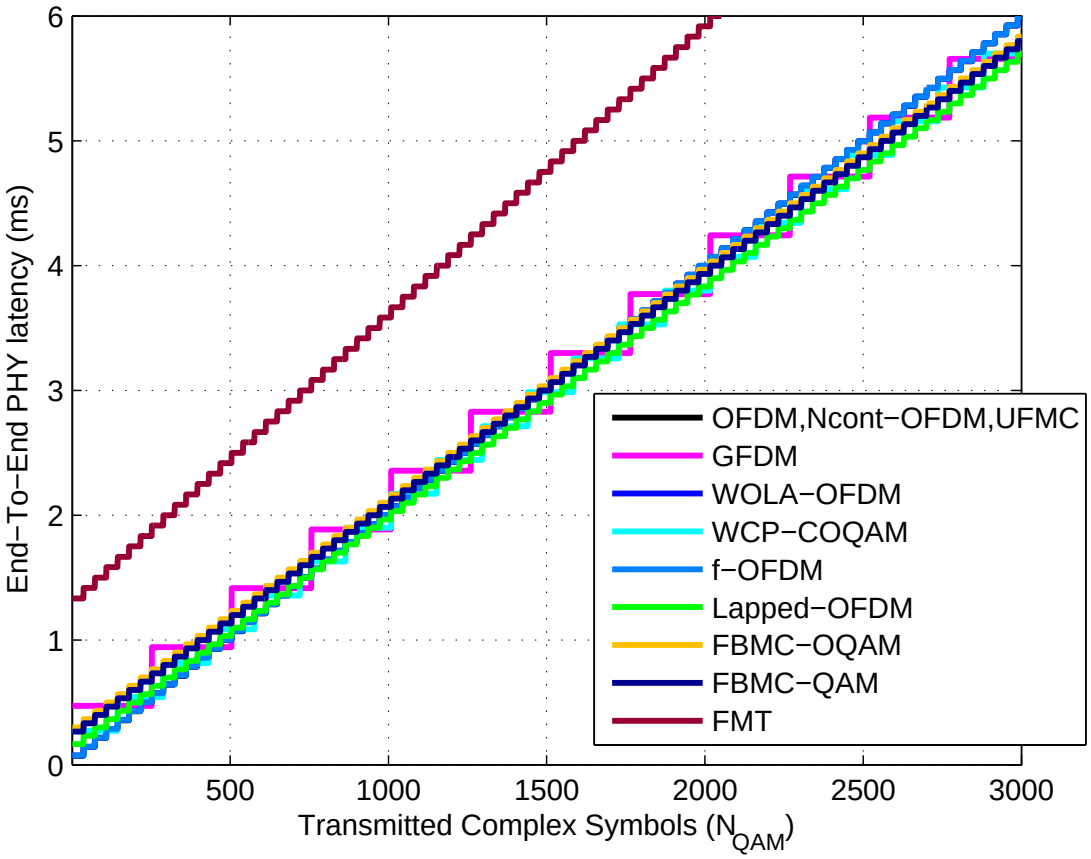

Figure 4-3: End-to-End Physical Layer latency (in ms) according to the number of transmitted N_{QAM} symbols for a user using 3 RB

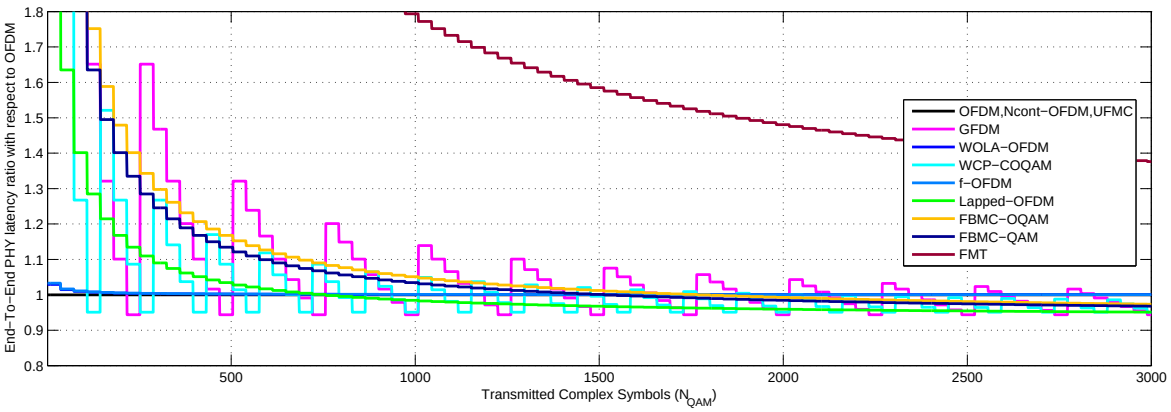

Figure 4-4: End-to-End Physical layer latency ratio with respect to traditional CP-OFDM scheme for a user which used 3 RB

square error (MSE)[2] on decoding the useful symbols of the user of interest in ideal noiseless channel. Note that normalized MSE is adopted since it remains the same for all constellation schemes. Both per-subcarrier MSE and average MSE are assessed vs. timing offset or carrier frequency offset. Actually, per-subcarrier MSE can provide a meaningful information about the distribution of asynchronous interference across useful subcarriers. Several cases of guard-bands are examined: $\delta = 0$, 15, 45 and 75 kHz. Note that pseudo-3D-MSE (per-subcarrier MSE), we use a color map indicating the MSE levels: from dark blue color when the MSE is less than or equal to -40dB to dark red color when the MSE is greater than or equal to -10dB.

4.4.1 Timing offset

In order to distinguish the degradation induced by timing synchronization errors from the one caused by CFO, we consider in this section that there is no CFO ($\varepsilon = 0$ Hz) between the interfering signal and the useful one. The timing misalignment τ varies from $-33.33\mu s$ to $+33.33\mu s$.

4.4.1.1 Waveforms with complex orthogonality

In CP-OFDM case, we can distinguish two regions: when $\tau < CP$, we observe in Figure 4-5 a dark blue region (MSE below -40 dB) which means that there is no asynchronous interference. Such a result is due to the fact that the orthogonality between subcarriers is maintained as long as the delay error τ does not exceed the CP duration. When τ is outside the CP interval, the orthogonality is no longer ensured. This loss of orthogonality gives rise to a strong level of asynchronous interference. We can see that the interference level slowly decreases as the spectral distance between the victim subcarrier and the interfering ones increases. Similarly, we observe a negligible enhancement when increasing the guard band. Such a behavior is due to the poor frequency localization of the rectangular transmit/receive OFDM filters.

In the case of CP-OFDM with transmit windowing 'Tx-W-OFDM' (Figure 4-6), we note that for small timing offset the interference level is particularly low but on smaller interval ($<$CP) compared to CP-OFDM. This can be explained by the fact that a part of the CP is used to absorb the windowing effects. When τ is outside the CP interval, we can observe a strong NMSE (dark-red color), at the edge subcarriers that are still heavily impacted by the asynchronous interference. Moreover, the inner subcarriers are not well enough protected against interference leading thus to a limited improvement compared to CP-OFDM. Such a limited performance can be explained by the fact that the rectangular receive filter brings an important amount of interference from the asynchronous user. Almost the same performance can be observed in Figure 4-7 for CP-OFDM scheme with receive windowing (Rx-W-OFDM) which can be explained, in this case, by the high spectrum side-lobes of the asynchronous transmitted signal CP-OFDM signal.

We move now to WOLA-OFDM (Figure 4-8), where additional remarks can be made. The interference level in the middle of the bandwidth becomes lower (approx. -35 dB) compared to the previous OFDM schemes. We can also see that blue colored area (MSE less than -30 dB) becomes larger when increasing the guard band. This can be explained by the fact that the WOLA processing applied at the receiver is able to suppress inter-user interference as well. Indeed, when users are not synchronized, the soft edges applied at the receiver help to reduce inter-user interference resulting from the mismatched FFT capture window.

[2]The normalized MSE is computed by dividing the MSE by the average power of the signal constellation

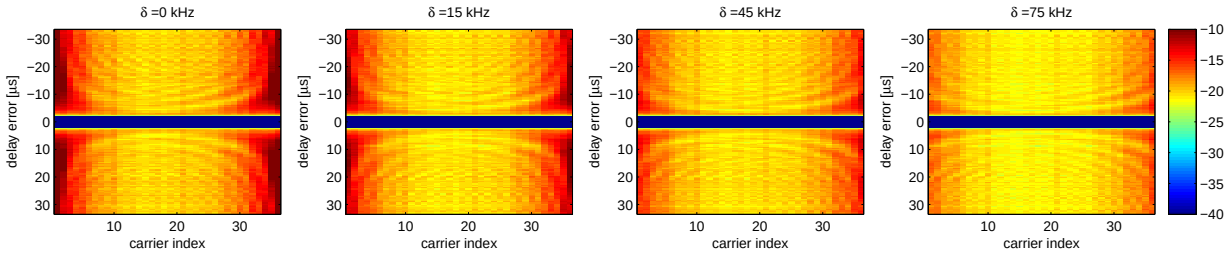

Figure 4-5: CP-OFDM: per-subcarrier NMSE against timing offset

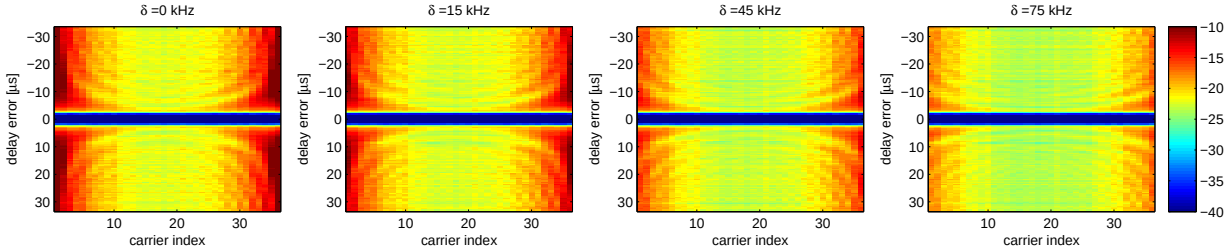

Figure 4-6: Tx-W-OFDM: per-subcarrier NMSE against timing offset

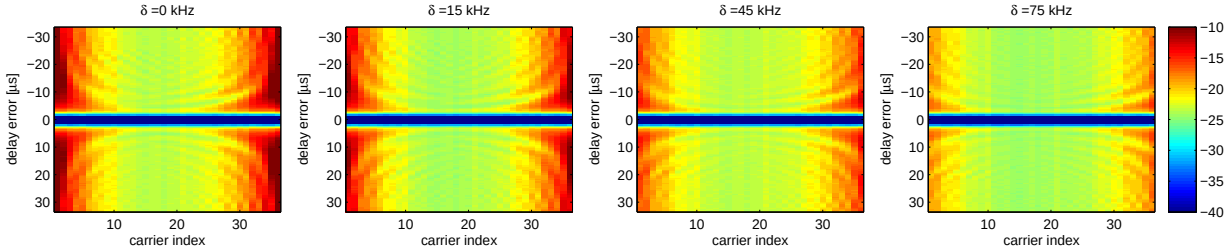

Figure 4-7: Rx-W-OFDM: per-subcarrier NMSE against timing offset

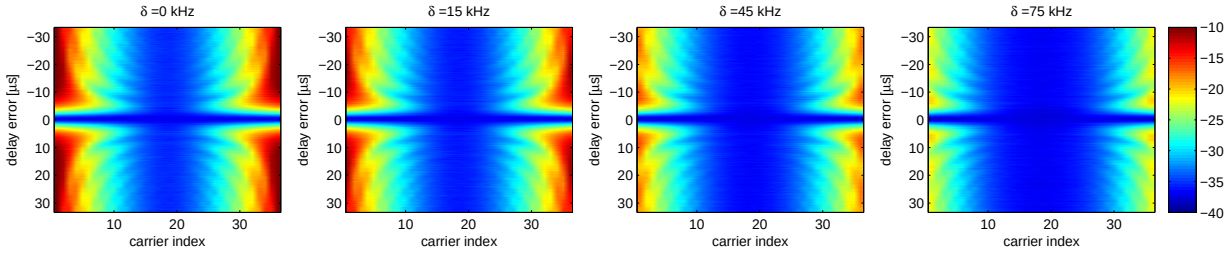

Figure 4-8: WOLA-OFDM: per-subcarrier NMSE against timing offset

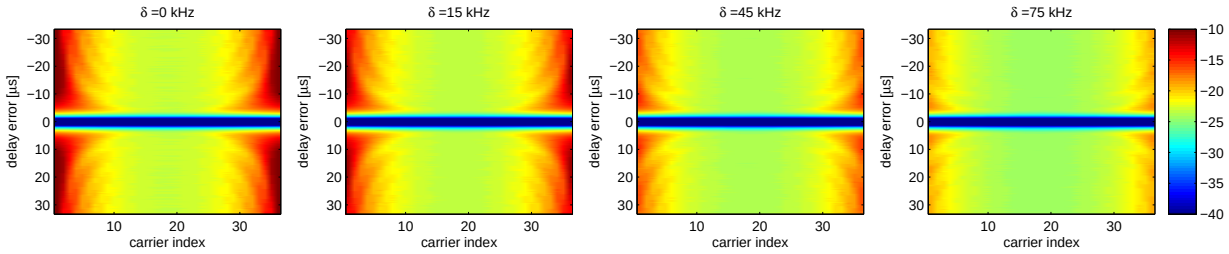

Figure 4-9: UFMC: per-subcarrier NMSE against timing offset

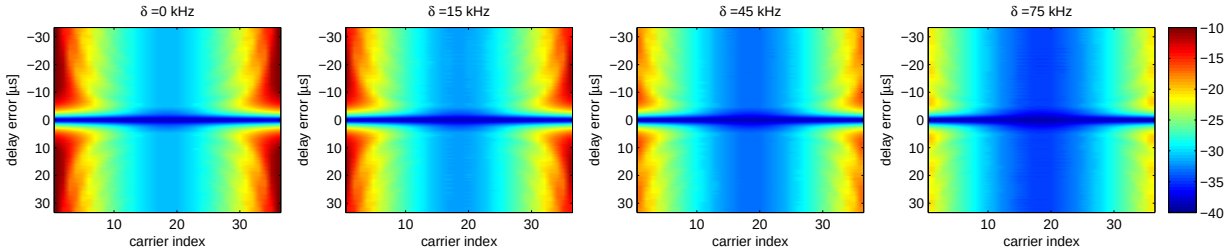

Figure 4-10: W-UFMC: per-subcarrier NMSE against timing offset

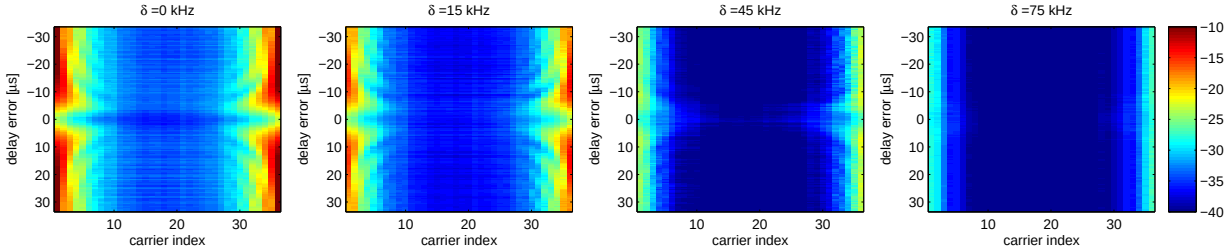

Figure 4-11: f-OFDM: per-subcarrier NMSE against timing offset

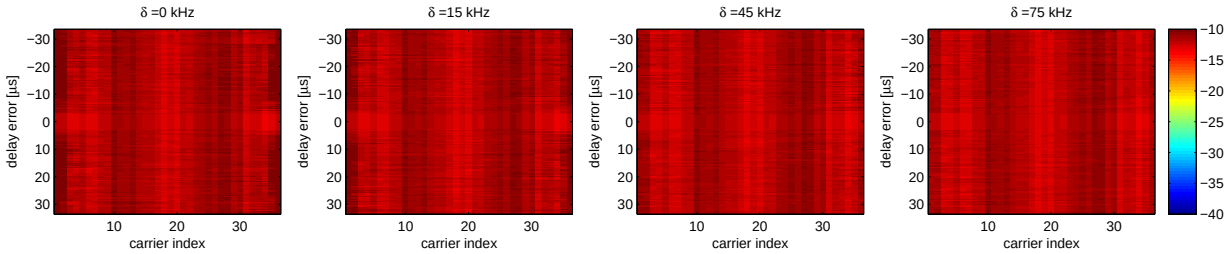

Figure 4-12: N-continuous OFDM: per-subcarrier NMSE against timing offset

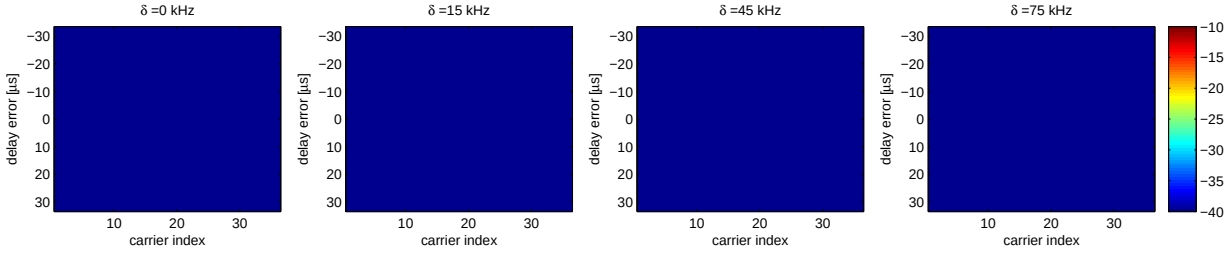

Figure 4-13: FMT: per-subcarrier NMSE against timing offset

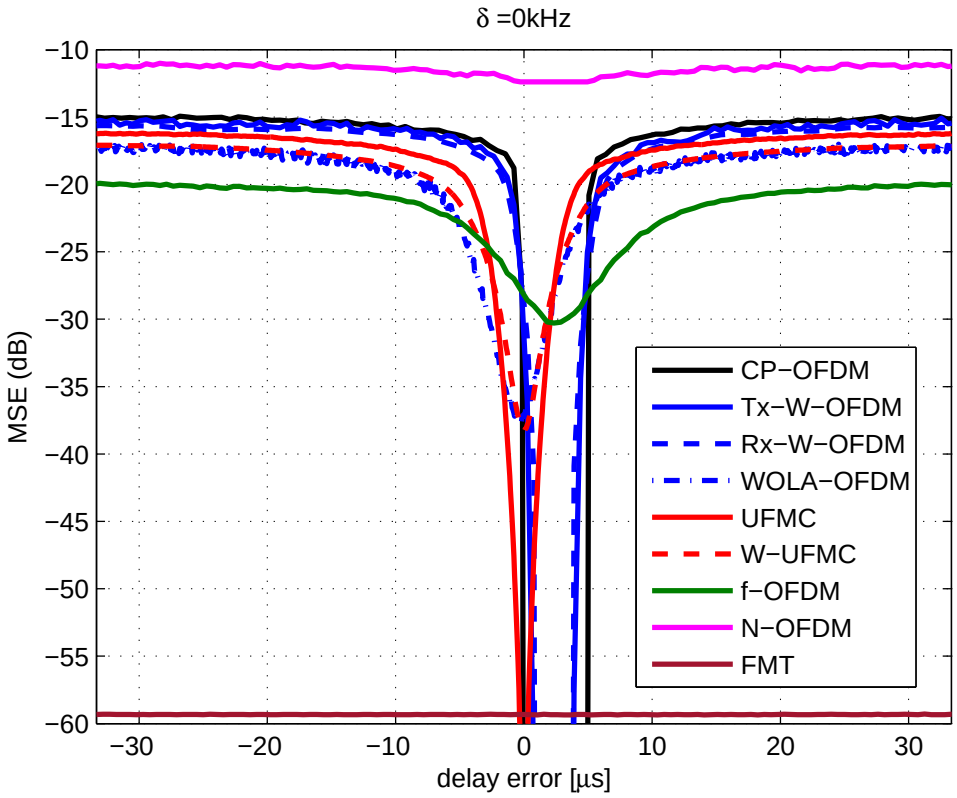
δ =0kHz
MSE (dB)
delay error [µs]
CP−OFDM
Tx−W−OFDM
Rx−W−OFDM
WOLA−OFDM
UFMC
W−UFMC
f−OFDM
N−OFDM
FMT

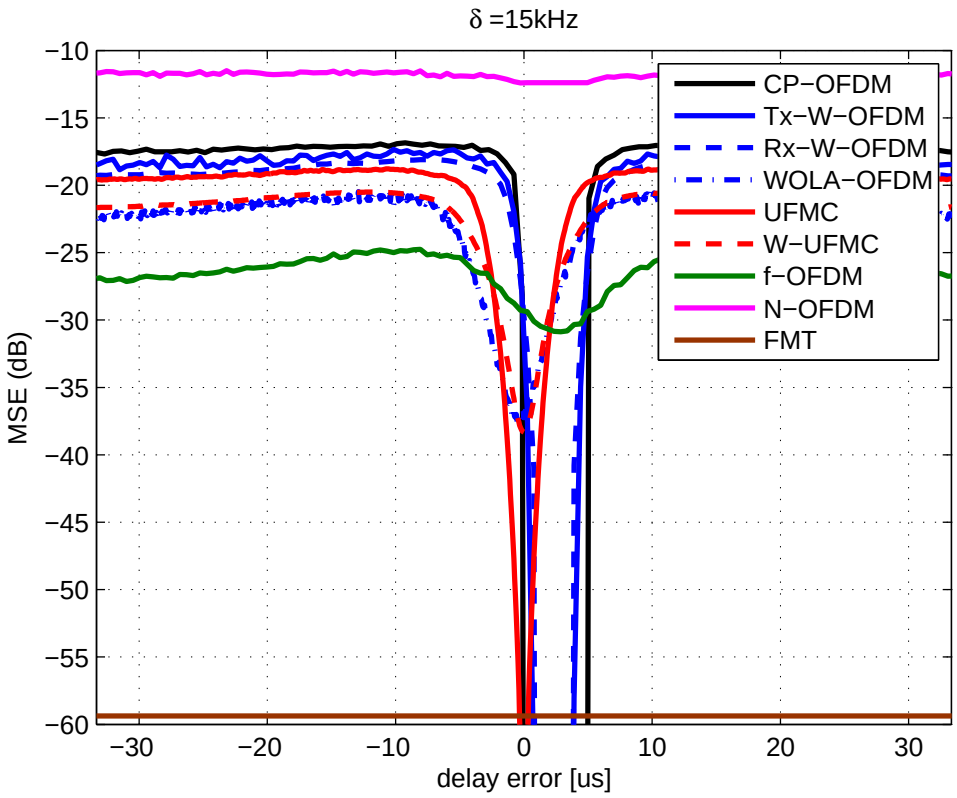
δ =15kHz
MSE (dB)
delay error [us]
CP−OFDM
Tx−W−OFDM
Rx−W−OFDM
WOLA−OFDM
UFMC
W−UFMC
f−OFDM
N−OFDM
FMT

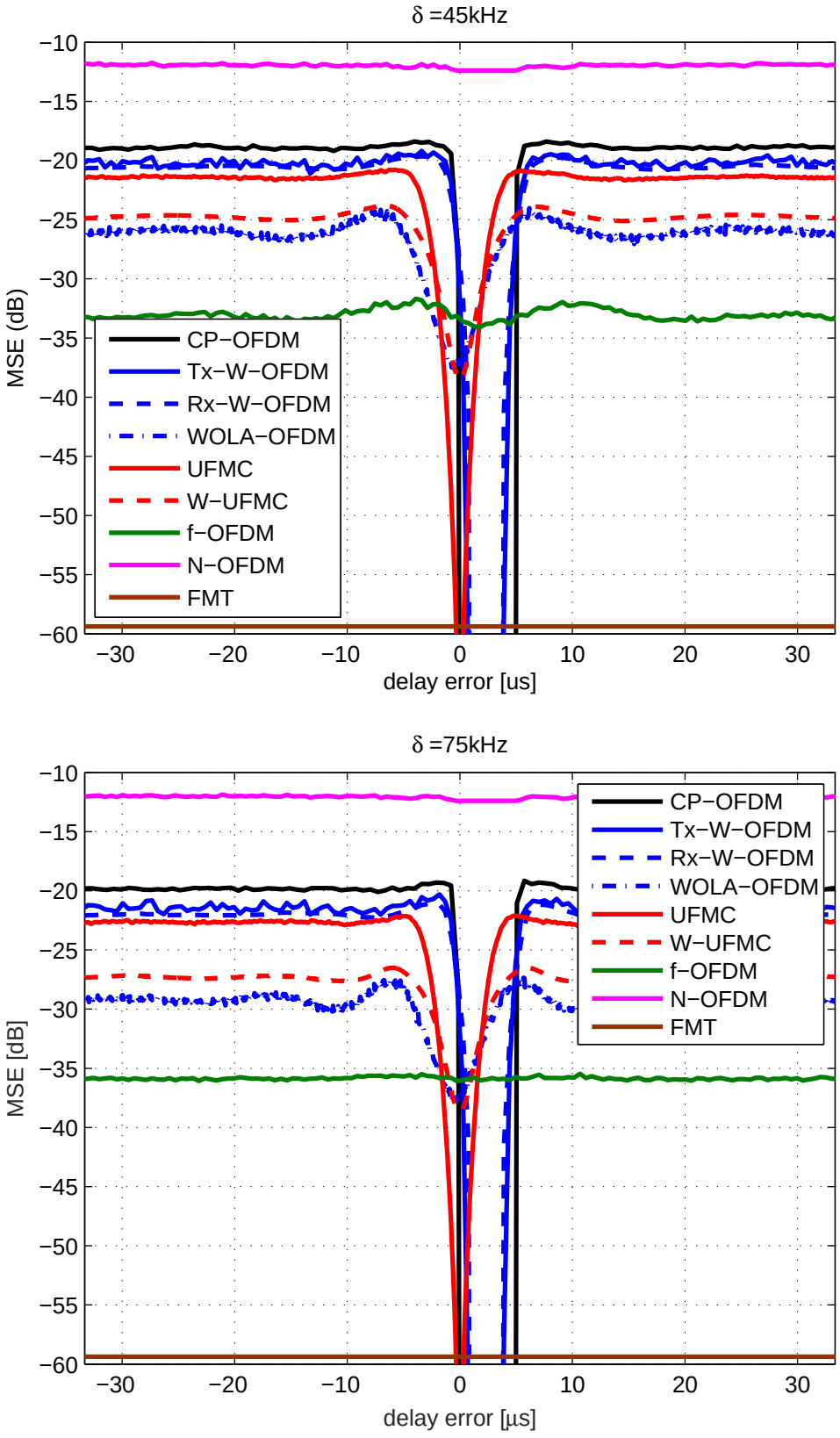

Figure 4-14: WFs with complex orthogonality: average MSE against timing offset

Thanks to the per-RB filtering, the UFMC scheme shows better performance compared to CP-OFDM (see Figure 4-9). However, the gain achieved by UFMC remains limited as in CP-OFDM with Tx or Rx windowing. Moreover, thanks to additional windowing at the receiver side (Figure 4-10), W-UFMC offers a higher gain compared to the basic scheme of UFMC when the timing offset is outside the CP region. Similar to previous windowed schemes, the CP region offering the lowest MSE is significantly reduced in W-UFMC because the ZP length is originally used to absorb the transmit filter response. Furthermore, when increasing the spectral distance of the victim subcarrier from the interfering ones, the interference level decay is more important compared to CP-OFDM but less significant when compared to WOLA-OFDM.

In the f-OFDM scheme (Figure 4-11), since filtering is applied at both transmitter and receiver sides, the inner subcarriers are more protected compared to the previous schemes. In fact, the long filters used in this waveforms offers a better frequency localization of the transmitted signals and a better protection against inter-user interference compared to WOLA-OFDM and W-UFMC. However, it is worth pointing out the fact the CP is completely used to absorb only a part of the transmit/receive filters responses.

Concerning the N-continuous OFDM waveform (Figure 4-12), one can see that the MSE is about or more than -10dB. However, this high level of MSE does not necessarily mean a high level of asynchronous interference. In fact, in this version, the precoding matrix is not explicitly known by the receiver, which means that the asynchronous interference is unfortunately hidden by distortion induced by the precoding matrix applied at the transmitter side.

In FMT case (Figure 4-13), we can observe that there is no (or negligible) asynchronous interference. Such a result is due the fact that there is no (or negligible) interaction between subcarriers. Indeed, each FMT subcarrier can be seen as a traditional single carrier modulation which respects the Nyquist criteria thanks to the very long transmit/receive FMT filters. Note that this excellent robustness against asynchronous interference is obtained to the detriment of latency which is very high in such a case.

The average MSEs of waveforms with complex orthogonality, obtained over all subcarriers, are plotted versus the timing offset for guard-bands $\delta = 0$, 15, 45 and 75 kHz, in Figure 4-14.

In the CP region, we can observe that CP-OFDM, Tx-W-OFDM and Rx-W-OFDM achieve the best performance with a MSE lower than -60 dB. It should be noted that the CP interval is shorter in Tx-W-OFDM and Rx-W-OFDM cases because a part of CP is used to absorb the windowing effect. In UFMC scheme, the CP region is reduced to a few sample periods due to the fact that the ZP is fully employed to absorb the transmit filter transient response. In WOLA-OFDM, W-UFMC and f-OFDM, the CP is no longer sufficient to deal with windowing or filtering effects giving rise to a slight distortion (between -40 to -35 dB) even in perfect synchronization case.

When the delay errors exceed the CP length, all schemes provide an improvement compared to CP-OFDM performance which is severely degraded. In contrast to the marginal gain achieved by Tx-W-OFDM, Rx-W-OFDM and UFMC systems, WOLA-OFDM, W-UFMC and f-OFDM schemes are offering more significant enhancements reaching up to 7, 10 and 16 dB for W-UFMC, WOLA-OFDM and f-OFDM, respectively (see $\delta = 75$kHz case).

As previously expected, N-continous OFDM system shows the worst performance which remains the same even when increasing the guard band size. Moreover, we can see that FMT outperforms the rest of waveforms by achieving the minimum MSE (about -60 dB) for the entire timing offset interval.

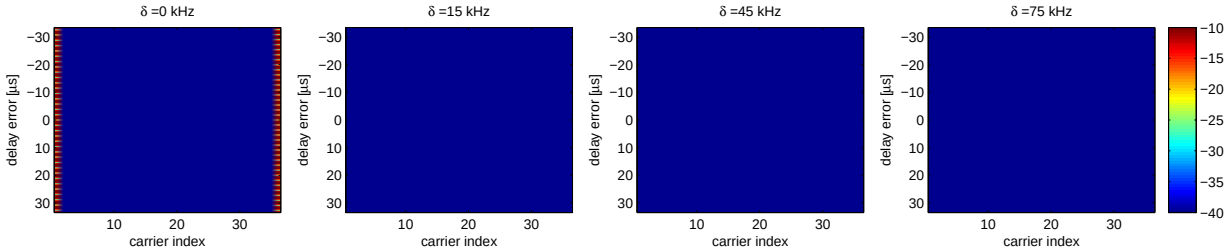

Figure 4-15: FBMC-OQAM: per-subcarrier NMSE against timing offset

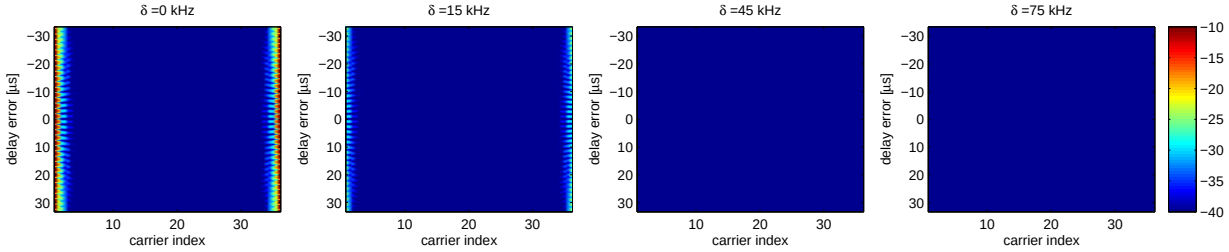

Figure 4-16: Lapped-OFDM: per-subcarrier NMSE against timing offset

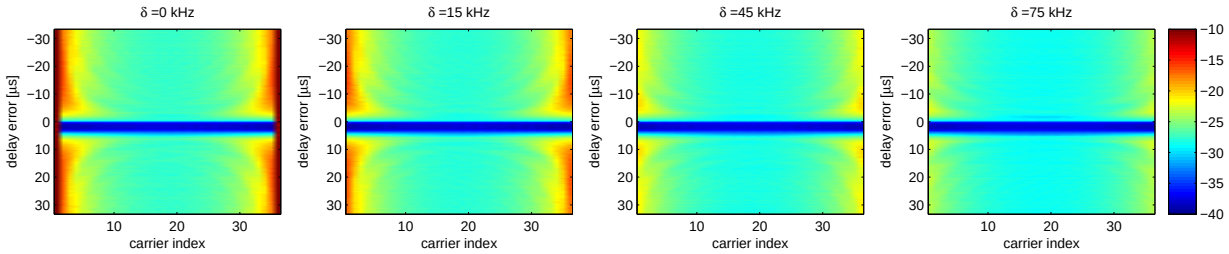

Figure 4-17: WCP-COQAM: per-subcarrier NMSE against timing offset

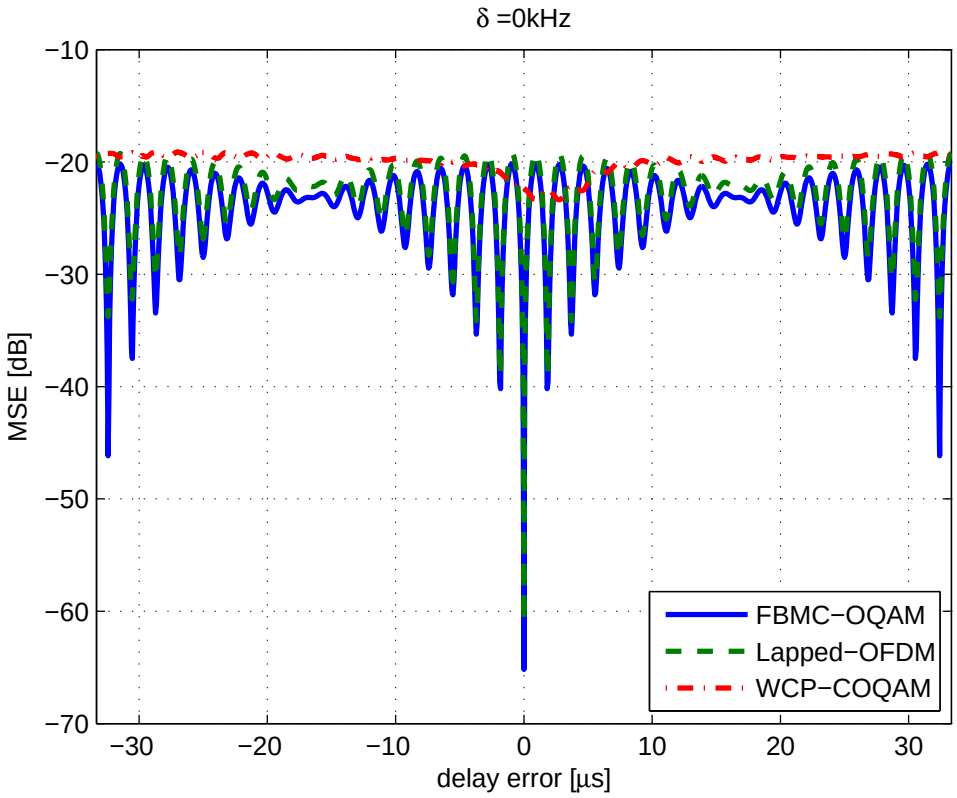
δ =0kHz
MSE [dB]
delay error [µs]
FBMC−OQAM
Lapped−OFDM
WCP−COQAM

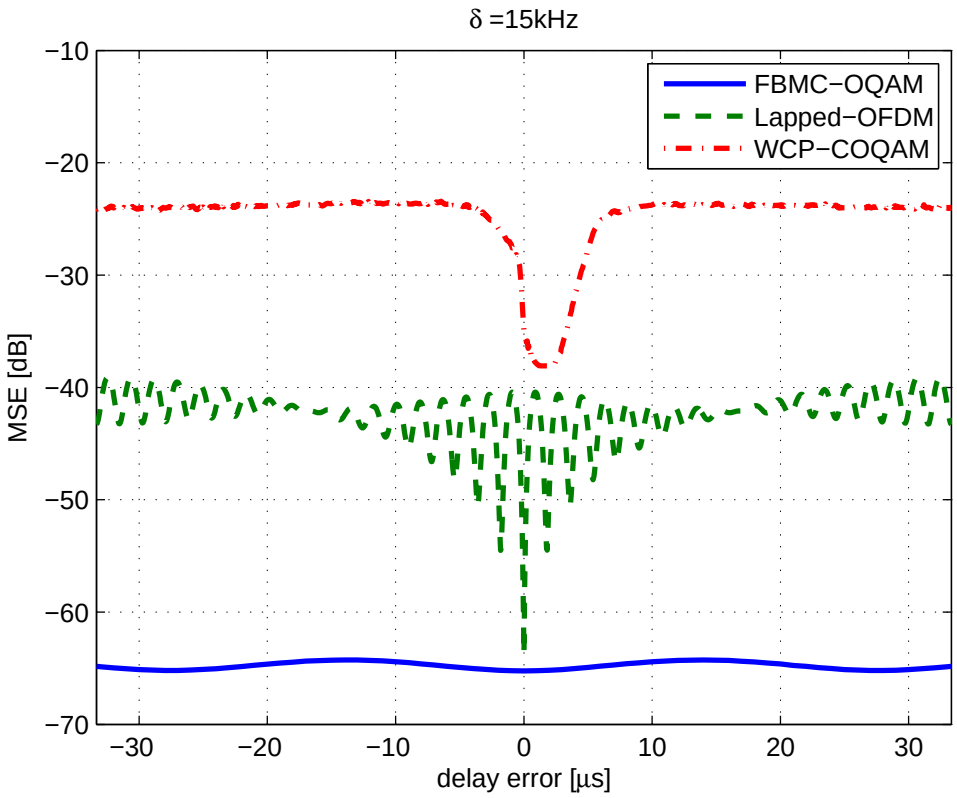
δ =15kHz
MSE [dB]
delay error [µs]
FBMC−OQAM
Lapped−OFDM
WCP−COQAM

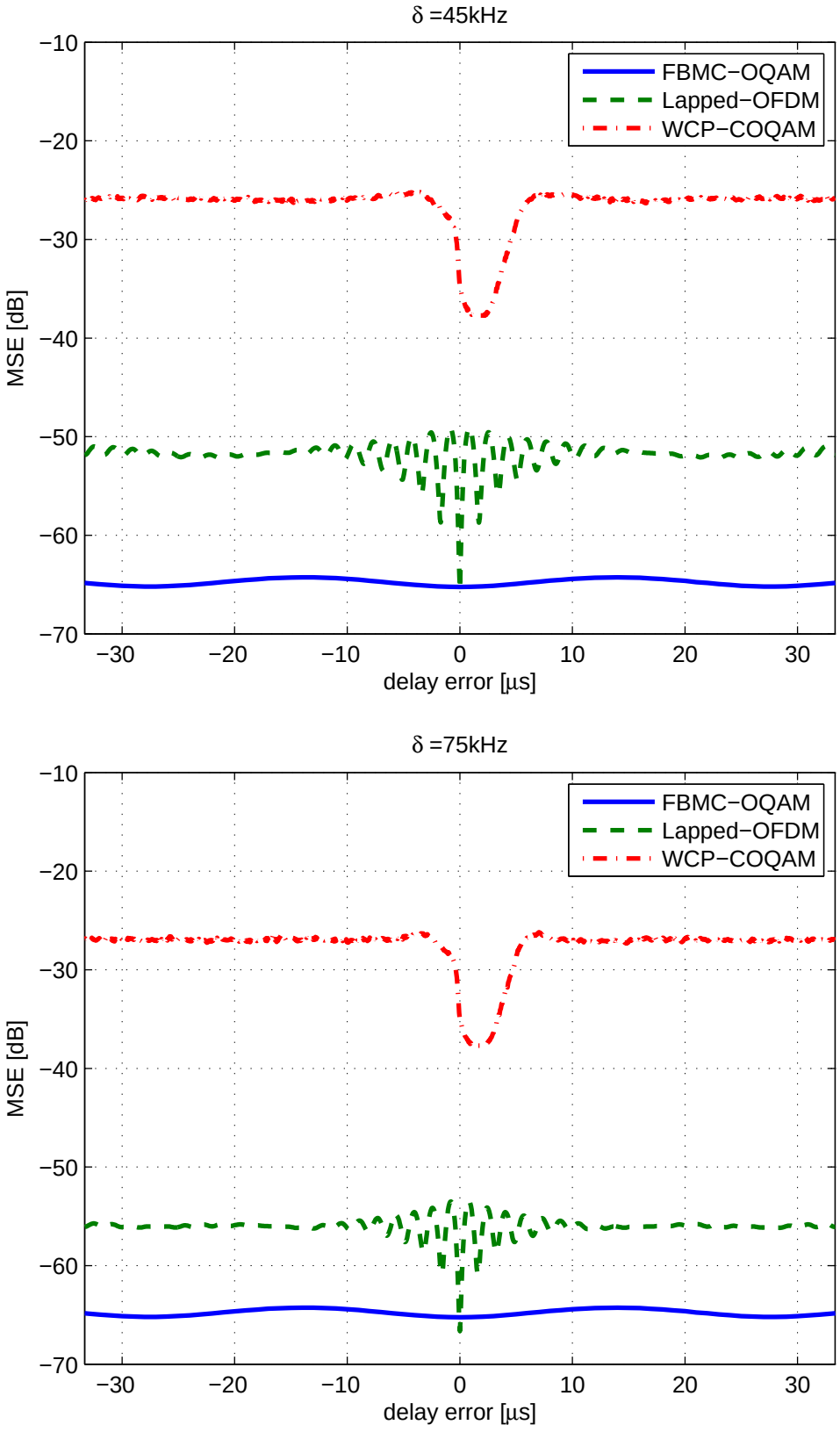

Figure 4-18: WFs with real orthogonality: average MSE against timing offset

4.4.1.2 Waveforms with real orthogonality

The per-subcarrier MSEs of FBMC-OQAM (using PHYDYAS prototype filter) and Lapped-OFDM are respectively shown in Figures 4-15 and 4-16. We can observe that a very small number of edge subcarriers are affected by interference thanks to the good spectral containment of FBMC-OQAM and Lapped-OFDM signals. Such a behavior is directly linked to the design of the prototype filter which is a key-property of FBMC waveforms. Indeed, FBMC prototype filters are commonly designed in order to minimize the interaction between subcarriers (e.g. in PHYDYAS case, a subcarrier overlaps at most with a single subcarrier on each side). When increasing the guard-band size, FBMC can reach the FMT performance by offering a MSE below -40 dB for the entire useful frequency band.

In contrast to FBMC-OQAM and Lapped-OFDM, WCP-COQAM shows a completely different behavior (see Figure 4-17). Let us recall that similarly to GFDM, a block based signal structure is adopted in WCP-COQAM thanks to the circular convolution property. In order to reduce the high-level spectrum side-lobes resulting from the inter-block discontinuities, a windowing is applied to the CP-COQAM signal. However, the windowing protection against asynchronous inter-user interference is less efficient compared to filtering one. This explains the poor WCP-COQAM performance in fully asynchronous case compared to FBMC-OQAM and Lapped-OFDM. However similar to CP based schemes, it should be pointed out that WCP-COQAM achieves negligible MSE inside the CP region.

The average MSEs of FBMC-OQAM, Lapped-OFDM and WCP-COQAM, computed over all subcarriers, are plotted w.r.t the timing offset for guard-bands $\delta = 0$, 15, 45 and 75 kHz, in Figure 4-18. One can see that all OQAM-based schemes provide almost the same performance (MSE about 20 dB) when there is no guard-band between the useful frequency band and the interfering one. Note that the obtained average MSE is inversely related to the frequency bandwidth of the user of interest. However, the average MSE becomes independent of the latter when a sufficient guard-band is separating the interfering spectrum from the useful one. Indeed, the FBMC-OQAM MSE reaches its minimum value (about $-65dB$) and remains constant for $\delta \geq 15$ kHz. The same result can be observed for Lapped-OFDM scheme but by inserting wider guard-bands. However, the WCP-COQAM still needs additional guard-band in order to reach its minimum MSE (about $-38dB$).

4.4.1.3 Non-orthogonal waveforms

The per-subcarrier MSE of MF-GFDM is shown in Figures 4-19 and 4-20 when the receiver is implemented without and with interference cancellation, respectively.

In the basic scheme (i.e. no interference cancellation), we can see that the MSE is almost the same for any subcarrier/timing offset. This strong MSE (dark orange color) is unfortunately meaningless to analyze the presence of asynchronous interference. In fact, since GFDM is non orthogonal, it suffers from high level of self interference which makes us unable to distinguish the asynchronous interference from the self-distortion. In order to overcome this limitation, let us analyze the MSE shown in Figure 4-20. One can see that asynchronous interference is more important on the edges of the useful frequency band. Thanks to transmit/receive filtering, the asynchronous interference decay becomes important when increasing the spectral distance between a given useful subcarrier and the interfering signal. Moreover, we can observe that the best performance is obtained when the timing offset is inside the CP interval except for the edge subcarriers when $\delta = 0$Hz. Note that the improved GFDM scheme (with interference cancellation) severely increases the complexity of the receiver since the interference is estimated by the reconstruction of the a-priori transmitted GFDM signal. It should be mentioned that

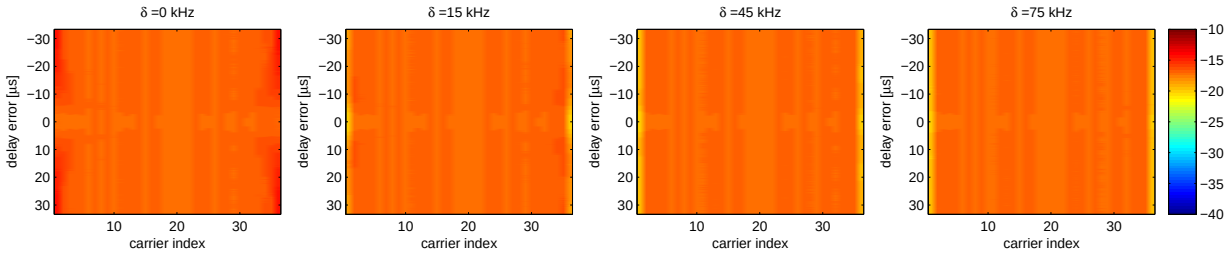

Figure 4-19: MF-GFDM no IC: per-subcarrier NMSE against timing offset

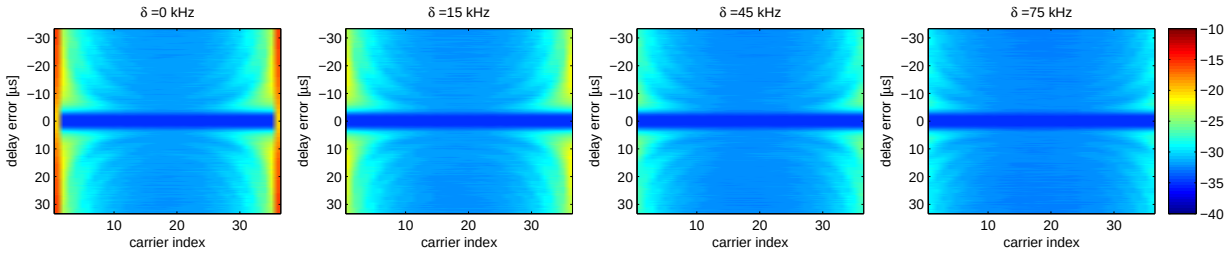

Figure 4-20: MF-GFDM w. IC: per-subcarrier NMSE against timing offset

the scenario considered is a noiseless case. These results are so a bound on the achievable performance. The interference cancellation scheme will suffer from noise and performance will be worst in case of AWGN channel

4.4.2 Carrier Frequency Offset

In this section, we assume that both users are perfectly synchronized in time domain but there is an offset between their respective carrier frequencies. The objective here is to examine the impact of CFO-induced inter-user interference on the performances of the various considered waveforms. The CFO ε considered here varies from -1.5kHz to $+1.5$kHz. Multiple guard-band sizes are also considered: $\delta = 0$, 15, 45 and 75 kHz. As mentioned in Section 3, the CFO shifts both interfering spectrum subbands in the same direction. This is why one of the guard-bands is reduced to $\delta - \varepsilon$kHz and the other is increased to $\delta + \varepsilon$kHz.

4.4.2.1 Waveforms with complex orthogonality

In Figures 4-21 and 4-22, we have the per-subcarrier MSE of CP-OFDM and Tx-W-OFDM systems. Both schemes provide roughly the same performance, where edges subcarriers are more sensitive to CFO compared to inner ones. In fact, the MSE at the edges becomes important even for negligible CFO (from 150Hz) while inner subcarriers keep best performances (MSE< -30dB) even when $\varepsilon = 1.5$kHz.

In Rx-W-OFDM and UFMC cases (Figures 4-23, 4-25), the subcarriers located at the middle of useful frequency band are more protected, compared to CP-OFDM, against CFO where the MSE is below -40dB (dark-blue color). Further subcarriers become preserved from asynchronous inter-user interference with large guard-bands. In fact, the MSE does not exceed -30dB in Rx-W-OFDM and -35dB in UFMC when $\delta =$75 kHz.

When it comes to WOLA-OFDM, W-UFMC and f-OFDM (Figures 4-24, 4-26 and 4-27), the same behavior can be reported. Indeed, except the sensitivity of edge subcarriers to CFO when there is no guard-band, WOLA-OFDM and W-UFMC provide good performance with a MSE below -35dB for any subcarrier/CFO point. However, f-OFDM needs wider guard-band

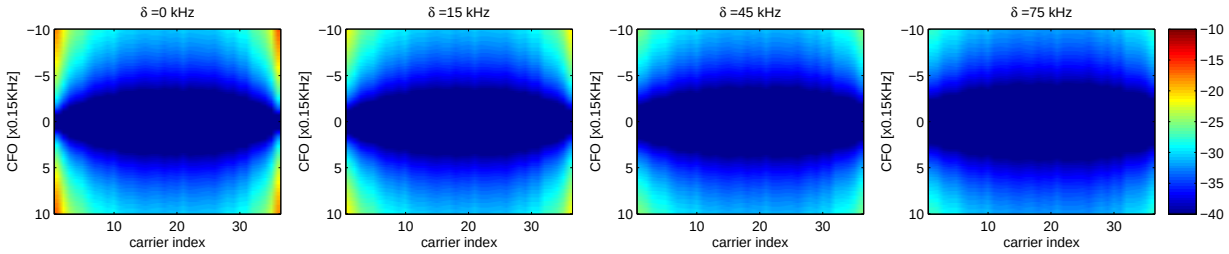

Figure 4-21: CP-OFDM: per-subcarrier NMSE against CFO

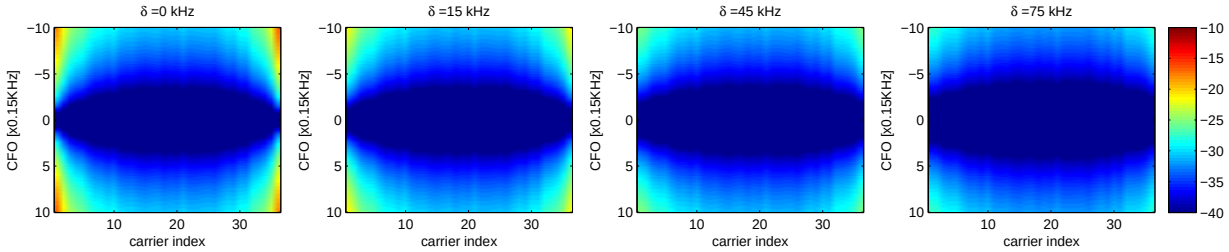

Figure 4-22: Tx-W-OFDM: per-subcarrier NMSE against CFO

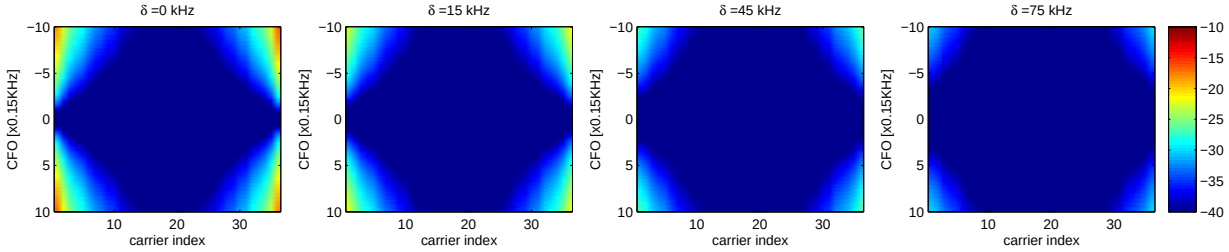

Figure 4-23: Rx-W-OFDM: per-subcarrier NMSE against CFO

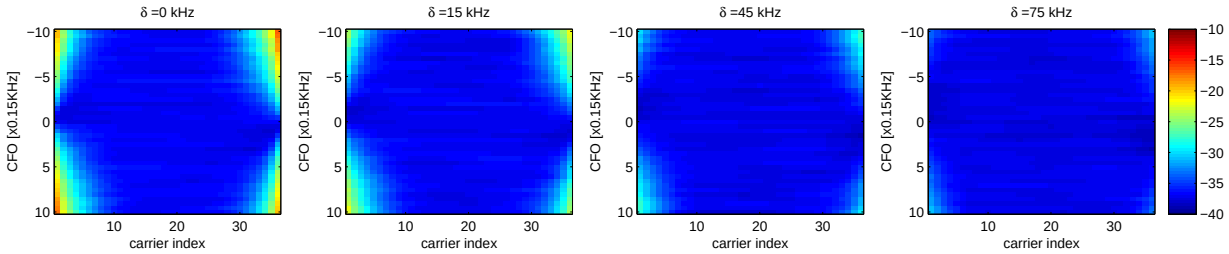

Figure 4-24: WOLA-OFDM: per-subcarrier NMSE against CFO

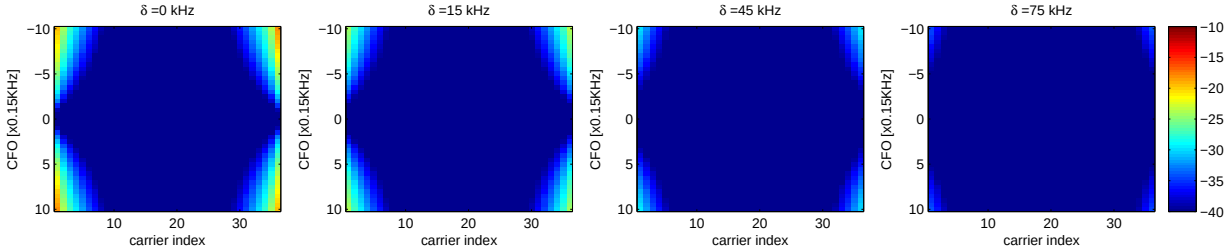

Figure 4-25: UFMC: per-subcarrier NMSE against CFO

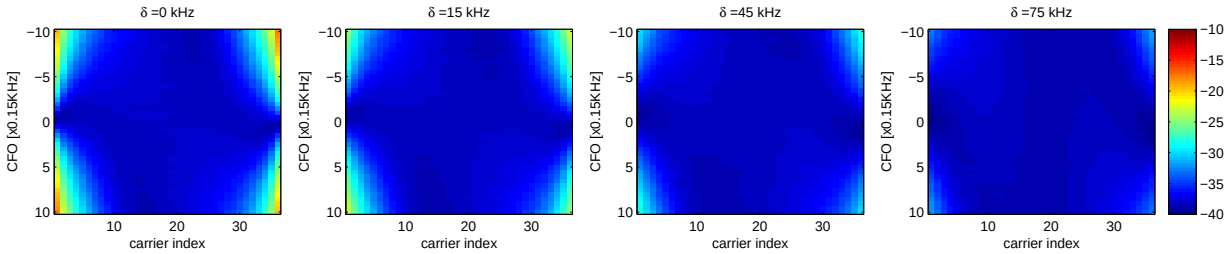

Figure 4-26: W-UFMC: per-subcarrier NMSE against CFO

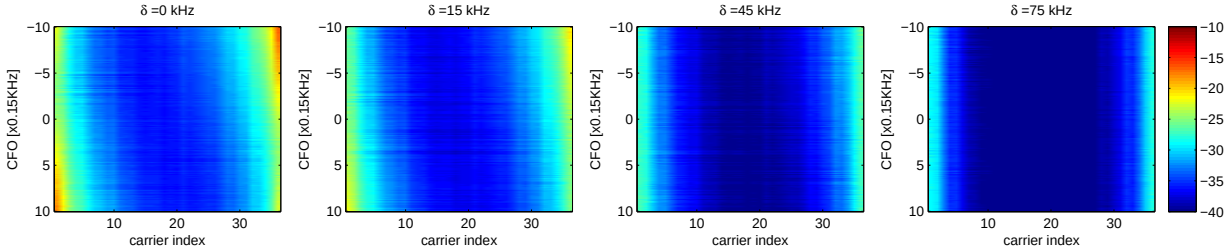

Figure 4-27: f-OFDM: per-subcarrier NMSE against CFO

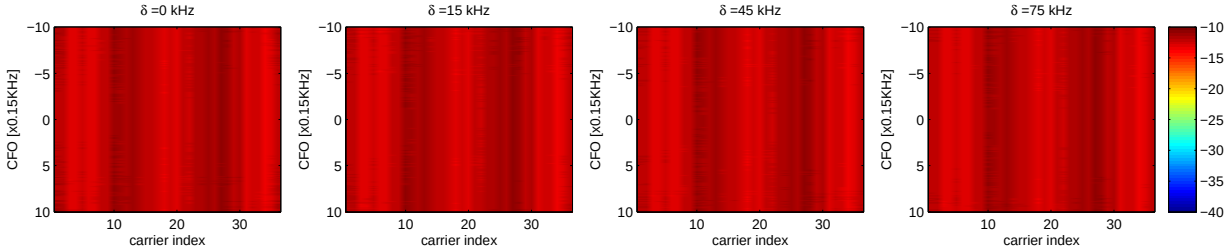

Figure 4-28: N-continuous OFDM: per-subcarrier NMSE against CFO

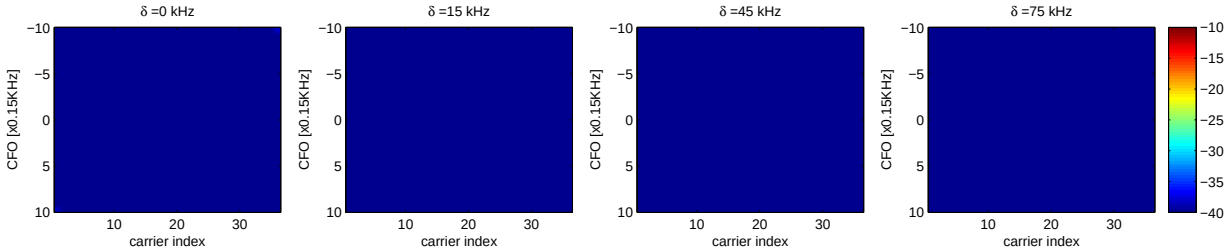

Figure 4-29: FMT: per-subcarrier NMSE against CFO

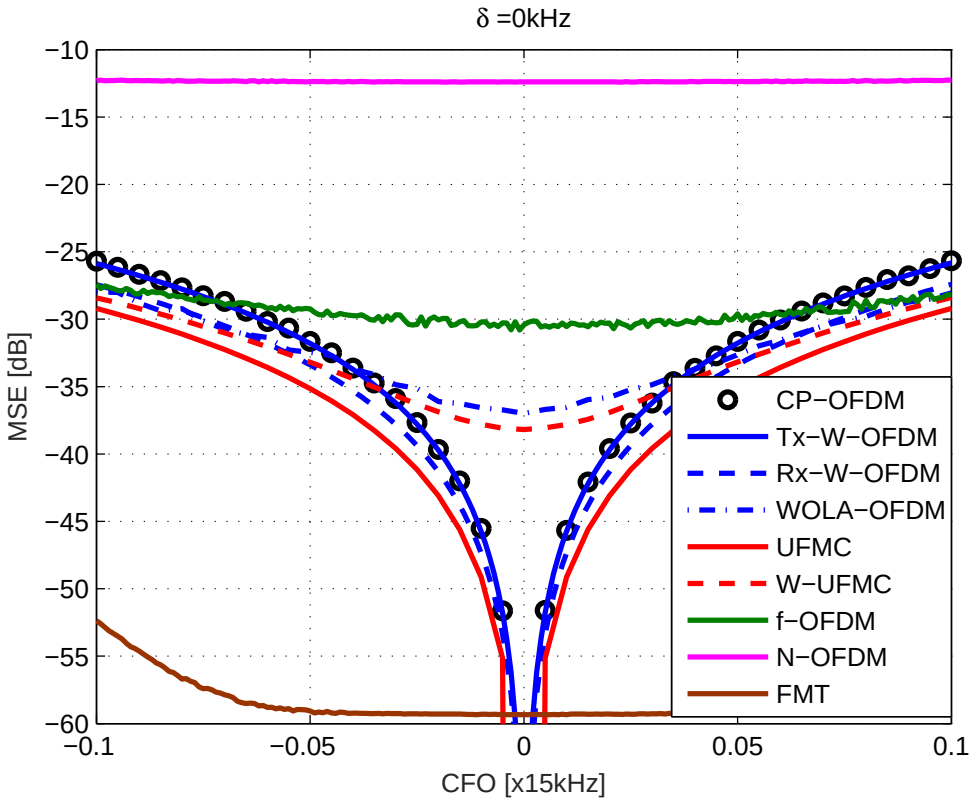
δ =0kHz
MSE [dB]
CFO [x15kHz]
CP−OFDM
Tx−W−OFDM
Rx−W−OFDM
WOLA−OFDM
UFMC
W−UFMC
f−OFDM
N−OFDM
FMT

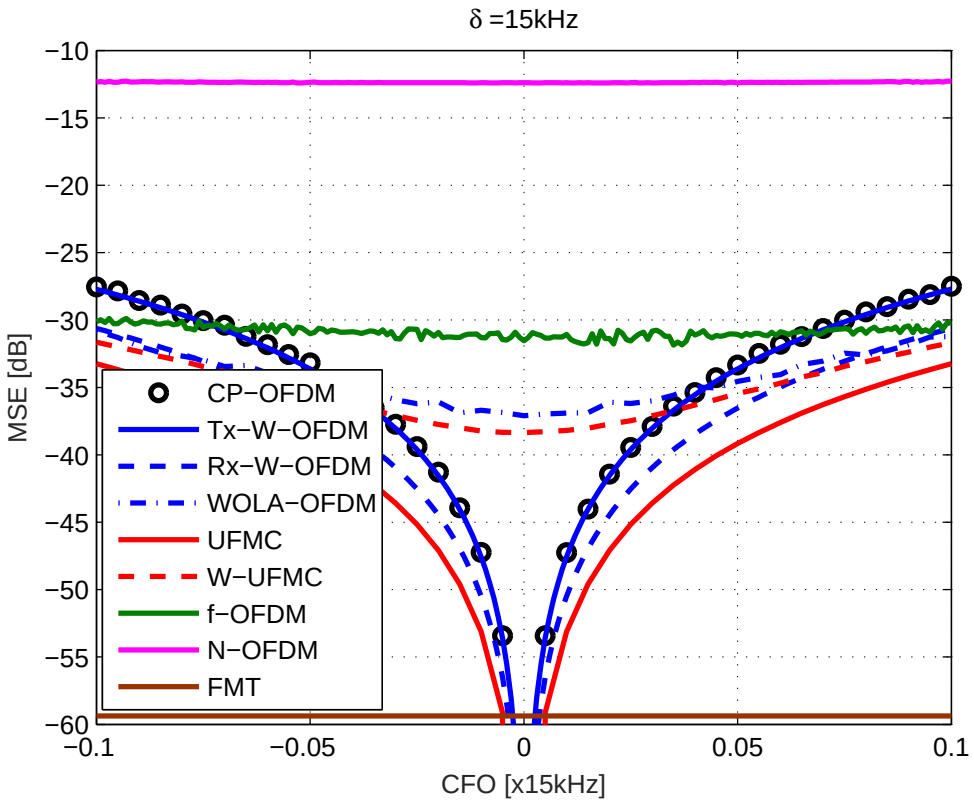
δ =15kHz
MSE [dB]
CFO [x15kHz]
CP−OFDM
Tx−W−OFDM
Rx−W−OFDM
WOLA−OFDM
UFMC
W−UFMC
f−OFDM
N−OFDM
FMT

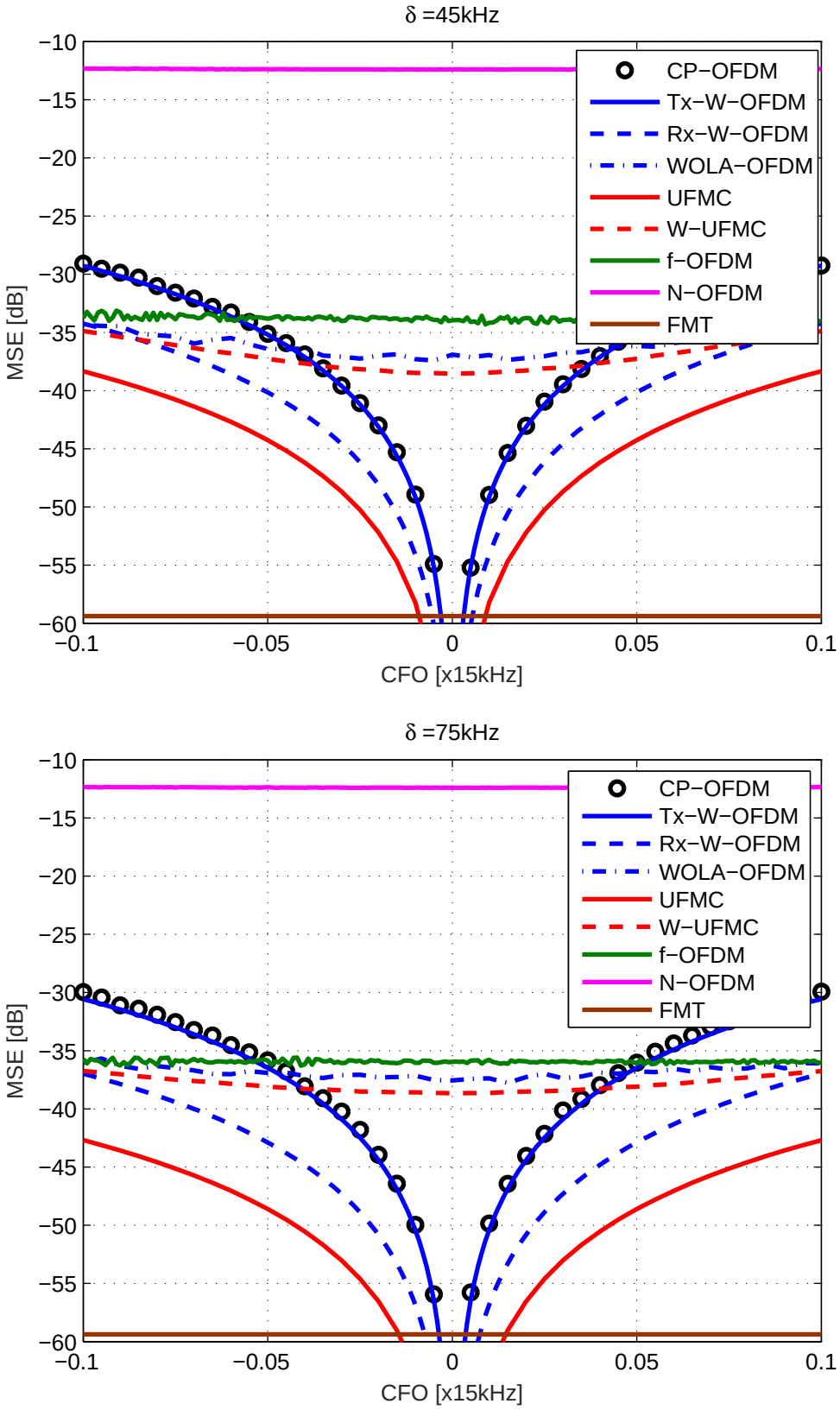

Figure 4-30: WFs with complex orthogonality: average MSE against CFO

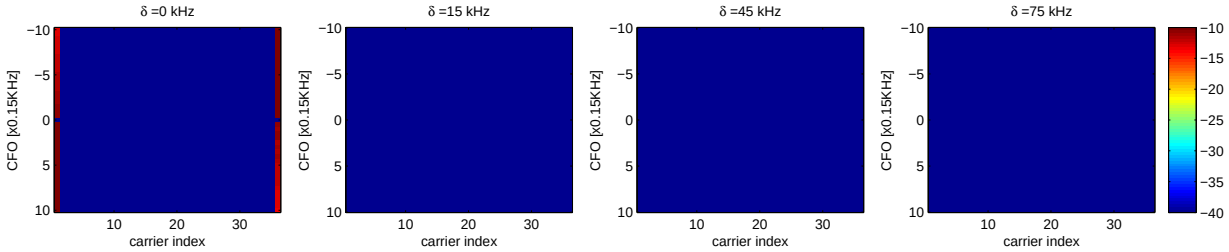

Figure 4-31: FBMC-OQAM: per-subcarrier NMSE against CFO

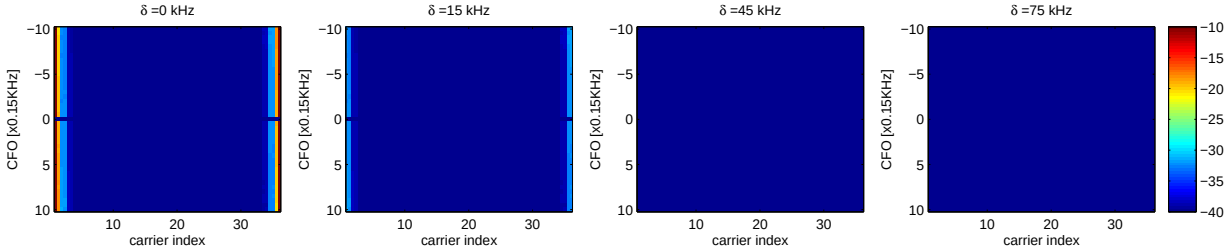

Figure 4-32: Lapped-OFDM: per-subcarrier NMSE against CFO

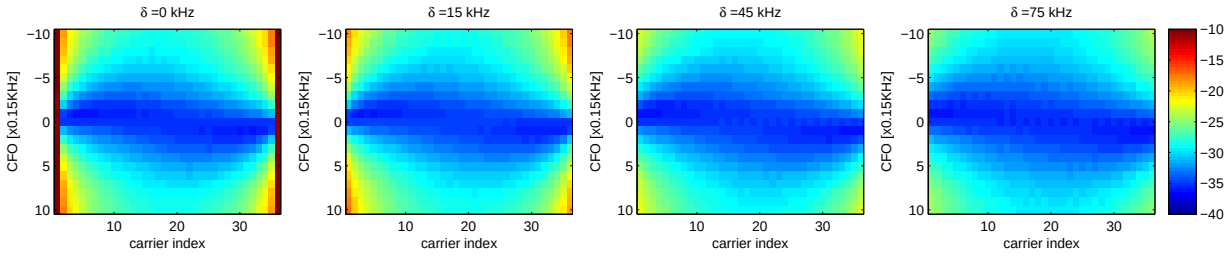

Figure 4-33: WCP-COQAM: per-subcarrier NMSE against CFO

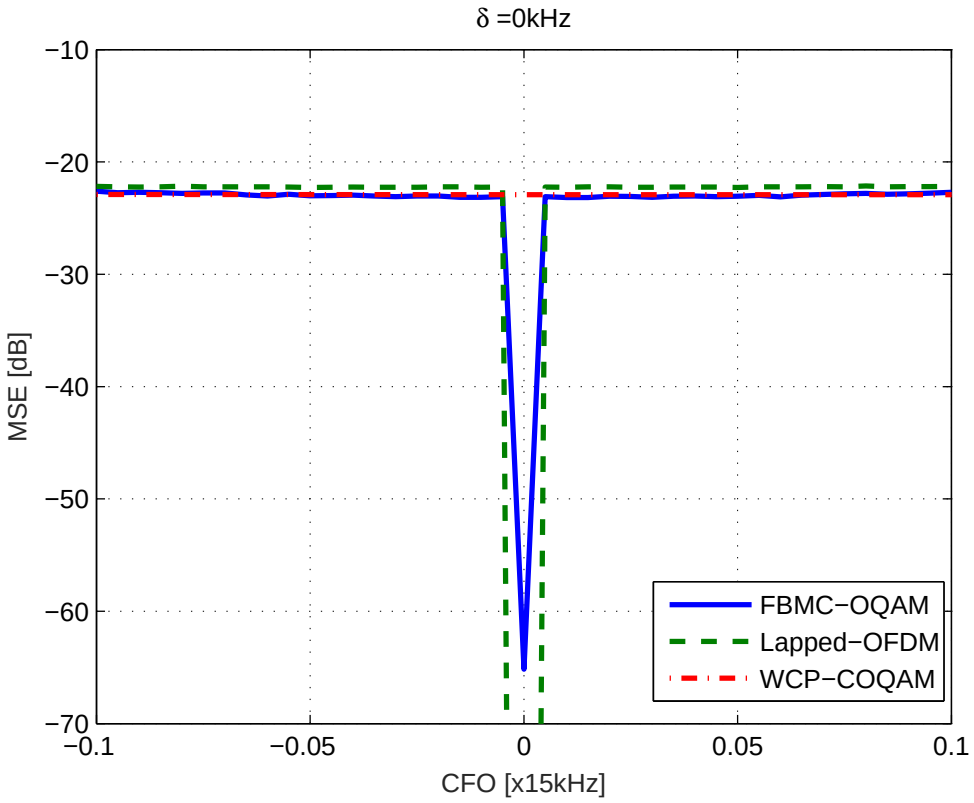
δ =0kHz
MSE [dB]
CFO [x15kHz]
FBMC−OQAM
Lapped−OFDM
WCP−COQAM
−10
−20
−30
−40
−50
−60
−70
−0.1
−0.05
0
0.05
0.1

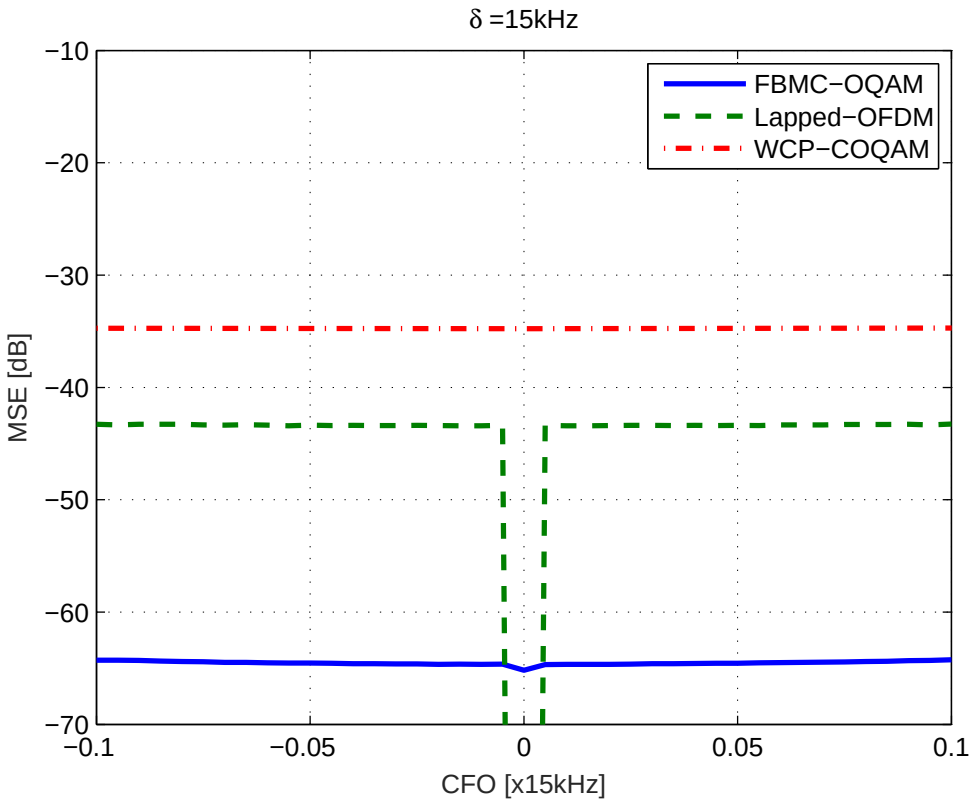
δ =15kHz
MSE [dB]
CFO [x15kHz]
FBMC−OQAM
Lapped−OFDM
WCP−COQAM
−10
−20
−30
−40
−50
−60
−70
−0.1
−0.05
0
0.05
0.1

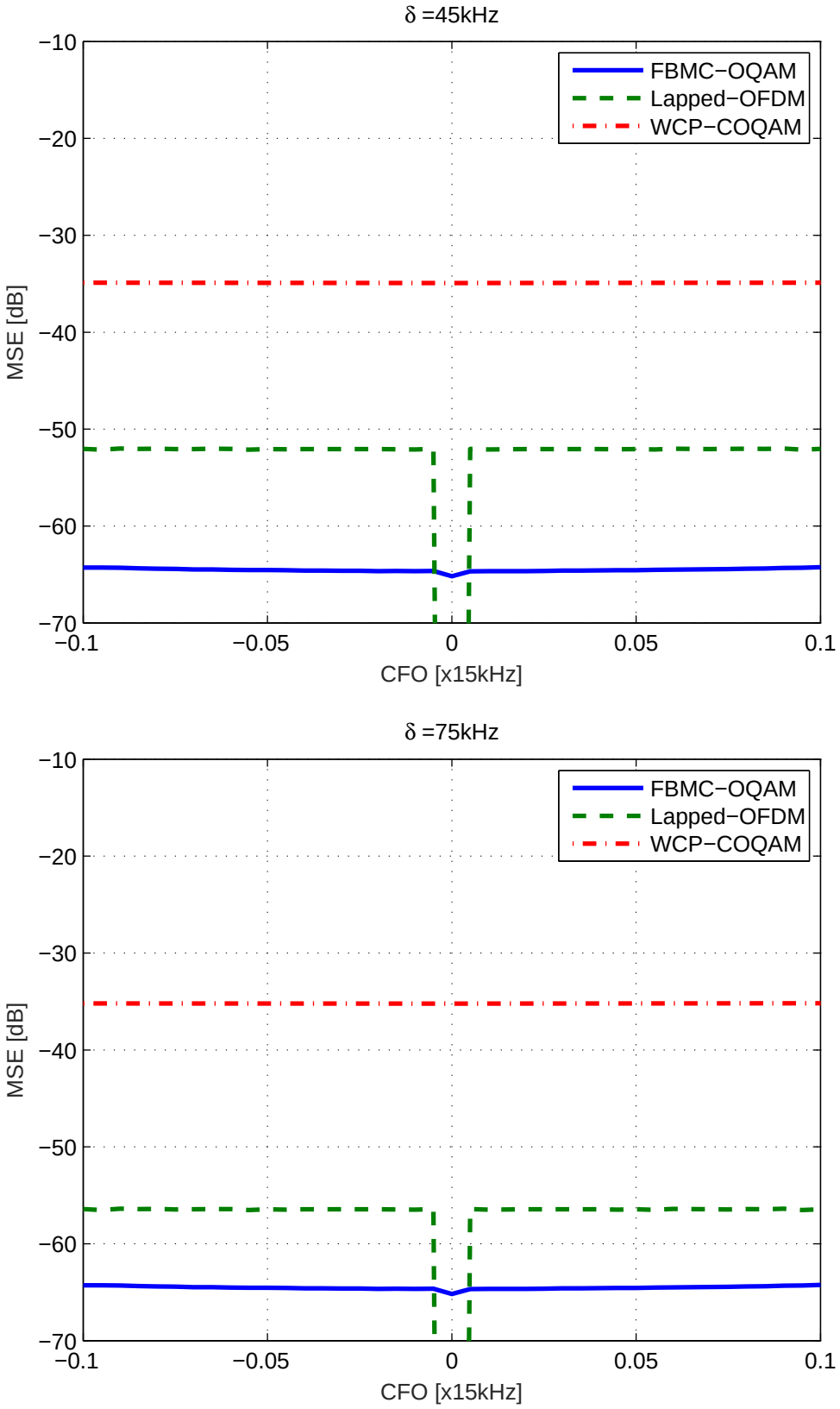

Figure 4-34: WFs with real orthogonality: average MSE against CFO

in order to ensure a uniform MSE for all useful subcarriers. Note that, f-OFDM inner subcarriers are more protected compared to WOLA-OFDM and W-UFMC where the MSE is lower than -40dB.

As discussed in the previous section, in N-continuous OFDM case, a uniform MSE of more than -10dB is shown for any subcarrier/CFO point (see Figure 4-28). We recall that this is due to the fact that the receiver does not have any knowledge about the precoding matrix applied at the transmitter in order to ensure the continuity between adjacent OFDM symbols.

In FMT case (Figure 4-29), the best performance is achieved where a negligible MSE (dark-blue color : MSE less than -40dB) is shown for all useful subcarriers. This can be explained by the fact that the orthogonality between subcarriers is maintained. Indeed, FMT subcarriers are arranged such that adjacent sub-bands do not overlap. Note that excess subcarrier bandwidth is reserved keeping thus non-overlapped subcarriers. It is worth pointing out here that the maximum CFO corresponds to 10% of the subcarrier spacing. So in case of higher CFO values ($> 50\%$ of the subcarrier spacing), the edge subcarriers become no longer protected against asynchronous inter-user interference.

The average MSEs of schemes with complex orthogonality, computed over all subcarriers, are plotted, in Figure 4-30, as function of CFO considering various guard-bands $\delta = 0$, 15, 45 and 75 kHz. Looking at the different MSE curves, we can distinguish three groups of waveforms w.r.t to the sensitivity to CFO:

- weak sensitivity: in this group, we have f-OFDM, N-continuous OFDM and FMT. The MSE is practically invariant w.r.t to CFO.
- mild sensitivity: WOLA-OFDM and W-UFMC MSE becomes more independent of CFO when increasing the guard-band size.
- strong sensitivity: the MSEs of the other waveforms is more important and rapidly grow with CFO.

4.4.2.2 Waveforms with real orthogonality

The per-subcarrier CFO-induced MSEs of FBMC-OQAM and Lapped-OFDM are depicted in Figures 4-31 and 4-32, respectively. As previously discussed, the robustness against asynchronism is ensured thanks to transmit/receive filtering that limits the interaction between a given subcarrier and its neighborhood. Indeed, one can see that, similar to timing asynchronism, only a small number of subcarriers are suffering from asynchronous inter-user interference (e.g. one subcarrier on each side in FBMC-OQAM case).

Due to the block-based structure which is built-in property of WCP-COQAM signal, this scheme is more sensitive to CFO-induced inter-user interference compared to FBMC-OQAM and Lapped-OFDM systems. In fact, one can observe that the asynchronous interference caused by other user is more important, impacting thus a higher number of useful subcarriers compared to other OQAM-based waveforms. Moreover, this interference is slowly decreasing w.r.t. to the spectral distance between a given victim subcarrier and the interfering signal.

The average MSE is plotted against the CFO for FBMC-OQAM, Lapped-OFDM and WCP-COQAM, when $\delta = 0$, 15, 45 and 75 kHz, in Figure 4-34. In the absence of guard-bands between the useful spectrum and the interfering one, all OQAM-based waveforms approximately show the same performance. It is worth pointing out that, the average MSE level does not really give a reliable information about the performances of the considered schemes, since it is inversely linked to the number of useful subcarriers. Similar to timing asynchronism case,

the FBMC-OQAM useful subcarriers become completely free of asynchronous interference from $\delta = 15$kHz, while more important guard-bands are required to reach the best performance of Lapped-OFDM. In WCP-COQAM case, an improvement of more than 10dB can be noticed by inserting a guard-band of 15kHz. However, the additional gain becomes marginal compared to $\delta = 15$kHz when considering wider guard-bands.

4.4.2.3 Non-orthogonal waveforms

The MF-GFDM performance in terms of per-subcarrier MSE against CFO is depicted in Figures 4-35 and 4-36 without and with interference cancellation, respectively.

Similar to the timing offset case, high level MSE (dark orange color) can be observed in the entire useful band for any CFO value, when there is no interference cancellation at the receiver side (see Figure 4-35). Such a results is a natural outcome of the presence of the intrinsic GFDM interference. In order to better understand the asynchronous interference effect on the performance of GFDM, let us observe the MSE depicted in Figure 4-36. Indeed, since the considered CFO does not exceed the subcarrier spacing (i.e. $|\varepsilon_{max}| = 1.5$kHz), we can see that only one subcarrier on each side is highly impacted by the asynchronous interference (see $\delta = 0$kHz). Moreover, increasing the guard-band size induces asynchronous interference decrease until this interference becomes almost negligible compared to the residual GFDM self-interference (see $\delta =$75kHz).

4.5 PAPR

All multicarrier schemes have in common the major problem of very high fluctuation of the instantaneous power of the signal to be transmitted. More specifically, the probability of having an instantaneous power 8 to 12 dB greater than the mean power is non negligible. These instantaneous power peaks produce signal excursions into the nonlinear region of operation of the power amplifier (PA) at the RF front-end, generating distortions and spectral regrowth. Thus, it is important to assess and compare the performance in terms of power fluctuation of the considered waveform.

In the literature, the Complementary Cumulative Distribution Function (CCDF) of the PAPR is a widely used performance criterion. The CCDF of the PAPR is defined as the probability that the PAPR per block of consecutive symbols exceeds a given level P_0:

$$\mathrm{CCDF}\left[PAPR\left(b\right)\right] = \mathrm{Prob}\left[PAPR\left(b\right) > P_0\right] \tag{4.1}$$

where $PAPR(b) = \frac{\max\left[|s(n)|^2\right]}{E\left[|s(n)|^2\right]}$,
b is a the block index,
$s(n)$ is the time domain block symbols
and $n = [0; N_{\mathrm{Block}} - 1]$,
N_{Block} is the considered block size[3].

The CCDF of PAPR is a representation that takes into account only one sample per block (which is the highest peak). From a practical point of view, it seems more relevant to consider all the samples that could go into the nonlinear area of the PA as they all generate distortion, instead of the samples with the highest power during the duration of a block. Therefore, it is

[3]Note that for OFDM, $N_{\mathrm{Block}} = N_{\mathrm{FFT}}$

interesting to analyze the CCDF of the instantaneous power (IAPR, Instantaneous to Average Power Ratio) given by [CBS06]:

$$\mathrm{CCDF}\left[\frac{|s(n)|^2}{E\left[|s(n)|^2\right]}\right] = \mathrm{Prob}\left[\frac{|s(n)|^2}{E\left[|s(n)|^2\right]} > P_0\right] \tag{4.2}$$

where n refers to the time index of the whole signal to be transmitted.

The comparisons of the CCDF of the IAPR and PAPR are presented in figure 4-37. Note that the block size N_{Block} used for the PAPR computation is the same for all the waveforms and has been set to 1024 since it refers to the size of a traditional CP-OFDM block symbol as configured for LTE. We can observe that, for a given number of subcarriers, traditional CP-OFDM provides the best PAPR and IAPR performances, which is in line with [CPGB16]. Nevertheless, all multicarriers waveforms presented in this document have almost equivalent IAPR and PAPR performances, even if GFDM and N-continuous waveforms have respectively 1 and 1.5 dB of degradation with respect to traditional CP-OFDM.

4.6 Complexity

This section aims at estimating the complexity of the transmitter and receiver schemes for the considered waveforms. The complexity will be assessed by counting the number of real multiplications per unit of time to perform both the modulation and demodulation process (equalization and (de)coding stages will not be taken into account in this evaluation). It has been preferred to assess the number of multiplications per unit of time in order to compare as fairly as possible the schemes that do not share the same sampling frequency. To do so, a burst of N_s symbols is considered. For the schemes that exhibit symbol overlapping, the complexity will be benchmarked when N_s tends to infinity.

From now, it will be assumed that one complex multiplication can be carried out with three real multiplications [Kra99]. F_s will denote the sampling frequency and T_s the sampling period. Moreover, the Cooley-Tukey implementation will be considered for the Fast Fourier Transforms (FFT).

4.6.1 WF with complex orthogonality

CP-OFDM

The complexity of the transmitter (resp. the receiver) is reduced to a N-point IFFT (resp. N-point IFFT), which leads to:

$$\mathrm{C}_{\mathrm{OFDM,Tx/Rx}} = \frac{3N}{2}\log_2(N) \tag{4.3}$$

The number of multiplications per unit of time is then:

$$\mathbb{C}_{\mathrm{OFDM,Tx/Rx}} = \frac{\mathrm{C}_{\mathrm{OFDM,Tx/Rx}} N_s}{N_s(N+N_{CP})T_s} = \frac{\mathrm{C}_{\mathrm{OFDM,Tx/Rx}}}{(N+N_{CP})}F_s \tag{4.4}$$

WOLA-OFDM

When it comes to WOLA-OFDM, the complexity also takes into consideration the windowing (real coefficients applied to complex data).

$$\mathrm{C}_{\mathrm{WOLA,Tx}} = \frac{3N}{2}\log_2(N) + 4\mathrm{W}_{\mathrm{Tx}} \tag{4.5}$$

$$\mathrm{C}_{\mathrm{WOLA,Rx}} = \frac{3N}{2}\log_2(N) + 4\mathrm{W}_{\mathrm{Rx}} \tag{4.6}$$

The number of multiplications per unit of time is then:

$$\mathbb{C}_{\mathrm{WOLA,Tx/Rx}} = \frac{\mathrm{C}_{\mathrm{WOLA,Tx/Rx}} N_s}{(W_{\mathrm{Tx}} + N_s(N+N_{CP}))T_s} \xrightarrow{N_s\to\infty} \frac{\mathrm{C}_{\mathrm{WOLA,Tx/Rx}}}{(N+N_{CP})} F_s \tag{4.7}$$

UFMC (UF-OFDM)

The data is processed at the RB level (B active Rbs out of N available). For each RB, first there is the predistortion stage with n complex multiplications. Then there is the transposition to the time domain with only n active sub carriers out of N. The IFFT is therefore mainly fed by null elements and its complexity can be reduced to $N + \frac{N}{2}\log_2(n)$ complex multiplications. The convolution with the baseband real filter (of length L) adds $N\lfloor\frac{L}{2}\rfloor$ multiplications (neglecting the rise and fall time of the convolution). Finally the upconversion to the carrier frequencies counts for $3(N+L-1)$ real multiplications.
At the receiver side, there is a $2N$-point FFT. A windowing can be considered in reception which adds $2L$ multiplications and this receiver is denoted as wUFMC .

$$\mathrm{C}_{\mathrm{UFMC,Tx}} = 3Bn + 3B\left(N + \frac{N}{2}\log_2(n)\right) + 3B(N+L-1) + 2BN\lfloor\frac{L}{2}\rfloor \tag{4.8}$$

$$\mathrm{C}_{\mathrm{UFMC,Rx}} = 3N\log_2(2N) \tag{4.9}$$

$$\mathrm{C}_{\mathrm{wUFMC,Rx}} = 3N\log_2(2N) + 2L \tag{4.10}$$

The number of multiplications per unit of time is then:

$$\mathbb{C}_{\mathrm{UFMC,Tx/Rx}} = \frac{\mathrm{C}_{\mathrm{UFMC,Tx/Rx}} N_s}{N_s(N+L-1)T_s} = \frac{\mathrm{C}_{\mathrm{UFMC,Tx/Rx}}}{(N+L-1)} F_s \tag{4.11}$$

It must be pointed out that reduced complexity schemes have been proposed for UF-OFDM [MZS+16][WS15].

Filtered OFDM

The complexity of this modulation scheme is induced by the (I)FFT and the filtering (convolution).

$$\mathrm{C}_{\mathrm{fOFDM,Tx/Rx}} = \frac{3N}{2}\log_2(N) + 3\left(N+N_{CP}\right)\lfloor\frac{L}{2}\rfloor \tag{4.12}$$

The number of multiplications per unit of time is then:

$$\mathbb{C}_{\mathrm{fOFDM,Tx/Rx}} = \frac{\mathrm{C}_{\mathrm{fOFDM,Tx/Rx}} N_s}{(L + N_s(N+N_{CP}))T_s} \xrightarrow{N_s\to\infty} \frac{\mathrm{C}_{\mathrm{fOFDM,Tx/Rx}}}{(N+N_{CP})} F_s \tag{4.13}$$

N-continuous OFDM

The complexity of the transmitter is induced by the FFT stage and the precoding (N^2 complex multiplications). The receiver is the same used in CP-OFDM.

$$\mathrm{C}_{\mathrm{N-ContOFDM,Tx}} = 3N^2 + \frac{3N}{2}\log_2(N) \tag{4.14}$$

$$\mathrm{C}_{\mathrm{N-ContOFDM,Rx}} = \frac{3N}{2}\log_2(N) \tag{4.15}$$

The number of multiplications per unit of time is then:

$$\mathbb{C}_{\mathrm{N-ContOFDM,Tx/Rx}} = \frac{\mathrm{C}_{\mathrm{N-ContOFDM,Tx/Rx}} N_s}{N_s(N+N_{\mathrm{CP}})T_s} \xrightarrow{N_s\to\infty} \frac{\mathrm{C}_{\mathrm{N-ContOFDM,Tx/Rx}}}{(N+N_{CP})}F_s \tag{4.16}$$

FMT

The FMT modulation is implemented by means of a polyphase network in both the transmitter and the receiver.

$$\mathrm{C}_{\mathrm{FMT,Tx/Rx}} = \frac{3M}{2}\log_2(N) + 2 * KN \tag{4.17}$$

The number of multiplications per unit of time is then:

$$\begin{aligned}\mathbb{C}_{\mathrm{FMT,Tx/Rx}} &= \frac{\mathrm{C}_{\mathrm{FMT,Tx/Rx}} N_s}{(KM + M(N_s-1))T_s} \\ &\xrightarrow{N_s\to\infty} \frac{\mathrm{C}_{\mathrm{FMT,Tx/Rx}}}{M}F_s\end{aligned} \tag{4.18}$$

4.6.2 WF with real orthogonality

FBMC-OQAM and Lapped-OFDM

The complexity of FBMC/OQAM and Lapped-OFDM is related to the (I)FFT, the real filtering stage and the phase offset. The difference between the two modulation schemes is the considered overlapping factor (typically 4 for FBMC/OQAM and 2 for Lapped-OFDM). The complexities of the transmitter and receiver schemes are identical.

$$\mathrm{C}_{\mathrm{FBMC-OQAM/Lapped,Tx/Rx}} = \frac{3M}{2}\log_2(M) + MK + M \tag{4.19}$$

The frequency-sampling scheme can also be considered. It works with a KM-point (I)FFT and a point-wise filtering with $2K-1$ multiplications per symbol, and a phase offset.

$$\mathrm{C}_{\mathrm{FS-FBMC,Tx/Rx}} = \frac{3KM}{2}\log_2(KM) + M(2K-1) + M \tag{4.20}$$

The number of multiplications per unit of time is then:

$$\begin{aligned}\mathbb{C}_{\mathrm{FBMC-OQAM,Tx/Rx}} &= \frac{\mathrm{C}_{\mathrm{FBMC-OQAM,Tx/Rx}} N_s}{(KM + \frac{M}{2}(N_s-1))T_s} \\ &\xrightarrow{N_s\to\infty} \frac{\mathrm{C}_{\mathrm{FBMC-OQAM,Tx/Rx}}}{\frac{M}{2}}F_s\end{aligned} \tag{4.21}$$

WCP-COQAM

The complexity of WCP-COQAM transmitter (pruned IFFT-based algorithm) can be divided by the OFDM stage with M carriers and the circular convolution stage with $2 * MK$ real multiplications and the windowing with $2 * 4 * W_{T_x}$ real multiplications. The complexity is normalized by the size of the block K. When it comes to the receiver scheme, the complexity is induced by the MK-point FFT, the point-wise filtering with $M(2K-1)$ and the $2K$-IFFT applied at each carrier. The complexity of the receiver is also normalized by the block length K.

$$\mathrm{C}_{\mathrm{WCP-COQAM,Tx}} = 3\frac{M}{2}\log_2(M) + 2MK + 8W_{T_x} \tag{4.22}$$

$$\mathrm{C}_{\mathrm{WCP-COQAM,Rx}} = 3\frac{M}{2}\log_2(KM) + 3M\log_2(2K) + \frac{M}{K}(2K-1) \tag{4.23}$$

The number of multiplications per unit of time is then:

$$\begin{aligned}\mathbb{C}_{\mathrm{WCP-COQAM,Tx/Rx}} &= \frac{\mathrm{C}_{\mathrm{WCP-COQAM,Tx/Rx}} N_s}{(KM + \frac{M}{2}(N_s-1))T_s} \\ &\xrightarrow{N_s\to\infty} \frac{\mathrm{C}_{\mathrm{WCP-COQAM,Tx/Rx}}}{\frac{M}{2}} F_s\end{aligned} \tag{4.24}$$

4.6.3 WF without orthogonality

FBMC-QAM

FBMC/QAM uses a dual-filterbank fed by M QAM symbols. The complexities of the transmitter and receiver schemes are identical [KYKS16].

$$\mathrm{C}_{\mathrm{FBMC-QAM,Tx/Rx}} = 2 \times \left(\frac{3M}{4}\log_2(\frac{M}{2}) + MK\right) \tag{4.25}$$

The number of multiplications per unit of time is then:

$$\begin{aligned}\mathbb{C}_{\mathrm{FBMC-QAM,Tx/Rx}} &= \frac{\mathrm{C}_{\mathrm{FBMC-QAM,Tx/Rx}} N_s}{(KM + M(N_s-1))T_s} \\ &\xrightarrow{N_s\to\infty} \frac{\mathrm{C}_{\mathrm{FBMC-QAM,Tx/Rx}}}{M} F_s\end{aligned} \tag{4.26}$$

GFDM

The complexity of the GFDM transmitter is given by the complexity of K FFTs of size M, the windowing process as well as the B filtering processes where B is the number of active carriers. The complexity is therefore given by:

$$\mathrm{C}_{\mathrm{GFDM,Tx}} = K\frac{3N}{2}\log_2(N) + 2KNN_{CP} + 2BNK^2 \tag{4.27}$$

The number of multiplications per unit of time is then:

$$\mathbb{C}_{\mathrm{GFDM,Tx}} = \mathrm{C}_{\mathrm{GFDM,Tx}}\frac{1}{KN + N_{CP}}F_s \tag{4.28}$$

Typical receivers for GFDM consider match filtering and successive interference cancellation [DMLF12]. Therefore the complexity of the receiver is very large and is not evaluated in this work.

4.6.4 Numerical Application

According to the aforementioned closed-form expressions and the configurations given in 3.2, it is possible to numerically assess the complexity of the different transmission and reception schemes as given in figures 4-38 and 4-39. A synthesis table is also proposed in 4-4 for the transmitter and in 4-5 for the receiver.

A classification of the waveforms regarding their filtering method can be considered: convolution, point wise, filter bank or no filtering. This study of complexity points out that filtering performed by convolution (UF-OFDM, WCP-COQAM, fOFDM) are highly inefficient in terms of implementation. On the contrary, point-wise filtering (WOLA) is efficiently realized. Waveforms with filter bank structure are in between. Regarding the receivers, the previous observation still holds.

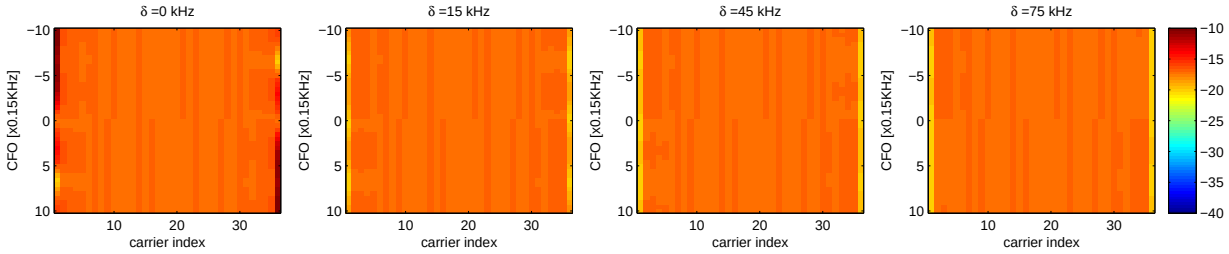

Figure 4-35: MF-GFDM no IC: per-subcarrier NMSE against CFO

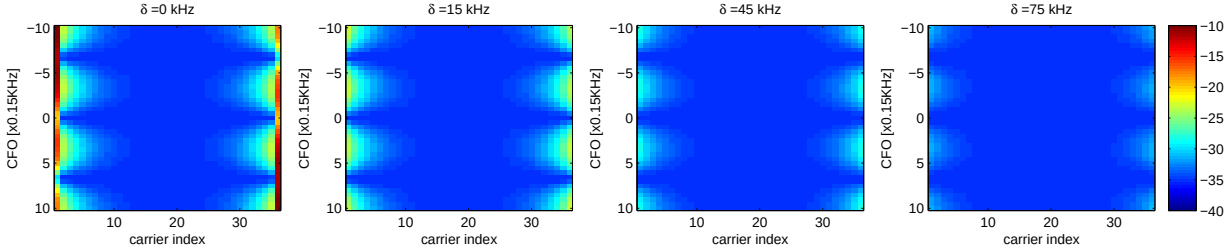

Figure 4-36: MF-GFDM w. IC: per-subcarrier NMSE against CFO

	5 RBs	25 RBs	50 RBs	Ranking (50 RBs)
CP-OFDM	1.00	1.00	1.00	1
WOLA	1.01	1.01	1.01	2
UF-OFDM	25.80	131.01	263.93	11
fOFDM	55.80	55.80	55.80	8
N-continuous OFDM	205.80	205.80	205.80	10
FMT	3.35	3.35	3.35	7
FBMC-OQAM	3.28	3.28	3.28	5
Lapped OFDM	2.71	2.71	2.71	4
FBMC-QAM	2.68	2.68	2.68	3
GFDM	16.18	35.96	60.68	9
WCP COQAM	3.30	3.30	3.30	6

Table 4-4: Tx complexity normalized with respect to OFDM

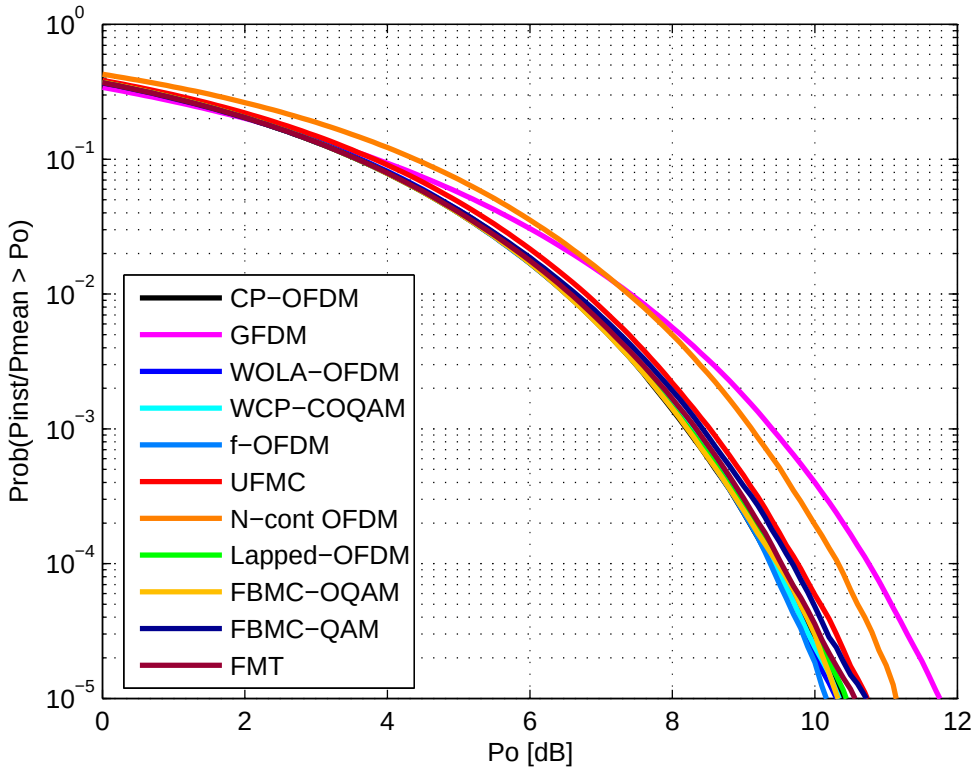

-a-

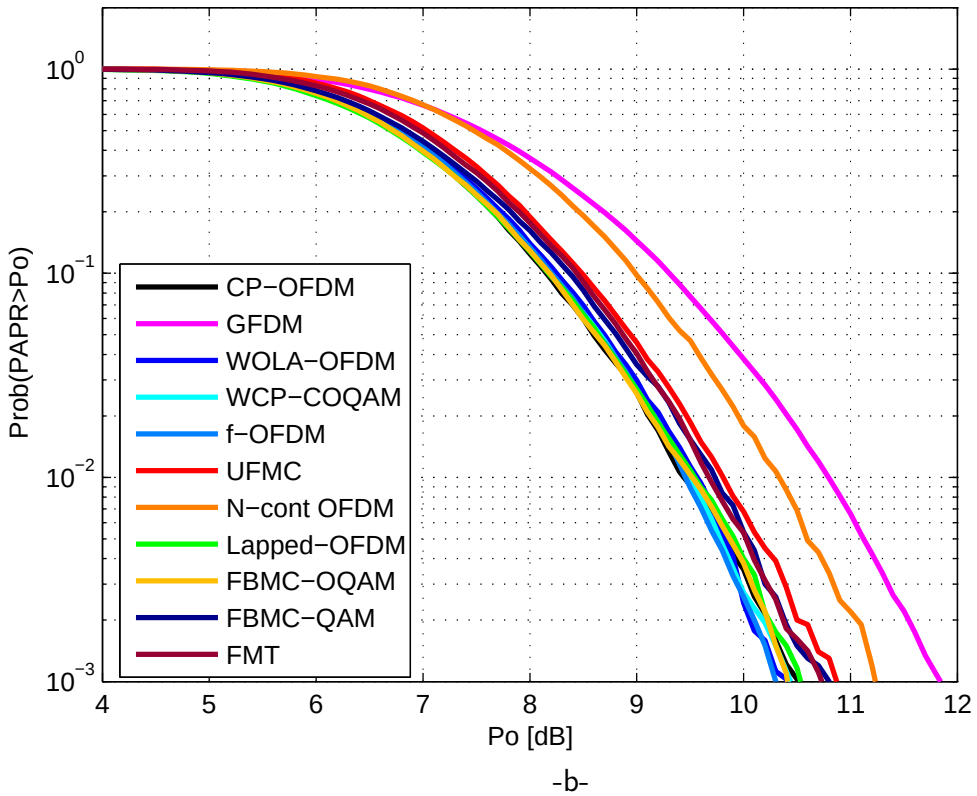

-b-

Figure 4-37: (a) Comparisons of the CCDF of the IAPR, (b) Comparison of the CCDF of the PAPR calculated over a block length of 1024 samples.

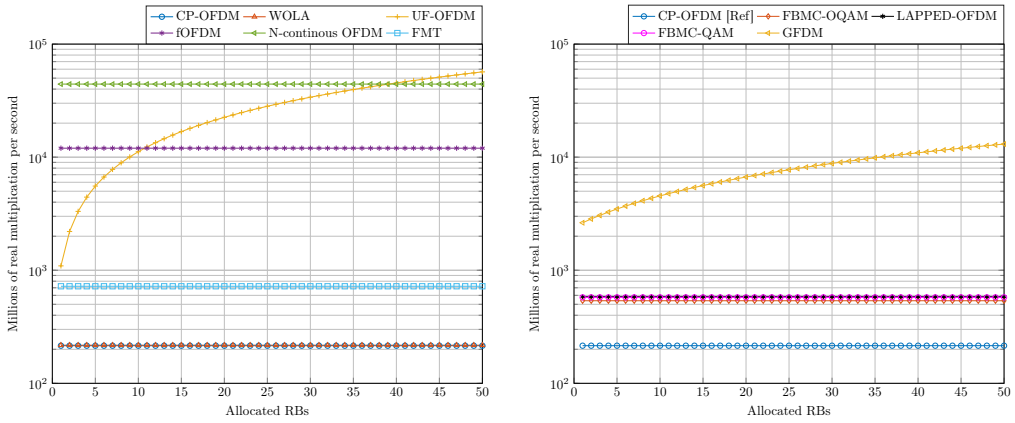

(a) (b)

Figure 4-38: Tx complexity synthesis for waveforms satisfying the complex orthogonality (a) and for waveforms that do not satisfy the complex orthogonality (b)

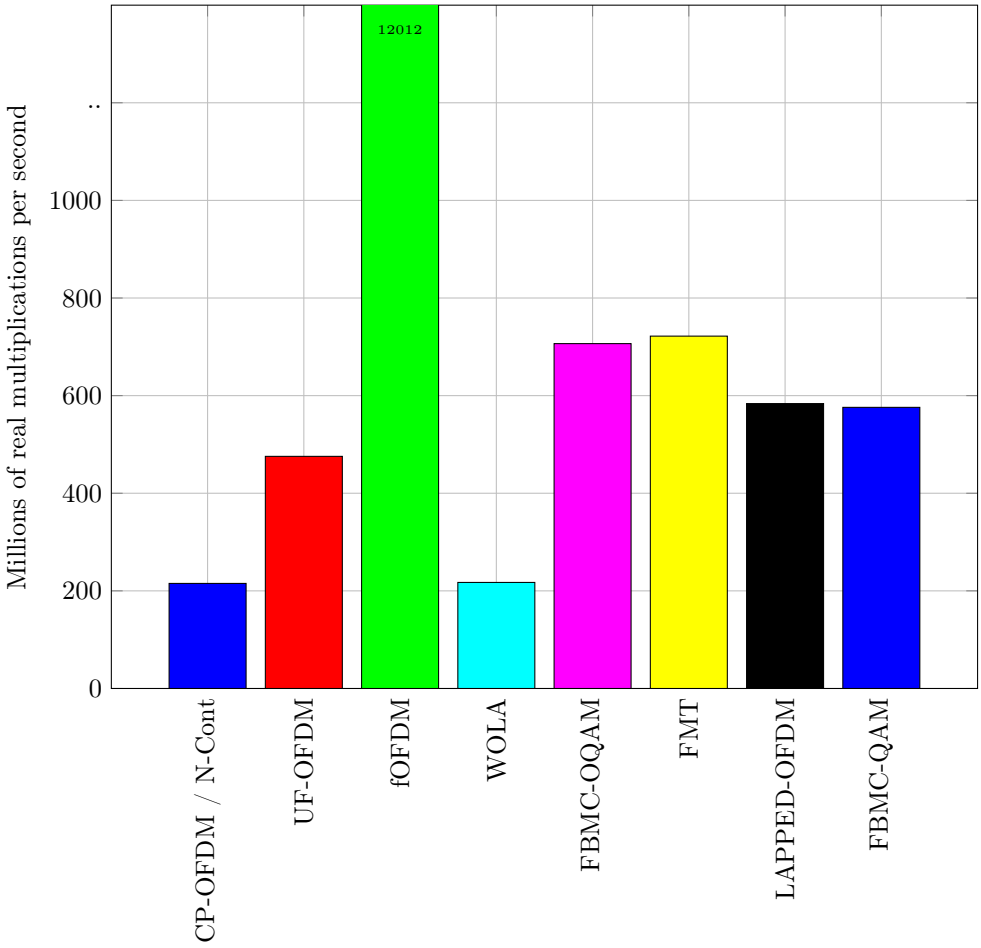

Figure 4-39: Rx complexity synthesis

4.7 MIMO Technology

4.7.1 Presentation and interests

A multi-input multi-output (MIMO) system [PGNB04] is a system which uses several antennas at both transmission and reception (Figure 4-40), contrary to a single-input single-output system which uses only one antenna at both sides.

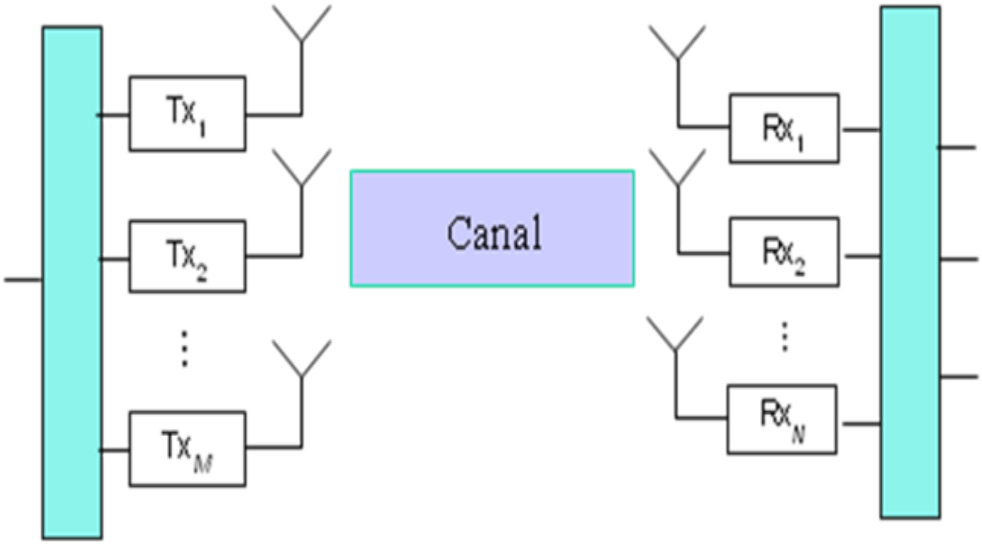

Figure 4-40: A MIMO system

For ideal propagation channel, i.e. for line of sight (LOS) radiocommunications, a MIMO system allows us to focus the transmitted energy in the receiver direction by steering a beam in the latter. In a same manner a beam may also be steered at reception in the transmitter direction. In this case, the MIMO system is a set of two beamformers (Figure 4-41), generating an improvement of the budget link for a given transmitted power.

For multi-paths propagation channels, a MIMO system allows us to extract the spatial diversity present at both transmission and reception (Figure 4-42) in order:

- to improve the budget link
- to spatially multiplex several statistically independent data streams at the same time on the same bandwidth.

The improvement of the budget link allows to increase the reliability, the range or the date rate of the communication by choosing higher order constellations. The spatial multiplexing allows to increase the data rate without any change in the constellation.

4.7.2 MIMO schemes

Two families of MIMO schemes at transmission, corresponding to closed-loop and open-loop schemes respectively may be implemented.

Closed-loop schemes correspond to schemes using channel state information (CSI) at transmission. In Frequency Division Duplexing (FDD) systems, this CSI is estimated by the receiver and sent to the transmitter through a feedback link (Figure 4-43). This requires slow variations of the channel and generates some additional "latency" in the processing. For this reason, these schemes are not selected for MTC links.

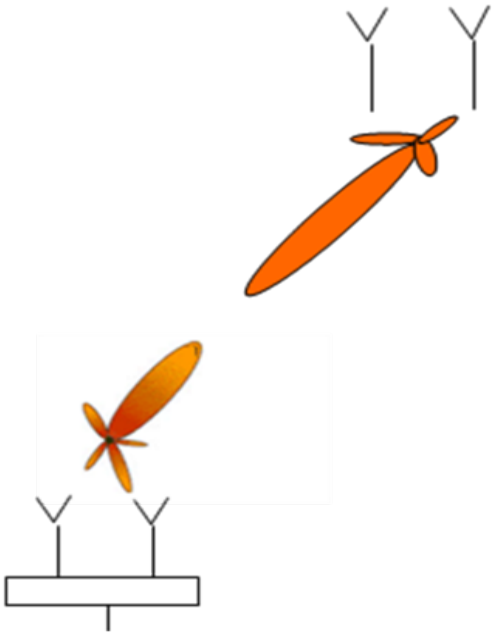

Figure 4-41: A MIMO system as a set of beamformers

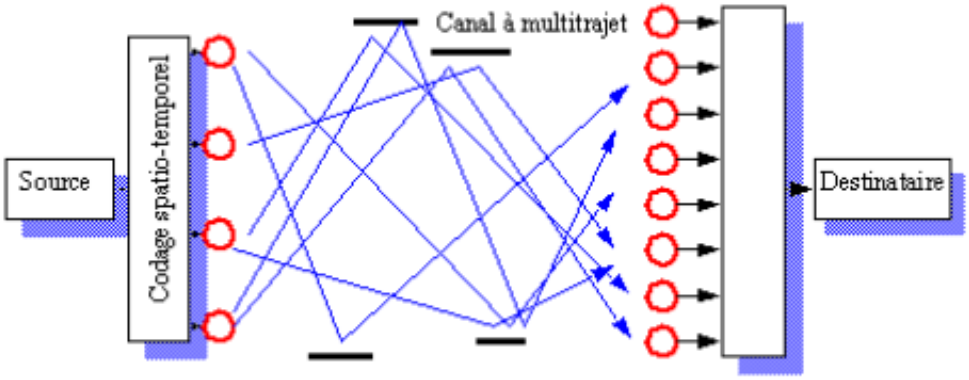

Figure 4-42: A MIMO system extracting Tx/Rx spatial diversity for multi-paths channels

Open-loop schemes do not use any CSI at transmission. Open-loop schemes which improve the budget link at reception do not implement spatial multiplexing but use spatio-temporal coding (STC) at transmission [TSC98]. The most famous STC, optimized for $N_t = 2$ transmit antennas, is the Alamouti STC [Ala98]. Among open-loop schemes which use spatial multiplexing we may cite the V-BLAST scheme [Fos96] or STC with spatial multiplexing such as the Golden code [BRV05]. The open-loop schemes are the ones which are considered in this project for MTC links.

4.8 Coupling of MIMO technology with MC waveforms

4.8.1 MIMO for OFDM waveforms

The coupling of the MIMO technology with OFDM waveforms consists in implementing the MIMO schemes on each sub-carrier of the OFDM waveform. This is a straightforward task thanks to the orthogonality of the sub-carriers in the complex domain whatever the selectivity

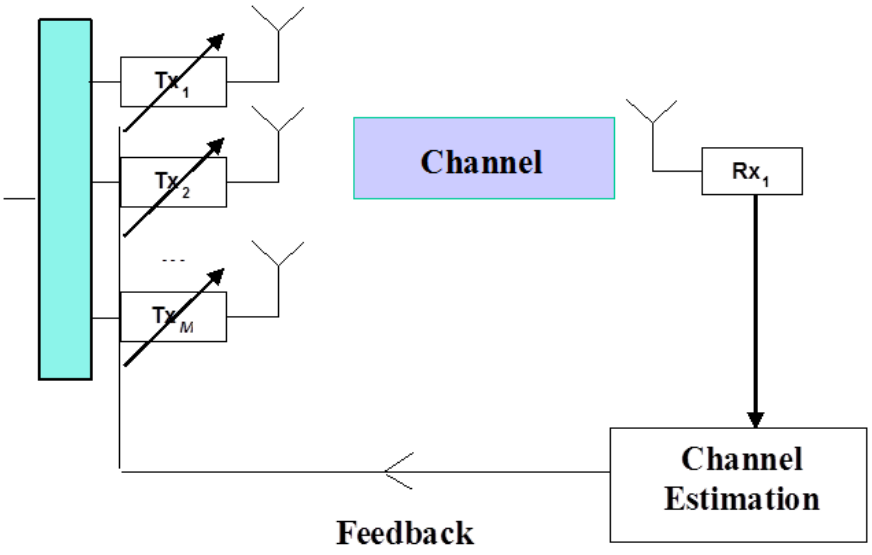

Figure 4-43: A MIMO system with feedback

degree of the propagation channel, provided that the CP size remains greater than or equal to the delay spread of the channel. Indeed, under this assumption, each sub-carrier sees a flat fading channel without any inter-symbol interference (ISI) and any inter-carrier interference (ICI), which allows us to obtain the performance of MIMO links for single carrier waveforms in flat fading channels. For this reason, the MIMO for CP-OFDM will be the reference for WONG5.

4.8.2 MIMO for filtered MC waveforms

On the contrary, the coupling of the MIMO technology with filtered MC-waveforms may be more difficult, depending on the amount of residual ISI and ICI at reception and the scheme considered. Indeed, Spatial Multiplexing with linear receivers applied to filtered MC waveforms give the same performance as CP-OFDM. However, when STC is considered the residual ISI and ICI could break the properties of the coding scheme.

Filtered MC waveforms which are said to be orthogonal in the complex domain (WOLA-OFDM, UFMC, N-Continuous OFDM, FMT) are in fact orthogonal only for propagation channels which are not too frequency selective. For such channels and for such MC waveforms, the use of MIMO technology is straightforward. However, it will be interesting to evaluate in the project the degree of frequency selectivity over which the performance of the MIMO schemes for these MC-waveforms degrade.

However, filtered MC waveforms which are not orthogonal in the complex domain (FBMC-OQAM, Laped-OFDM-OQAM, WCP-COQAM, FBMC-QAM, GFDM) generate both ISI and ICI at reception. These interference explain the strong performance degradation of most of the standard MIMO schemes used for CP-OFDM, even for propagation channels which are relatively weakly frequency selective . For this reason, new MIMO schemes, aiming at mitigating the effects of ISI and ICI, are required for non orthogonal filtered MC waveforms. This is the purpose of WP 4 of the project.

Waveforms	Normalized complexity	Rank
CP-OFDM	1.00	1
WOLA	1.01	3
UF-OFDM	2.21	4
fOFDM	55.80	10
N-continuous OFDM	1.00	2
FMT	3.35	8
FBMC-OQAM	3.28	7
Lapped OFDM	2.71	6
FBMC-QAM	2.68	5
WCP-COQAM	4.10	9

Table 4-5: Rx complexity normalized with respect to OFDM

5. Potential candidates for MTC

To give an overview on all of the considered waveforms performances discussed in Part 4, we introduce in Figure 5-1 radar plots where each corner corresponds to a given criteria:

- PSD (near neighborhood): We focused on the PSD level at spectral distance of 75kHz. Here, the gain in dB of each waveform compared to CP-OFDM is considered. We have adopted a linear scale between 0dB of CP-OFDM and 80dB corresponding to the FMT gain. This metric can be useful for quantifying the necessary spectral distance between different asynchronous users within the same multicarrier system.
- PSD (far neighborhood): In this case, we have focused on the asymptotic PSD level (i.e. very large spectral distance). This axis has been constructed similarly to the previous one. However, we have limited the minimum PSD level to -100dB. This metric can be useful for quantifying the required guard-band separating two asynchronous multicarrier systems.
- Spectral efficiency (short bursts): The spectral efficiency of each waveform is normalized to the CP-OFDM one where a linear scale has been adopted. Concerning the burst size, we have considered the extreme case where we have a single multicarrier block.
- Spectral efficiency (long bursts): The evaluation is similar to the previous metric except the burst size. In fact, this case corresponds to the asymptotic behavior where the burst is formed by an infinity of multicarrier blocks
- Latency (short bursts): similar to the spectral efficiency (short bursts).
- Latency (long bursts): similar to the spectral efficiency (long bursts).
- Robustness to timing offset: As done in the PSD axis, we focus here on the MSE gap in dB between each waveform and CP-OFDM in a fully asynchronous scenario ($\tau = T/2$). A linear scale has been adopted between 0dB for CP-OFDM and 45dB achieved by FBMC-OQAM. Note that the considered results are related to a guard-band of $\delta = 75$kHz between the user of interest and asynchronous interfering ones.
- Robustness to CFO: similar to the robustness against timing offset axis. Here, the considered guard band is also $\delta = 75$kHz.
- Receiver complexity: For this criteria, we focused on the inverse of the waveform complexity which is previously normalized to the CP-OFDM one (see Table 4-5). Also, a linear scale has been adopted.
- Transmitter complexity (Narrow-Band case): similar to the receiver complexity axis. Note here, that the narrow-band case corresponds to 5RBs column of Table 4-4.
- Transmitter complexity (Broad-Band case): similar to the receiver complexity axis. Here, the broad-band case corresponds to 50RBs column of Table 4-4.

In order to make easier the comparison overview, the radar plots have been splitted into three groups according the orthogonality classification of the waveforms: complex orthogonality in Figure 5-2, real orthogonality in Figure 5-3 and without orthogonality in Figure 5-4. Note that for three figures, we keep CP-OFDM as a reference. Moreover, we have introduced radar plots for each criteria where the corners correspond to the studied waveforms in Figure 5-5.

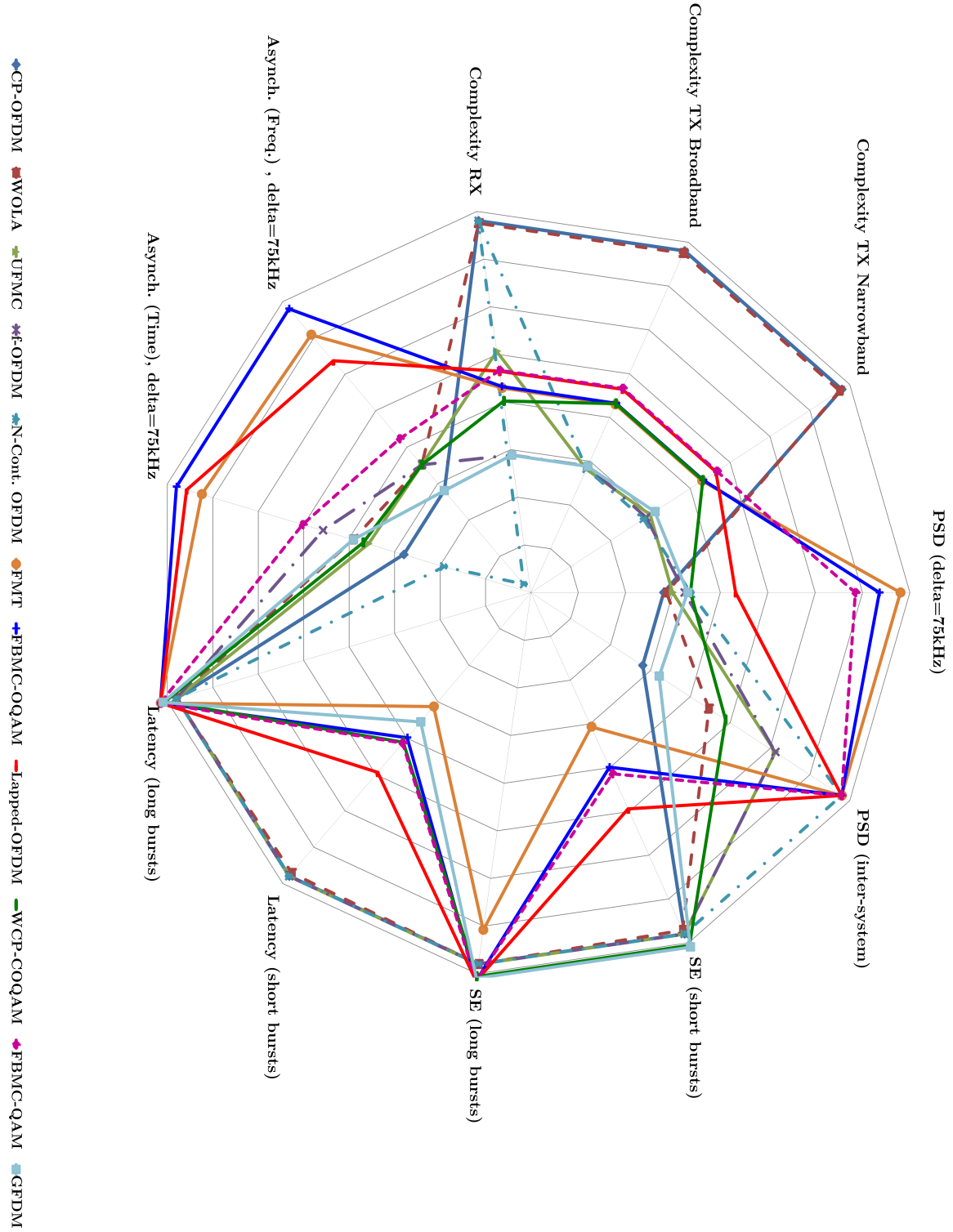

Figure 5-1: Performance overview: all waveforms

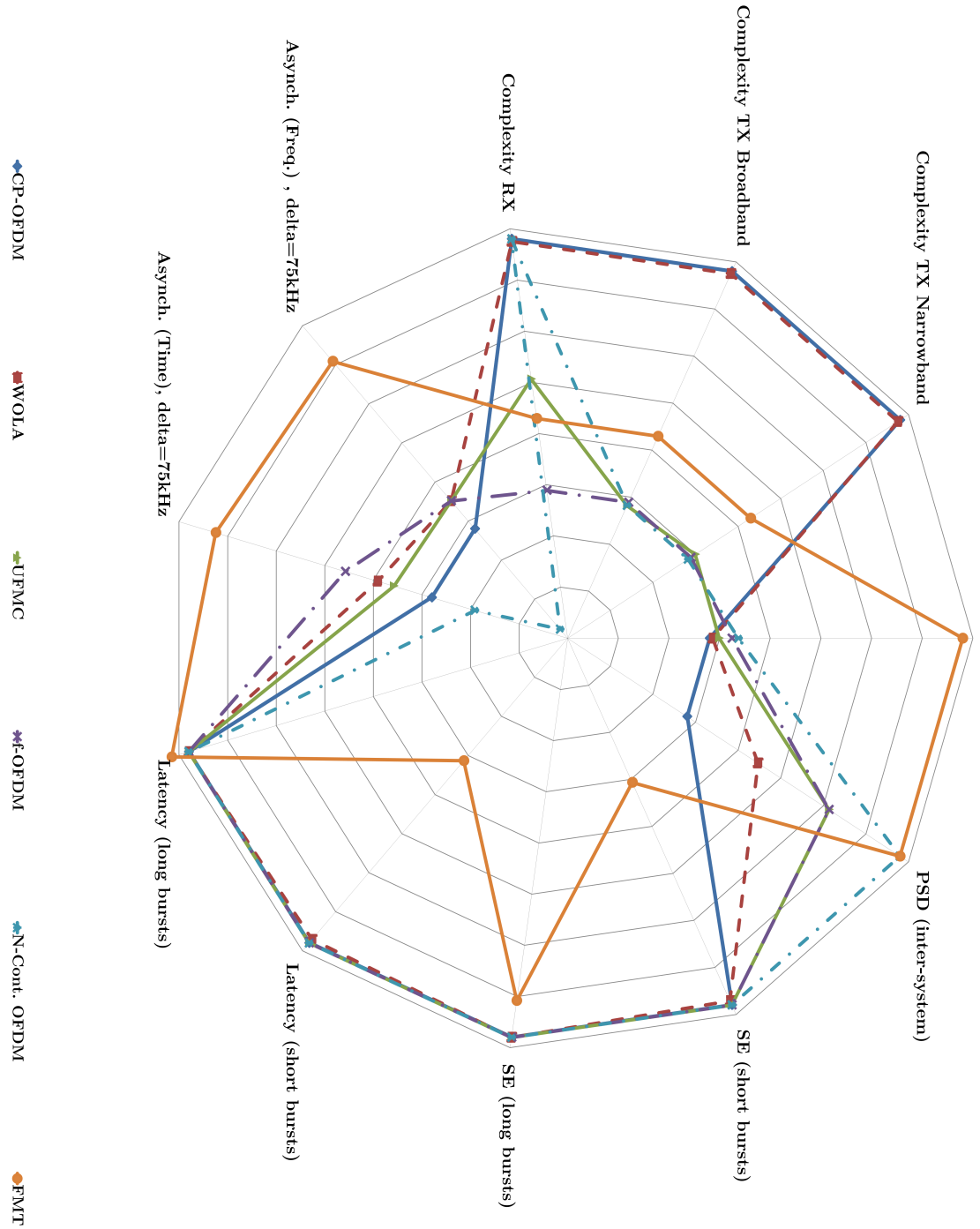

Figure 5-2: Performance overview: waveforms with complex orthogonality

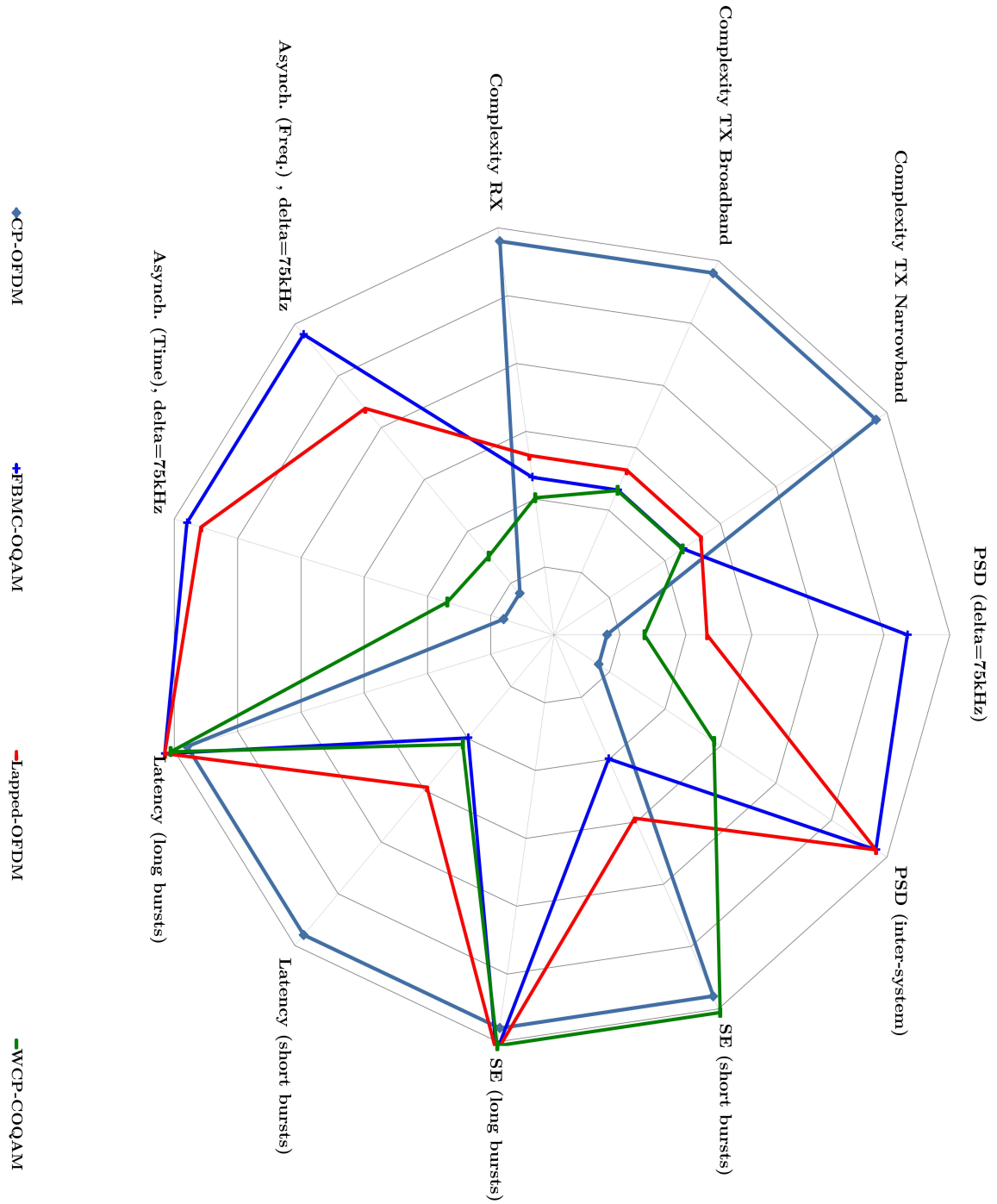

Figure 5-3: Performance overview: waveforms with real orthogonality

Figure 5-4: Performance overview: waveforms without orthogonality

PSD (delta=75kHz)

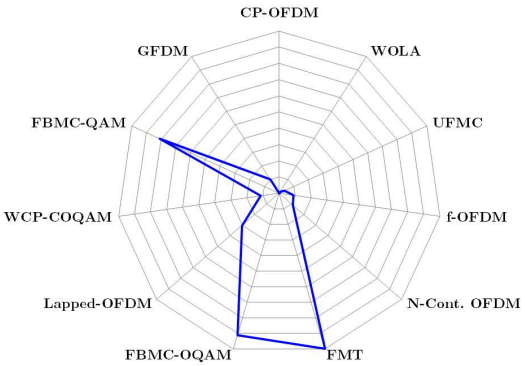

PSD (inter-system)

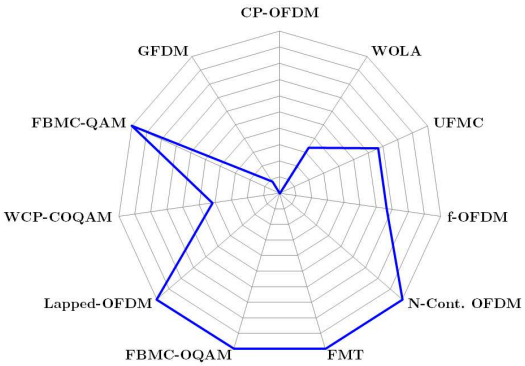

SE (short bursts)

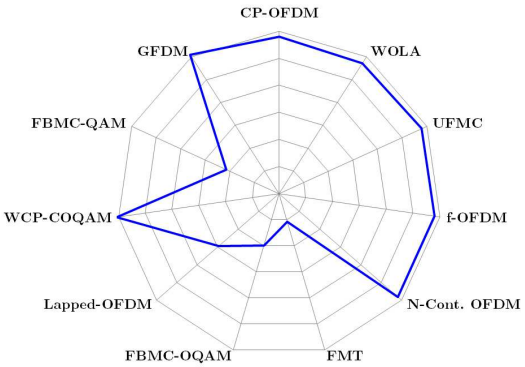

SE (long bursts)

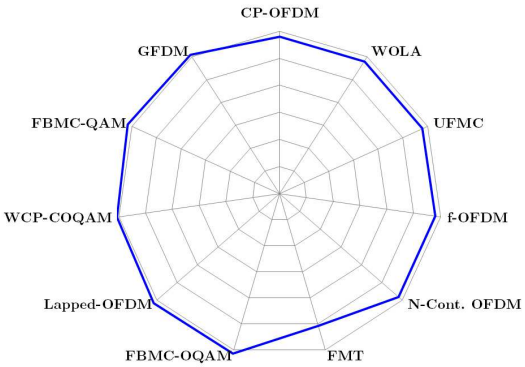

Latency (short bursts)

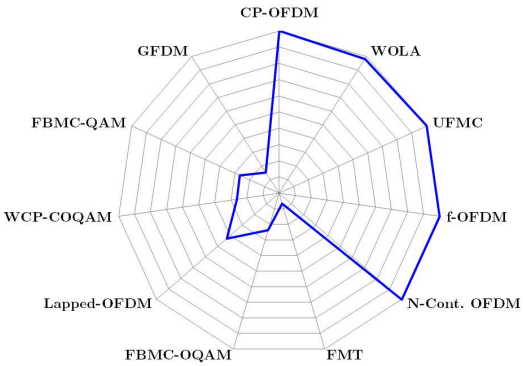

Latency (long bursts)

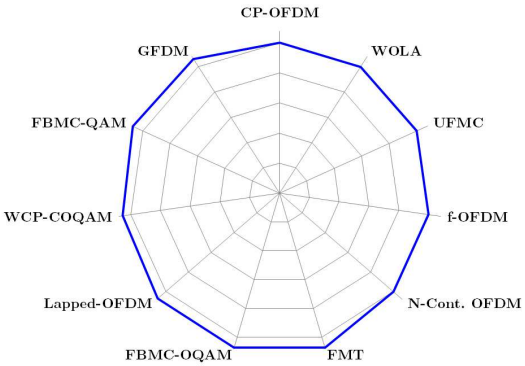

Asynch. (Time), delta=75kHz

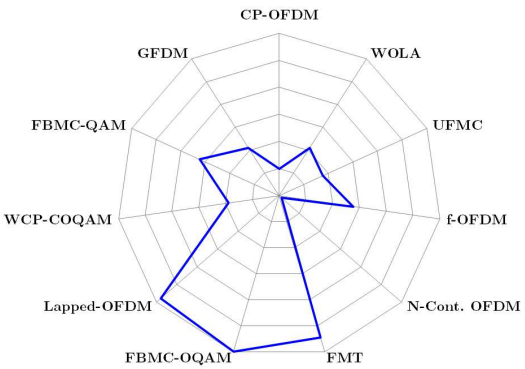

Asynch. (Freq.) , delta=75kHz

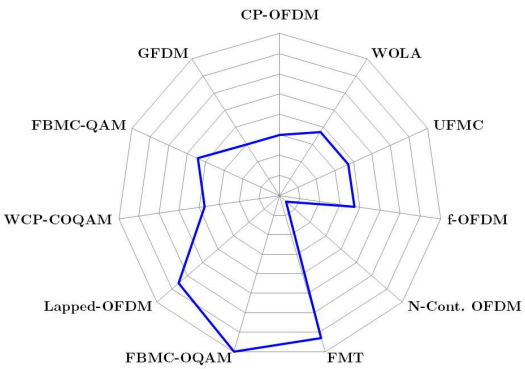

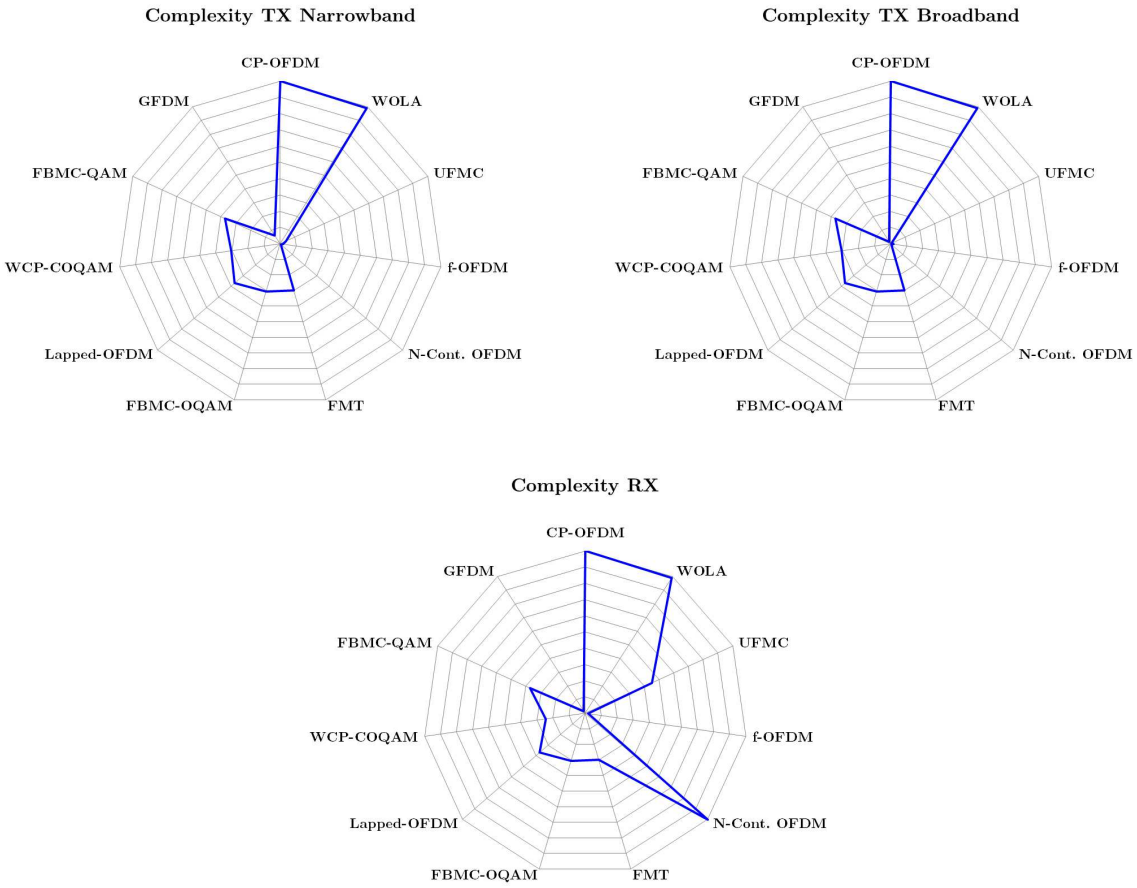

Figure 5-5: Performance overview

5.1 WONG5 choice

As said in Part 1, the objectives of deliverable D2.1 were to analyze, compare and finally define a restricted set of post-OFDM waveforms adapted to the C-MTC context.

It is not straightforward to rank the different criteria that have been analyzed at the light of C-MTC context. Nevertheless, from D1.1 and D1.2, it has been highlighted that some criteria were of prime importance for C-MTC as: **low latency, asynchronous capabilities, high reliability, high energy efficiency and spectral efficiency**.

The **PSD criterion** can be related to the resistance to asynchronous users in the time domain. In fact, a WF with a very bad localized PSD will exhibit very bad performances concerning resistance to timing errors. Nevertheless, a WF with quite good spectral localization can have quite bad performances concerning resistance to timing errors if the receiving filter is not well localized in frequency. For instance, UFMC and f-OFDM have a similar performance concerning their PSD (see Figures 4-1 and 4-2) but f-OFDM is better concerning timing offsets (see Figures 4-9, 4-10 and 4-11) because of the receiving filter used in this WF. In conclusion, we will put higher emphasis on the criterion "resistance to timing offsets" compared to the criterion "PSD".

Complexity has been also compared for all WFs. Following figure 4-38 and figure 4-39, some WFs have a complexity lower than four times the complexity of CP-OFDM. For this set of WFs, complexity will not be a discriminant criterion. On the contrary a second set of WFs has a very high complexity (order of 100) compared to CP-OFDM: UFMC, f-OFDM, N Continuous-OFDM and GFDM. For this second set of WFs, complexity can be a discriminant criterion.

Concerning **energy efficiency** related to High Power Amplifiers necessary back off, Figure 4-37 tells us that all considered WFs have a similar PAPR/IAPR and thus will exhibit similar energy efficiency. This last criterion is thus not discriminant.

Lapped-OFDM and FBMC-OQAM waveforms are very similar. The only slight difference consists in a different shaping filter. In the following, we will consider only FBMC-OQAM waveform as a generic WF with orthogonality in the real domain and very good frequency localization.

In the Table 5-1, only discriminant criteria have been taken into account:

- Latency
- End to End physical latency
- Resistance to timing offsets
- Resistance to CFO
- Complexity
- Spectral efficiency

"PSD" and "energy efficiency" criteria have been discarded because of the above reasons.

CP-OFDM will be kept as a reference WF.

N-continuous OFDM is discarded because of its very bad performance concerning timing errors and CFO together with high complexity. Note that, in order to properly recover data, the transmission of the precoding matrix to the receiver is required, otherwise, this scheme will suffer from a high level of EVM.

Waveforms	Latency	E2E Lat.	Time Asynch.	Freq. Asynch.	S.E.(short bursts)	S.E. (long bursts)	Complexity
CP-OFDM	+	+	−	+	+	+	+
	+		−				+
	+		−				+
WOLA-OFDM	+	+	+	+	+	+	+
	+						+
UFMC	+	+	+	+	+	+	−
	+						−
	+						−
fOFDM	+	+	+	+	+	+	−
	+		+				−
	+		+				−
N-Cont. OFDM	+	+	−	−	+	+	−
	+		−	−			−
	+		−	−			−
FMT	−	+	+	+	−	+	+
	−		+	+	−		
	−		+	+	−		
FBMC-OQAM	−	+	+	+	−	+	+
			+	+			
			+	+			
WCP-COQAM	−	+	+	+	+	+	+
FBMC-QAM	−	+	+	+	−	+	−
			+	+			−
			+	+			−
GFDM	−	+	+	+	+	+	−
							−
							−

Table 5-1: Waveforms vs. criteria

FMT is not retained because of its bad latency and its bad spectral efficiency. For this WF there is a tradeoff between latency and spectral efficiency. Note that, if we want a better spectral efficiency we need a filter with a smaller roll-of factor and thus we need a very long impulse response filter and thus a higher latency.
WCP-COQAM will be discarded because of poor performances concerning timing errors and CFO.
GFDM is not considered because it has a very high complexity at the receiver side if interference cancellation is considered and, furthermore, has poor performances concerning timing errors and CFO.

The set of considered WFs for the rest of the WONG5 project will be:

Waveforms with complex orthogonality and windowing/filtering applied to a group of subcarriers:

- WOLA-OFDM: very similar to CP-OFDM concerning latency. Small added complexity due to windowing processing at the emitter side (PSD) and at the receiver (asynchronous interference protection). Good performances concerning timing errors and CFO.
- UFMC/UF-OFDM: very similar to CP-OFDM concerning latency. Added complexity due to filtering processing at the emitter side (PSD). Good performances concerning timing errors and CFO.
- f-OFDM: very similar to CP-OFDM concerning latency. Added complexity due to filtering processing at both emitter and receiver side. Good performances concerning timing errors and CFO.

Waveforms with real orthogonality and filtering applied to single subcarrier:

- FBMC-OQAM : higher latency for ultra-small packets but very good performances concerning timing errors and CFO. Added complexity due to filtering processing at both emitter and receiver side.

Waveforms without orthogonality and filtering applied to single subcarrier:

- FBMC-QAM : higher latency for ultra-small packets but very good performances concerning timing errors and CFO. Added complexity due to filtering processing at both emitter and receiver side and to the interference canceller at the receiver side. This WF has been added to the set of candidates WFs because, despite the receiver complexity, it will be interesting to study non orthogonal WFs and their adaptation to MIMO systems.

6. References

[AJM13] M. J. Abdoli, M. Jia, and J. Ma. Weighted circularly convolved filtering in OFDM/OQAM. In *2013 IEEE 24th Annual International Symposium on Personal, Indoor, and Mobile Radio Communications (PIMRC)*, pages 657–661, Sept 2013.

[AJM15] J. Abdoli, M. Jia, and J. Ma. Filtered ofdm: A new waveform for future wireless systems. In *2015 IEEE 16th International Workshop on Signal Processing Advances in Wireless Communications (SPAWC)*, pages 66–70, June 2015.

[Ala98] S. M. Alamouti. A simple transmit diversity technique for wireless communications. *IEEE Journal on Selected Areas in Communications*, 16(8):1451–1458, Oct 1998.

[AS97] O.E. Agazzi and N. Seshadri. On the use of tentative decisions to cancel intersymbol interference and nonlinear distortion (with application to magnetic recording channels). *Information Theory, IEEE Transactions on*, 43(2):394 –408, mar 1997.

[BDN14] Vincent Berg, Jean-Baptiste Dore, and Dominique Noguet. A flexible fs-fbmc receiver for dynamic access in the tvws. In *Cognitive Radio Oriented Wireless Networks and Communications (CROWNCOM), 2014 9th International Conference on*, pages 285–290. IEEE, 2014.

[Bel10] M. Bellanger. Efficiency of Filter Bank Multicarrier Techniques in Burst Radio Transmission. In *Global Telecommunications Conference (GLOBECOM 2010), 2010 IEEE*, pages 1–4, Dec 2010.

[Bel12] Maurice Bellanger. Fs-fbmc: A flexible robust scheme for efficient multicarrier broadband wireless access. In *Globecom Workshops (GC Wkshps), 2012 IEEE*, pages 192–196. IEEE, 2012.

[BLRR+10] M Bellanger, D Le Ruyet, D Roviras, M Terré, J Nossek, L Baltar, Q Bai, D Waldhauser, M Renfors, T Ihalainen, et al. Fbmc physical layer: a primer. *PHYDYAS, January*, 2010.

[BMT15] Maurice Bellanger, Davide Mattera, and Mario Tanda. Lapped-ofdm as an alternative to cp-ofdm for 5g asynchronous access and cognitive radio. In *Vehicular Technology Conference (VTC Spring), 2015 IEEE 81st*, pages 1–5. IEEE, 2015.

[BRV05] J. C. Belfiore, G. Rekaya, and E. Viterbo. The golden code: a 2 times;2 full-rate space-time code with nonvanishing determinants. *IEEE Transactions on Information Theory*, 51(4):1432–1436, April 2005.

[BT07] Norman C Beaulieu and Peng Tan. On the effects of receiver windowing on OFDM performance in the presence of carrier frequency offset. *IEEE Transactions on Wireless Communications*, 6(1):202–209, 2007.

[CBS06] C. Ciochina, F. Buda, and H. Sari. An analysis of ofdm peak power reduction techniques for wimax systems. In *2006 IEEE International Conference on Communications*, volume 10, pages 4676–4681, June 2006.

[CEOC00] G. Cherubini, E. Eleftheriou, S. Oker, and J. M. Cioffi. Filter bank modulation techniques for very high speed digital subscriber lines. *IEEE Communications Magazine*, 38(5):98–104, May 2000.

[CPGB16] M. Chafii, J. Palicot, R. Gribonval, and F. Bader. A necessary condition for waveforms with better papr than ofdm. *IEEE Transactions on Communications*, 64(8):3395–3405, Aug 2016.

[DMLF12] R. Datta, N. Michailow, M. Lentmaier, and G. Fettweis. GFDM interference cancellation for flexible cognitive radio PHY design. In *Proc. IEEE Vehicular Technology Conference (VTC Fall)*, pages 1–5, Sept 2012.

[DRT16] J-B Dore, Daniel Rovira, and Sylvain Traverso. Wong5 project, deliverable 1.1: Scenario description of critical - machine type communications. *ANR, Tech. Rep*, 2016.

[FB11] Behrouz Farhang-Boroujeny. Ofdm versus filter bank multicarrier. *IEEE signal processing magazine*, 28(3):92–112, 2011.

[FBM16] B. Farhang-Boroujeny and H. Moradi. OFDM Inspired Waveforms for 5G. *IEEE Commun. Surveys Tutorials*, 18(4):2474–2492, 2016.

[FKB09] G. Fettweis, M. Krondorf, and S. Bittner. GFDM - generalized frequency division multiplexing. In *Proc. IEEE 69th Vehicular Technology Conference (VTC)*, pages 1–4, April 2009.

[Fos96] G. J. Foschini. Layered space-time architecture for wireless communication in a fading environment when using multi-element antennas. *Bell Labs Technical Journal*, 1(2):41–59, Autumn 1996.

[GMM+15] I. Gaspar, M. Matthe, N. Michailow, L. Leonel Mendes, D. Zhang, and G. Fettweis. Frequency-shift Offset-QAM for GFDM. *IEEE Communications Letters*, 19(8):1454–1457, Aug 2015.

[HDR03] F. J. Harris, C. Dick, and M. Rice. Digital receivers and transmitters using polyphase filter banks for wireless communications. *IEEE Transactions on Microwave Theory and Techniques*, 51(4):1395–1412, Apr 2003.

[HiS16] Huawei HiSilicon. f-ofdm scheme and filter design. In *R1-165425*, May 2016.

[Kra99] Steven G Krantz. *Handbook of Complex Variables*. Birkhäuser Basel, 1999.

[KYKS16] C. Kim, Y. H. Yun, K. Kim, and J. Y. Seol. Introduction to qam-fbmc: From waveform optimization to system design. *IEEE Communications Magazine*, 54(11):66–73, November 2016.

[LFAB95] Bernard Le Floch, Michel Alard, and Claude Berrou. Coded orthogonal frequency division multiplex [tv broadcasting]. *Proceedings of the IEEE*, 83(6):982–996, 1995.

[LS14] H. Lin and P. Siohan. Multi-carrier modulation analysis and WCP-COQAM proposal. *EURASIP Journal on Advances in Signal Processing*, 2014(1):1, 2014.

[Med12] Yahia Medjahdi. *Interference modeling and performance analysis of asynchronous OFDM and FBMC wireless communication systems*. PhD thesis, Conservatoire national des arts et metiers-CNAM, 2012.

[MGK+12] N. Michailow, I. Gaspar, S. Krone, M. Lentmaier, and G. Fettweis. Generalized frequency division multiplexing: Analysis of an alternative multi-carrier technique for next generation cellular systems. In *International Symposium on Wireless Communication Systems (ISWCS)*, pages 171–175, Aug 2012.

[MKLF12] N. Michailow, S. Krone, M. Lentmaier, and G. Fettweis. Bit error rate performance of generalized frequency division multiplexing. In *Proc. IEEE Vehicular Technology Conference (VTC Fall)*, pages 1–5, Sept 2012.

[MTLR+11] Yahia Medjahdi, Michel Terré, Didier Le Ruyet, Daniel Roviras, and Ali Dziri. Performance analysis in the downlink of asynchronous ofdm/fbmc based multi-cellular networks. *IEEE transactions on wireless communications*, 10(8):2630–2639, 2011.

[MWG+02] B. Muquet, Zhengdao Wang, G. B. Giannakis, M. de Courville, and P. Duhamel. Cyclic prefixing or zero padding for wireless multicarrier transmissions? *IEEE Transactions on Communications*, 50(12):2136–2148, Dec 2002.

[MZS+16] M. Matthe, D. Zhang, F. Schaich, T. Wild, R. Ahmed, and G. Fettweis. A Reduced Complexity Time-Domain Transmitter for UF-OFDM. In *2016 IEEE 83rd Vehicular Technology Conference (VTC Spring)*, pages 1–5, May 2016.

[PGNB04] A. J. PAULRAJ, D. A. GORE, R. U. NABAR, and H. BOLCSKEI. An overview of mimo communications - a key to gigabit wireless. *Proceedings of the IEEE*, 92(2):198–218, Feb 2004.

[Qua] Qualcomm, Incorporated. R1-162199 - Waveform candidates.

[Sal67] B Saltzberg. Performance of an efficient parallel data transmission system. *IEEE Transactions on Communication Technology*, 15(6):805–811, 1967.

[SW14a] F. Schaich and T. Wild. Relaxed synchronization support of universal filtered multi-carrier including autonomous timing advance. In *2014 11th International Symposium on Wireless Communications Systems (ISWCS)*, pages 203–208, Aug 2014.

[SW14b] F. Schaich and T. Wild. Waveform contenders for 5g - ofdm vs. fbmc vs. ufmc. In *2014 6th International Symposium on Communications, Control and Signal Processing (ISCCSP)*, pages 457–460, May 2014.

[SWC14] F. Schaich, T. Wild, and Yejian Chen. Waveform contenders for 5G - suitability for short packet and low latency transmissions. In *Proc. IEEE 79th Vehicular Technology Conference (VTC Spring)*, pages 1–5, May 2014.

[Tra16] S. Traverso. A family of square-root nyquist filter with low group delay and high stopband attenuation. *IEEE Communications Letters*, 20(6):1136–1139, June 2016.

[TSC98] V. Tarokh, N. Seshadri, and A. R. Calderbank. Space-time codes for high data rate wireless communication: performance criterion and code construction. *IEEE Transactions on Information Theory*, 44(2):744–765, Mar 1998.

[VBRB06] S. Van Beneden, J. Riani, and J.W.M. Bergmans. Cancellation of Linear Intersymbol Interference for Two-Dimensional Storage Systems. In *Communications, 2006. ICC '06. IEEE International Conference on*, volume 7, pages 3173 –3178, june 2006.

[vdBB09a] J. van de Beek and F. Berggren. Evm-constrained ofdm precoding for reduction of out-of-band emission. In *2009 IEEE 70th Vehicular Technology Conference Fall*, pages 1–5, Sept 2009.

[vdBB09b] J. van de Beek and F. Berggren. N-continuous ofdm. *IEEE Communications Letters*, 13(1):1–3, January 2009.

[VIS+09] Ari Viholainen, Tero Ihalainen, Tobias Hidalgo Stitz, Markku Renfors, and Maurice Bellanger. Prototype filter design for filter bank based multicarrier transmission. In *Signal Processing Conference, 2009 17th European*, pages 1359–1363. IEEE, 2009.

[VWS+13] V. Vakilian, T. Wild, F. Schaich, S. ten Brink, and J. F. Frigon. Universal-filtered multi-carrier technique for wireless systems beyond lte. In *2013 IEEE Globecom Workshops (GC Wkshps)*, pages 223–228, Dec 2013.

[WS15] T. Wild and F. Schaich. A Reduced Complexity Transmitter for UF-OFDM. In *2015 IEEE 81st Vehicular Technology Conference (VTC Spring)*, pages 1–6, May 2015.

[WSC14] T. Wild, F. Schaich, and Y. Chen. 5g air interface design based on universal filtered (uf-)ofdm. In *2014 19th International Conference on Digital Signal Processing*, pages 699–704, Aug 2014.

[WWS15] X. Wang, T. Wild, and F. Schaich. Filter optimization for carrier-frequency- and timing-offset in universal filtered multi-carrier systems. In *2015 IEEE 81st Vehicular Technology Conference (VTC Spring)*, pages 1–6, May 2015.

[WWSdS14] X. Wang, T. Wild, F. Schaich, and A. Fonseca dos Santos. Universal filtered multi-carrier with leakage-based filter optimization. In *European Wireless 2014; 20th European Wireless Conference*, pages 1–5, May 2014.

[YKK+15] Yeo Hun Yun, Chanhong Kim, Kyeongyeon Kim, Zuleita Ho, Byunghwan Lee, and Ji-Yun Seol. A new waveform enabling enhanced qam-fbmc systems. In *Signal Processing Advances in Wireless Communications (SPAWC), 2015 IEEE 16th International Workshop on*, pages 116–120. IEEE, 2015.

[ZLRM12] R. Zakaria, D. Le Ruyet, and Y. Medjahdi. On ISI cancellation in MIMO-ML detection using FBMC/QAM modulation. In *Wireless Communication Systems (ISWCS), 2012 International Symposium on*, pages 949 –953, aug. 2012.

[ZMSR16] R. Zayani, Y. Medjahdi, H. Shaiek, and D. Roviras. WOLA-OFDM: a potential candidate for asynchronous 5G. In *IEEE Global Communications Conference (GLOBECOM)*, 2016.

[ZR14] Rostom Zakaria and Didier Le Ruyet. Intrinsic interference reduction in a filter bank-based multicarrier using QAM modulation . *Physical Communication*, 11:15–24, 2014. Radio Access Beyond OFDM(A).

Glossary and Definitions

Acronym	Meaning
ACL	Adjacent Channel Leakage
C-MTC	Critical-Machine Type Communications
CCDF	Complementary Cumulative Distribution Function
COQAM	Circular Offset QAM
CFO	Carrier Frequency Offset
CP	Cyclic Prefix
EVM	Error Vector Magnitude
FBMC	Filter Bank Multi-Carrier
FFT	Fast Fourier Transform
FMT	Filtered Multi-Tone
f-OFDM	filtered-OFDM
FS	Frequency Spreading
GFDM	Generalized Frequency Division Multiplexing
IAPR	Instantaneous-to-Average Power Ratio
LTE	Long Term Evolution
MF	Matched Filter
MIMO	Multi-Input Multi-Output
MSE	Mean Square Error
OFDM	Orthogonal Frequency Division Multiplexing
OLA	Overlap and Add
OLS	Overlap and Save
OOB	Out-Of-Band
PAPR	Peak-to-Average Power Ratio
PPN	Poly-Phase Network
PSD	Power Spectral Density
RB	Resource Block
RRC	Root Raised-Cosine
Rx-W-OFDM	CP-OFDM with receive windowing
Tx-W-OFDM	CP-OFDM with transmit windowing
UFMC (i.e. UF-OFDM)	Universal-Filtered Multi-Carrier (i.e. Universal-Filtered OFDM)
UOI	User Of Interest
WCP	Windowed Cyclic Prefix
WF	WaveForm
WOLA	Weighted Overlap and Add
ZP	Zero Padding